ALMA MATER STUDIORUM
UNIVERSITÀ DI BOLOGNA

DOTTORATO DI RICERCA IN

SCIENZE BIOTECNOLOGICHE, BIOCOMPUTAZIONALI, FARMACEUTICHE E FARMACOLOGICHE

Ciclo 36

Settore Concorsuale: 06/A2 - PATOLOGIA GENERALE E PATOLOGIA CLINICA

Settore Scientifico Disciplinare: MED/04 - PATOLOGIA GENERALE

EXPLORING THE EFFECT OF RAD51/BRCA2 INHIBITION TO PURSUE SYNTHETIC LETHALITY WITH PARPi IN *IN-VITRO* MODELS OF PANCREATIC CANCER

Presentata da: Laura Poppi

Coordinatore Dottorato
Maria Laura Bolognesi

Supervisore
Marinella Roberti

Co-supervisore
Giuseppina Di Stefano

Esame finale anno 2024

ALMA MATER STUDIORUM
UNIVERSITÀ DI BOLOGNA

Ph.D. PROGRAMME IN

BIOTECHNOLOGICAL, BIOCOMPUTATIONAL,
PHARMACEUTICAL AND PHARMACOLOGICAL SCIENCES

Cycle 36th

Academic recruitment field: 06/A2 – GENERAL PATHOLOGY AND CLINICAL PATHOLOGY

Academic discipline: MED04 – GENERAL PATHOLOGY

EXPLORING THE EFFECT OF RAD51/BRCA2 INHIBITION TO PURSUE SYNTHETIC LETHALITY WITH PARPi IN *IN-VITRO* MODELS OF PANCREATIC CANCER

Ph.D. student: Laura Poppi

Coordinator of the Ph.D. programme
Maria Laura Bolognesi

Supervisor
Marinella Roberti

Co-supervisor
Giuseppina Di Stefano

Final exam, 2024

[This page is intentionally left blank]

TABLE OF CONTENTS

ABSTRACT……4

KEYWORDS……...……...5

ABBREVIATIONS……..……5

1. INTRODUCTION……...9

1.1 Cancer overview……...……...9

1.1.1 Pancreatic cancer……...…….……...10

1.1.2 Pancreatic ductal adenocarcinoma ……..…..…….……..11

1.2 The concept of synthetic lethality……..……..…13

1.3 Overview of the DNA damage response…..……..……..…16

1.3.1 DNA single-strand breaks and PARP-1…….…….18

1.3.2 PARP-1 inhibitors…….…..19

1.3.3 Talazoparib…….....20

1.3.4 DNA double-stranded breaks…….….21

1.3.5 Focus on homologous recombination……..…….…..22

1.3.6 RAD51 and BRCA2, the HR core proteins……..……..….25

2. AIM OF THE THESIS……..…..29

3. SECTION I - The BRC4 peptide: a tool for studying the effects of RAD51/BRCA2 inhibition……..……32

3.1 Introduction……..……..32

3.2 Materials and methods……..……33

3.2.1 Cell cultures…….……...33

3.2.2 BRC4 peptide……..……33

3.2.3 Homologous recombination quick assay (HR-QA)……..…..33

3.2.4 Cell immunofluorescence assay……..……34
3.2.5 Cell viability assay…….…….34
3.2.6 Western blot assay…….……..35

3.3 Results and Discussion……..…….…….....36
3.3.1 BRC4 peptide inhibits HR activity……..……..…….36
3.3.2 Evaluation of RAD51 nuclear foci as a marker for compromised HR…….…..36
3.3.3 HR impairment increases the cytotoxic effects of anticancer drugs……...37
3.3.4 Proteomic profile of BxPC-3 cells following myrBRC4 peptide treatment……..….39
3.3.5 Validation of FANCI, FANCD2, and RPA3 protein downregulation in pancreatic cancer cells……..……40

3.4 Conclusions – SECTION I……...……...42

4. SECTION II - Biological validation of a RAD51-BRCA2 small molecule inhibitor as a promising candidate to synergize with PARPi in 2D and 3D models of pancreatic cancer…….....45

4.1 Introduction……..……..45

4.2 Material and methods……..……....46
4.2.1 Cell cultures…….……...46
4.2.2 Organoids cultures…….….46
4.2.3 Homologous recombination quick assay (HR-QA)…….47
4.2.4 mClover Lamin A Homologous Recombination assay (mCl-HR)……..……47
4.2.5 Cell immunofluorescence assay…….…….47
4.2.6 Cell viability assay……..48
4.2.7 Cell death inhibitor assay……....48
4.2.8 Organoid viability assay..…..…….…..49
4.2.9 Immunofluorescence organoid assay…….…….49

4.3 Results and Discussion……..……..50
4.3.1 Evaluation of HR impairment following **46** treatment through different assays…....50
4.3.2 Analysis of **46**/talazoparib combination in three different BRCA2-proficient pancreatic cancer cell lines…….……54

4.3.3 Analysis of **46**/talazoparib combination in 3D models of pancreatic adenocarcinoma……..……...58

4.4 Conclusions – SECTION II……..…….62

5. CONCLUSIONS……...……..64

6. BIBLIOGRAPHY……..……....66

ABSTRACT

Synthetic lethality (SL) is an innovative framework for discovering novel anticancer treatments for personalized targeted therapies. Two genes are synthetically lethal if the inhibition of either gene alone has no effect on cell viability, but their simultaneous impairment leads to cell death. In this context, the Food and Drug Administration approved in 2014 the PARP inhibitor (PARPi) olaparib for oncology patients with BRCA1/2 mutations.

My Ph.D. research project is focused on pancreatic cancer, an oncological need. It is aimed at exploiting a new paradigm, dubbed "fully small-molecule-induced synthetic lethality", which was already presented in previous studies by the research group of Professors A. Cavalli (Italian Institute of Technology) and M. Roberti (University of Bologna). It is based on the possibility of triggering SL by using only small molecules: a PARPi and a RAD51/BRCA2 disruptor that mimics the BRCA2-defective condition.

RAD51 and BRCA2 are two key proteins in the homologous recombination (HR) pathway. Their interaction is mediated by eight motifs of BRCA2, among which the fourth (BRC4) has the highest affinity for RAD51. The first section of this thesis describes the effects on cell cultures of a synthetic BRC4 peptide, which reproduced the expected outcomes of HR pathway inhibition, such as the reduction of RAD51 nuclear foci following DNA damage and the increased response to chemotherapeutic agents. A subsequent proteomic study in BRC4-exposed cultures led to identify a statistically significant downregulation of three proteins (FANCI, FANCD2, RPA3) involved in the DNA damage response.

The second section of the thesis is focused on the biological characterization of compound **46**, a RAD51/BRCA2 inhibitor identified by IIT colleagues. **46** was studied on both 2D and 3D pancreatic cancer models in combination with the PARPi talazoparib. Taken together, the obtained results suggested that the talazoparib-46 combination is a potential inducer of SL.

KEYWORDS

Synthetic lethality; anticancer drug discovery; pancreatic cancer; homologous recombination; DNA repair; PARP inhibition; BRCA2; RAD51; BRC4; chemo/radiosensitizer; small molecule inhibitor; organoids.

ABBREVIATIONS

^{19}F NMR: ^{19}Fluorine Nuclear Magnetic Resonance

AKT: ak strain transforming kinase (protein kinase B)

APTX: aprataxin

ARID1A: AT-rich interactive domain-containing protein 1A

ATM: ataxia-telangiectasia mutated protein

ATR: ataxia-telangiectasia and Rad3-related protein

ATRIP: ATR-interacting protein

BARD1: BRCA1 associated RING domain 1

BCL-2: B-cell lymphoma protein 2

BER: base excision repair

BRCA1-2: breast cancer susceptibility proteins 1 and 2

CHK1-2: checkpoint kinases 1 and 2

CKS1B: Cyclin-dependent kinases regulatory subunit 1B

C-MYC: cellular myelocytomatosis oncogene encoded protein

CSL: conditional synthetic lethality

CtIP: CtBP (carboxy-terminal binding protein) interacting protein

DBS: DNA double strand breaks

DDR: DNA damage repair

D-loop: displacement loop

DNA-PK: DNA-dependent protein kinase

ds: double-strand

DSBR: double-strand break repair

EPT: exocrine pancreatic tumour

ExoI: exonuclease 1

FA: Fanconi Anemia

FDA: food and drugs administration

FOLFIRINOX: folinic acid, *5*-fluroruracil, irinotecan, and oxaliplatin

H2AX: histone family member X

HER2: human epidermal growth factor receptor 2

HR: homologous recombination

KRAS: Kirsten rat sarcoma virus protein

LIG3: DNA ligase IIIα

MAD2: mitotic arrest deficient 2-protein

MMR: mismatch repair

mo: months

MRE11: double-strand break repair meiotic recombination protein

NBS1: Nijmegen breakage syndrome protein 1

NCSL: non-conditional synthetic lethality

NER: nucleotide excision repair

NET: neuroendocrine pancreatic tumour

NHEJ: non-homologous end joining

NSCLC: non–small-cell lung cancer

OS: overall survival

P53: tumour protein 53

PALB2: partner and localizer of BRCA2

PAR: poly-ADP-ribose

PARP: poly-ADP ribose polymerase

PARPi: PARP inhibitor

PDAC: pancreatic ductal adenocarcinoma

PI3K: phosphoinositide 3-kinase

PI5P4Ks: phosphatidylinositol-5-phosphate 4-kinases

PLK1: polo-like kinase 1

PNKP: polynucleotide kinase phosphatase

POL β: DNA polymerase β

POLδ: DNA polymerase δ

PP2A: protein phosphatase 2A

RAD51-54: radiation-sensitive proteins 50 and 51

RBBP8: retinoblastoma-binding protein 8

ROS: reactive oxygen species

RPA: replication protein A

SAR: structure–activity relationship

SCLC: small-cell lung cancer

SDSA: synthesis-dependent strand annealing

SL: synthetic lethality

SSB: single strand break

STAG2: stromal antigen 2

SWI/SNF: (switch/sucrose nonfermenting) chromatin remodeling complex

SWS1: Short-wavelength sensitive opsin

SWSAP1: SWIM-type zinc finger 7 associated protein 1

TLZ: talazoparib

WHO: World Health Organization

XRCC1-3: X-ray repair cross-complementing proteins 1-3

γH2AX: phosphorylated H2AX

[This page is intentionally left blank]

1. INTRODUCTION

1.1 Cancer overview

In the mid-19th century, the pathologist Rudolf Virchow postulated that “the body is a cell state in which every cell is a citizen. Disease is merely the conflict of the citizens of the state brought about by the action of external forces.” [1] His "cellular theory" proposed that all diseases, including cancer, originated from alterations within cells. To date, according to the World Health Organization (WHO), cancer is referred to as a class of diseases in which a mass of aberrant cells divides without control and possibly invades nearby tissues following different progression stages, which are peculiar for each tumour type (Fig. 1).[2–4] It is noteworthy that the term "cancer" originates from the Latin word for crab, which was associated with the description of a malignancy; as a crab grasps with its claws, a malignant tumour holds on the invaded tissues.

Cancer represents the second leading cause of death worldwide, behind cardiovascular disease. In 2020, an approximate total of 19.3 million new cancer cases were estimated globally, and they are expected to rise by 47 % in twenty years.[5] To date, lung cancer is the leading cause of cancer death among both men and women, followed by liver and stomach; breast cancer is the second leading cause of cancer cell death in women.[6,7] Although continuous research efforts have notably reduced mortality rates for several cancers like breast, prostate, and colorectal, advancements in the diagnosis and treatment are crucially needed for other types of cancers, such as pancreatic cancer, which is the third leading cause of cancer-related death in USA, Germany, Italy, Austria, Czechia, Finland, Hungary, Malta, Spain and Switzerland.[8,9]

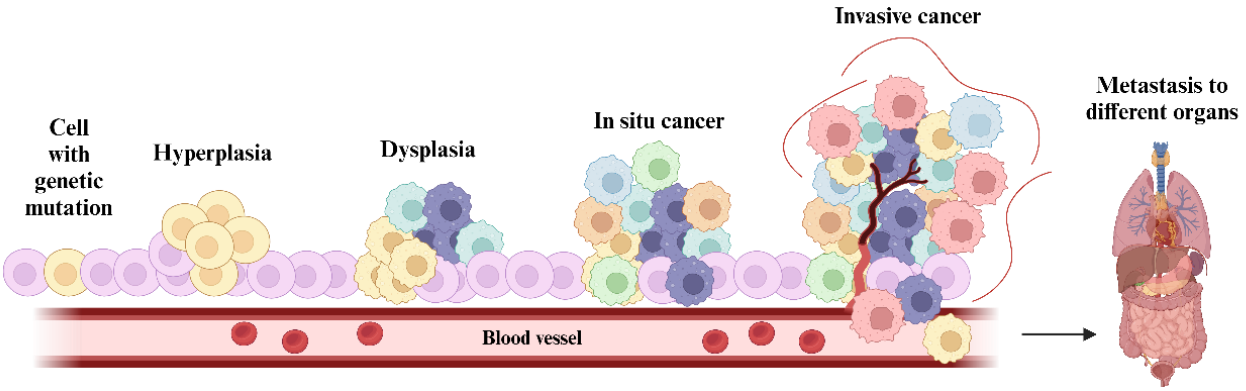

Figure 1. Exemplification of tumour development stages*. A cell carrying mutations divides fast leading to hyperplasia. The cell descendants divide excessively, accumulating different mutations and becoming abnormal (dysplasia). The mass of abnormal cells is defined as a tumour. If it is still contained within its original tissue, it is called in-situ cancer. Additional mutations may allow the tumour to spread into the blood or lymph nodes and establish new tumours (metastases) in different organs.*

1.1.1 Pancreatic cancer

Pancreatic cancer is a highly aggressive malignancy characterized by rapid progression, fatal outcome, and reduced therapy effectiveness. It is the 7th leading cause of cancer-related death worldwide, characterized by a low 5-year survival rate of 9%.[10,11] In 2020, approximately 500,000 new cases of pancreatic cancer were documented globally. The global rate incidence calculated in 2020 was 4.9 *per* 100000 and is predicted to increase globally to 18.6 *per* 100000 in 2050.[9,12,13] Its extreme malignancy is due to the lack of early symptoms and a consequent rapid tumour progression from stage 0 (carcinoma in situ, resectable) to stage IV (advanced or metastatic cancer) (Fig. 2);[11,14] moreover, 50% of patients are found to develop metastasis by the time of diagnosis, and 75% die within a year from the diagnosis.[10,15]

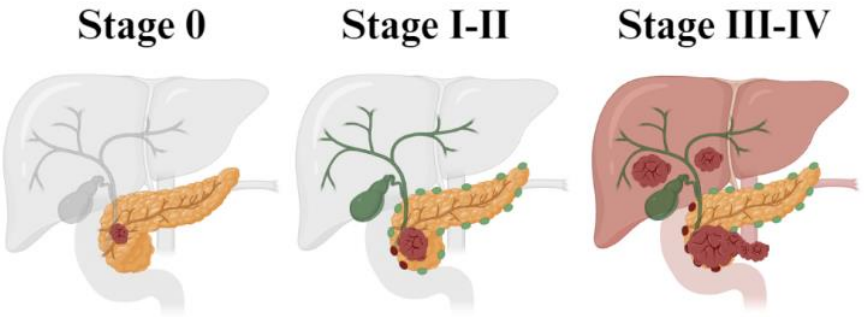

Figure 2. *Pancreatic cancer stages. Stage 0: no spread. Pancreatic cancer is limited to the top layers of cells in the ducts of the pancreas. Stage I-II: the tumour has spread to nearby lymph nodes. Stage III-VI: the tumour has spread to nearby organs.*

The poor prognosis and lack of effective treatments urge for increased research efforts in developing new treatment regimens, making pancreatic cancer an important oncological need.

Pancreatic cancer is divided into two categories: neuroendocrine pancreatic tumour (NET) which is the rarest form (less than 5% of all pancreatic cancer cases) and onsets from the endocrine tissue of the pancreas made by small cell clusters called islets (or islets of Langerhans); exocrine pancreatic tumour (EPT), which includes more than 95% of all pancreatic cancers and develops from the exocrine gland and pancreatic ducts.[11]

EPTs are subdivided into four different subtypes, which are listed below. (Fig. 3)

1. **Ductal adenocarcinoma**: it occurs in the lining of pancreatic ducts and accounts for more than 90 % of diagnosed pancreatic cancers.[16]
2. **Squamous carcinoma**: it is an extremely rare EPT form (0.5 – 2 %), with only a few documented case reports and no available standard treatments or guidelines.[17]

3. **Adenosquamous carcinoma**: its estimated incidence is between 0.38 and 10 % of all EPTs. Regarding the histological pattern, it shows both ductal adenocarcinoma and squamous carcinoma features.[18]

4. **Colloid carcinoma**: it is a histological variant of ductal adenocarcinoma, characterized by abundant stromal mucin and floating malignant cells that reach 50% of the tumour volume. It accounts for only 1–3% of EPT forms.[19]

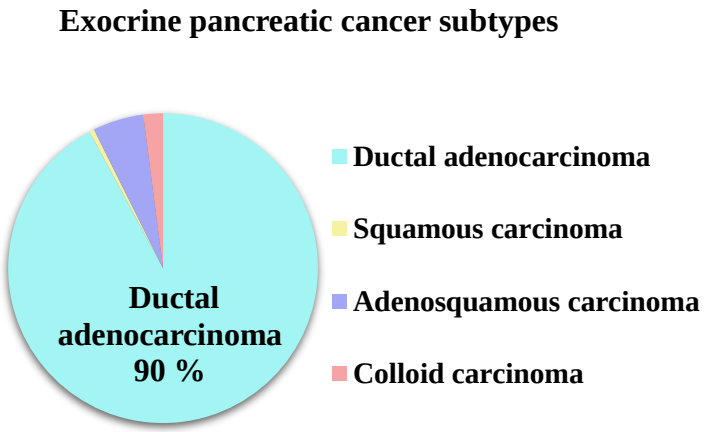

Figure 3. *Representative scheme of EPTs subtypes. Pancreatic ductal adenocarcinoma represents the major EPT subtype.*

1.1.2 Pancreatic ductal adenocarcinoma

The present thesis study is focused on pancreatic ductal adenocarcinoma (PDAC). It represents more than 90 % of all pancreatic cancers and has a 5-year overall survival of about 10%.[16,20] Risk factors for PDAC are pancreatitis, which is a local inflammation in the pancreas; systemic inflammation caused by metabolic disorders such as obesity and type II diabetes mellitus; smoking; excessive alcohol consumption; and inherited cancer predisposition.[21,22] The only curative treatment is surgery resection followed by adjuvant chemotherapy, but only 10-20 % of patients exhibit the main criteria for resectable PDAC tumours, such as position (head or uncinate process), no arterial and venous proximity, no other organ involvement and absence of metastases.[23–25] Therefore, chemotherapy becomes the first-line treatment for locally advanced and metastatic pancreatic cancer (Table 1). The currently available treatment is based on gemcitabine plus nab-paclitaxel and/or FOLFIRINOX (FOLinic acid, 5-Fluroruracil, IRINotecan, and Oxaliplatin), which has been approved by the Food and Drugs Administration (FDA). [26–31]

Type of treatment	Type of PDAC	Approval by FDA	Clinical endpoint	Ref
Single-agent Gemcitabine	Locally advanced/metastatic	1996	median survival of ≈ 6 mo	32
Gemcitabine + Erlotinib vs Gemcitabine	Locally advanced/unresectable/ metastatic	2005	improved OS by 10 days	33
FOLFIRINOX vs Gemcitabine	Metastatic	2011	Improved OS by 11 mo	34
Gemcitabine + nab-paclitaxel vs Gemcitabine	Metastatic	2013	Improved OS by 8.5 mo	35
Gemcitabine + Capacitabine vs Gemcitabine	Resectable	2022	Improved OS by 28 mo	36,37

Table 1. Landmark FDA-approved treatment for pancreatic ductal adenocarcinoma*. (OS) = overall survival (PDAC) = pancreatic adenocarcinoma. (mo) = months.*

Currently, the development of acquired chemoresistance appears as one of the most impactful obstacles in decreasing PDAC patients' survival. The main reasons affecting therapy efficacy are metabolic alterations which increase the availability of metabolic substrates allowing a fast energy supply for PDAC growth;[38] aberrant expressions of genes associated with cellular survival and apoptosis resistance (e.g. the phosphoinositide 3-kinase-PI3K, the B-cell lymphoma 2-BCL-2);[39] alterations in drug efflux pumps;[40] overexpression of enzymes implicated in cellular drug metabolism (e.g. aldehyde dehydrogenases);[41] overexpression of the ABC transporter genes, whose function is to extrude drugs out of the cell.[42] Therefore, the availability of effective treatment regimens for PDAC still remains an important need in oncological medicine.

1.2 The concept of synthetic lethality

Synthetic lethality (SL) was first described in the early 20th century by Calvin Bridges, an American geneticist.[43] He was studying the fruit fly *Drosophila melanogaster* model and identified gene mutations compatible with cell viability when presented separately, but resulting in cell death when appearing together in the same cell. Twenty years later, the same phenomenon was observed and cited by Theodore Dobzhansky in a different fruit fly model (*Drosophila pseudoobscura*).[44] Then, several studies conducted also in *Saccharomyces cerevisiae* reported the finding of several synthetic lethal partners of cell-division-cycle genes (CDC45 and CDC54) mutated.[45]

The original concept of SL is based on the assumption that the simultaneous perturbation, in terms of mutation, overexpression, or gene inhibition of two genes is lethal, whereas the impairment of either gene alone is consistent with cell viability.[46] (Fig. 4)

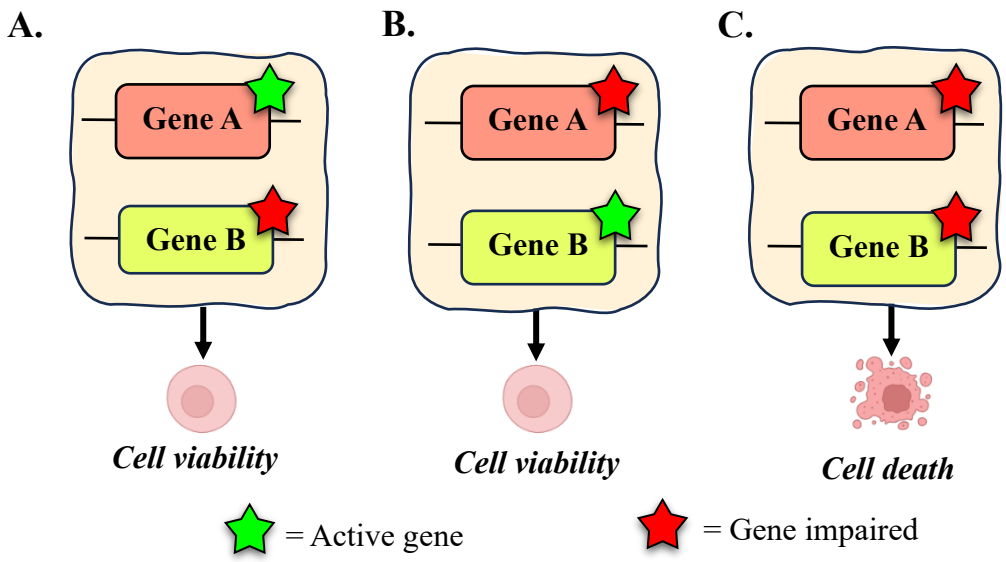

Figure 4. Schematic representation of synthetic lethality concept*. Two genes are synthetic lethal when their simultaneous impairment results in cell death.* ***A.B****. Alteration of either gene A or gene B does not affect viability.* ***C****. Inactivation of both at the same time is lethal.*

SL is now emerging as an important cancer therapeutic paradigm, able to exploit genetic vulnerabilities in tumoral cells while sparing normal cells, thus overcoming the limitations of conventional chemotherapy. It can be used to selectively kill cancer cells by identifying the cancer-associated molecular changes that are absent in healthy cells, specifically targeting their synthetic lethal partners.

Several studies have expanded the concept of SL, defining different sub-classifications that increase its complexity, aiming to provide a more comprehensive knowledge of SL.[47–50]

In this paragraph two SL subtypes are briefly discussed: conditional synthetic lethality (CSL) and non-conditional synthetic lethality (NCSL), which are described below and reported schematically in Fig. 5.[51]

1. *Conditional synthetic lethality* (CSL) refers to the variation in synthetic lethal outcomes observed in different tumoral cells of the same cancer type. The main reason is due to internal or external factors, such as hypoxia, levels of reactive oxygen species (ROS), and the use of drugs or radiation, that lead to tumoral cell heterogeneity, resulting in condition-dependent genetic interactions.[52,53] An example is reported in a glioblastoma model. Treatment of glioblastoma cell lines characterized by a mutation in the STAG2 (stromal antigen 2) gene with PARP (poly adenosine diphosphate [ADP] – ribose) polymerase inhibitors resulted in synthetic lethality only after chemotherapy with the DNA-damaging agent temozolomide.[54]

2. *Non-conditional synthetic lethality* (NCSL) could be further divided into synthetic dosage lethality (SDL) and classic synthetic lethality (CSL);

- SDL is based on the evidence that cancer cells often exhibit oncogene overexpression, which can be due to multiple genetic events, such as somatic copy number alterations, or epigenetic changes that increase gene transcription.[45,55] Identifying and inhibiting synthetic lethal partners of the overexpressed oncogenes can result in cancer cell death. Recent SDL studies in the yeast *Saccharomyces cerevisiae*, by using homologs of genes commonly overexpressed in cancers, have highlighted SDL partners, which are conserved in human cancer cells. The first reported is mitotic arrest deficient 2 (MAD2), which is a protein involved in the mitotic spindle checkpoint. It is described as overexpressed in several tumoral types (malignant lymphoma, liver and lung cancer, and colorectal carcinoma) and exhibited SDL in combination with the knockdown or the inhibition of protein phosphatase 2A (PP2A), a protein that regulates by dephosphorylation the function of many critical cellular molecules such as protein kinase B (AKT), tumour protein (P53), cellular myelocytomatosis oncogene (C-MYC).[56–58] Several studies identified as an oncogene commonly overexpressed in lung, breast, and liver cancers, the Cyclin-dependent kinases regulatory subunit 1 (CKS1B), which binds the catalytic subunit of cyclin-dependent protein kinases. Its SDL-reported partner is polo-like kinase 1 (PLK1), which is a protein involved in the M phase of the cell cycle.[59–61] Additionally, it is well documented that a large number of tumours are characterized by Kirsten rat sarcoma virus (KRAS) or MYC oncogene activation, which are still considered undruggable

targets. The identification and inhibition of synthetic lethal targets of KRAS/MYC could have a corresponding anti-cancer therapeutic effect.[62,63]

- CSL occurs when a loss of function mutation of a single gene sensitizes tumoral cells to the inhibition of a different gene involved in a complementary pathway.[64] Several examples of CSL are reported. TP53 mutated breast cancer cells rely on phosphatidylinositol-5-phosphate 4-kinases (PI5P4Ks) for their growth; its inhibition could be a highly effective treatment option for TP53 deficient cancers.[65] Furthermore, defects in AT-rich interactive domain 1A (ARID1A), which is a component of the SWItch/Sucrose Non-Fermentable (SWI/SNF) chromatin remodelling complex, sensitize tumoral cells to inhibitors of ATR (Ataxia-Telangiectasia and Rad3-related) protein kinase, which is a critical component of the DNA damage repair (DDR) cellular pathway.[66] It is well known that, compared to healthy cells, neoplastic cells are characterized by a high genetic instability, which is commonly caused by impaired DDR pathways. The direct consequence is that cancer cells become vulnerable to DNA damage and addicted to the conserved repair pathways' activity. A landmark achievement in the application of CSL in the therapeutic field is the administration of PARP inhibitor (PARPi) to breast cancer patients carrying mutations in the breast cancer susceptibility genes 1 and 2 (BRCA1 and BRCA2).[67,68] It represents one of the most effective cancer therapies in the last decade. The reason is that patient cancer cells become unable to set efficient DNA repair due to the simultaneous inhibition of two different DNA repair pathways. BRCA1/2 genes are essential components of homologous recombination (HR) repair, a pathway involved in repairing the DNA double-strand breaks (DBSs), while PARP is involved in the single strand breaks (SSBs) repair pathway. The inhibition of PARP in BRCA1/2 mutated cells results in catastrophic DSBs during replication and, ultimately, in cell death.[69]

Overall, NCSL and CSL provide important advice for revealing cancer-specific susceptibilities and identifying cancer-specific treatments.

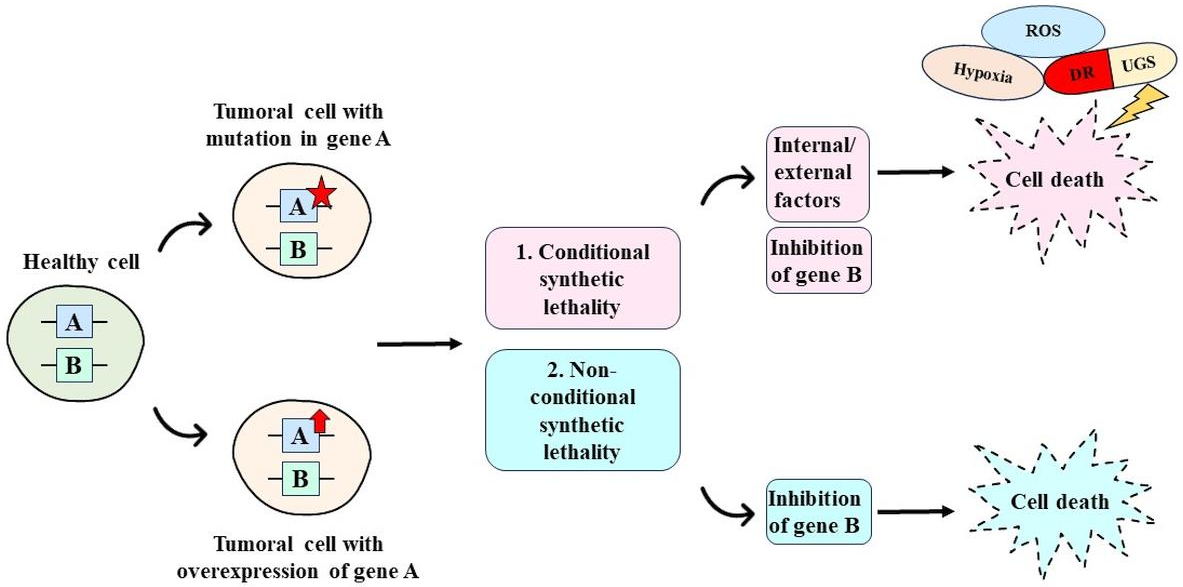

Figure 5. *Exemplification of synthetic lethality. SL is divided into conditional synthetic lethality and nonconditional synthetic lethality.* ***1. Conditional synthetic lethality.*** *Synthetic lethal interactions may be reliant on specific internal factors, such as hypoxia, high ROS, or external factors, such as drugs/radiation. Without these conditions, inhibition of gene B in cells with a mutation/ overexpression in gene A is consistent with cell viability.* ***2. Non-conditional synthetic lethality.*** *Mutation/overexpression of gene A alone is viable in tumoral cells. Inhibition of gene B in cells results in cell death.*

1.3 Overview of the DNA damage response

The maintenance of genomic integrity is a process crucial for the sustenance of cellular functions. Alterations of the genetic sequence are a hallmark of genome instability, which can ultimately results in the development of several diseases, including cancer.[70] Several endogenous and exogenous DNA damaging factors, such as ROS, ultraviolet (UV) light, and chemotherapeutic agents, can lead to different types of DNA injuries; it has been reported that human cells are characterized by 10^4-10^5 DNA lesions per day.[71] Each of them prompts the DDR that provides the activation of different DNA repair pathways as well as cell cycle checkpoints, DNA damage tolerance, and, eventually, the induction of cell death.[72]

Six major DNA repair pathways are used to identify and remove the different incurred damages, depending on both the damage type and the phase of the cell cycle during which they occur. (Fig.6) The Nucleotide Excision Repair (NER) identifies and corrects bulky DNA lesions caused by ultraviolet (UV) radiation, intrastrand crosslinks induced by drugs, and cyclopurines generated by reactive oxygen species (ROS), acting as a "cut-and-paste" like mechanism.[73] Hereditary

deficiencies in the NER pathway commonly lead to sensitivity to UV, manifesting as Xeroderma Pigmentosum disease, and increased cancer incidence at a young age.[74,75]

The Base Excision Repair (BER) pathway corrects base alterations such as deamination, oxidation, and alkylation.[76,77] It is also involved in the repair of SSBs, which are discontinuities in one strand of the DNA double helix originating during programmed DNA metabolic events or induced by ROS or alkylating agents.[78] These abnormalities represent one of the most common DNA damage types.[79] Defects in the BER pathway lead to genomic instability and cellular transformation, which progressively result in cancer onset.[80]

The Mismatch Repair (MMR) pathway is activated following base-base mismatches and insertion/deletion mis-pairs within the duplex DNA, which can occur during DNA replication. Inactivation of MMR results in the accumulation of errors in the DNA sequence, leading to the so-called microsatellite instability, which characterizes specific types of tumours, such as colorectal cancer.[81,82]

The Fanconi Anemia (FA) pathway is involved in the recognition and repair of interstrand crosslinks, lesions that are caused by endogenous metabolites or drugs, such as aldehydes and mitomycin C, respectively. In these lesions, the complementary DNA strands are linked through a covalent bond, which prevents transcription and replication.[83] Moreover, the FA pathway interplays with other DNA repair processes, such as the HR pathway described below.[84] Mutations in the FA genes cause the FA autosomal recessive disorder, which culminates in cancer onset.[85]

The most deleterious type of DNA injury is the DSB, which occurs when the two complementary strands of the DNA helix are broken simultaneously. It is reported that a single unrepaired DSB can result in aneuploidy, genetic aberration, or cell death. The main causes of DSB are different exogenous or endogenous factors, such as ionizing radiation, chemical agents, or even natural impediments that cause a block in the progression of the replication fork.[86,87] The two main mechanisms involved in repairing DNA DSBs are non-homologous end joining (NHEJ) and HR.

NHEJ is the predominant pathway since it can occur through all cell cycle phases. It employs a variety of enzymes that modify DSB DNA ends until they are compatible for ligation, making itself a potentially error-prone repair pathway. [88] On the other hand, HR is a high fidelity pathway that occurs during the S/G2 phase since it involves the sister chromatid as a DNA donor to restore any lost information. [89]

Although every type of DNA damage is preferentially repaired by its corresponding specific mechanism, all the pathways are strictly connected and intertwined, leading to a complex and well-coordinated network able to sense and transmit the damage signals to effector proteins, maintaining genome integrity. Currently, the inhibition of specific DNA damage responses, together with the

induction of DNA damage by using chemotherapy and radiotherapy, is considered an effective strategy to kill cancer cells.

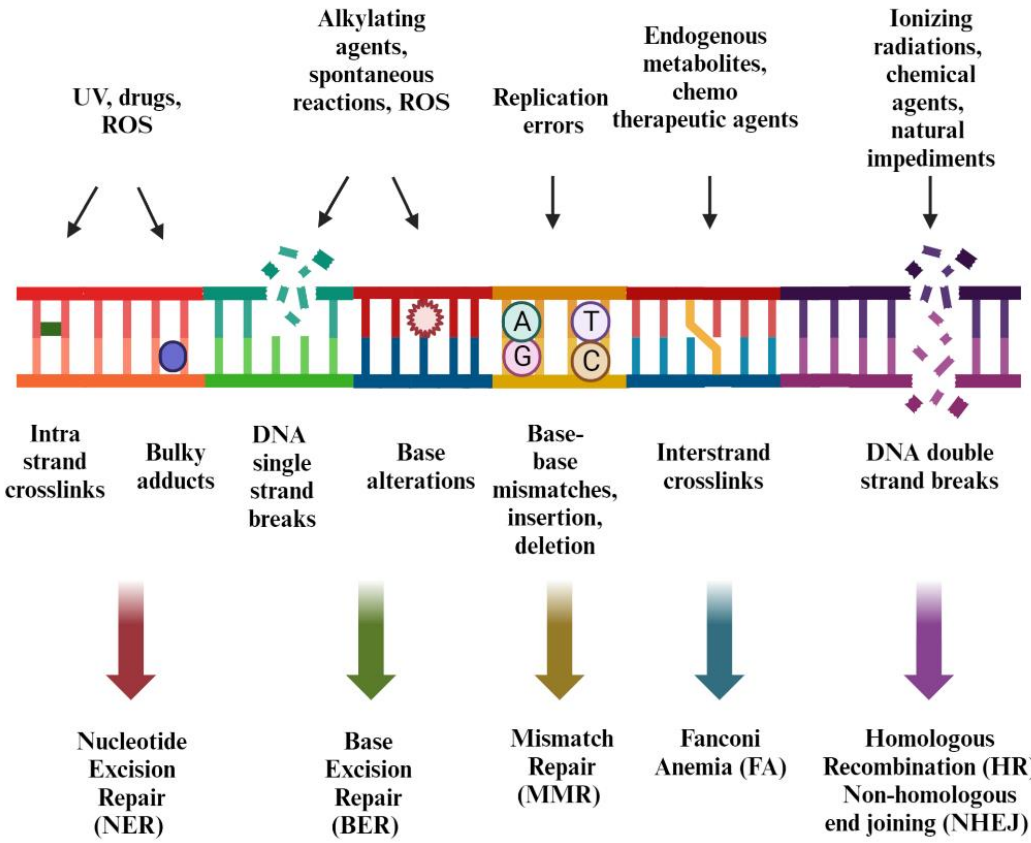

Figure 6. *Schematic representation of DNA damage repair mechanisms.*

1.3.1 DNA single-strand breaks and PARP-1

DNA SSBs represent the most common type of DNA damage, arising more than 10,000 times per mammalian cell each day.[90] Unrepaired SSBs during DNA replication can be converted to the more deleterious DNA DSBs through the collapse of the replication fork.[91] SSBs are discontinuities in one strand of the DNA double helix and can arise from oxidized nucleotides/bases during oxidative stress, intermediate products of DNA repair pathways, and abortive activity of topoisomerases during gene transcription.[92–95]

PARP are part of a group of 17 proteins crucial in various stages of cellular processes. These proteins are involved in stress response, chromatin modification, DNA repair, and in triggering cell death by inducing apoptosis.[96] Among the PARP proteins, PARP-1 plays a pivotal role in the BER

pathway, which is one of the major cellular mechanisms used to repair SSBs.[97] In detail, when a SSB occurs in the DNA, PARP-1 is recruited at the DNA damage site by using its amino-terminal DNA binding domain. Then, it acts as a damaged sensor and starts attaching adenosine diphosphate (ADP)-ribose units (derived from the ADP donor nicotinamide adenine dinucleotide-NAD^+) to itself and other target proteins through a process called poly-ADP-ribosylation (PARylation).[98] This post-translational modification serves as a signal for recruiting different proteins to the damaged site. These include XRCC1 (X-ray repair cross-complementing protein 1), which acts as a scaffold protein facilitating the coordination and recruitment of enzymes involved in the SSB repair, such as the end-processing enzymes polynucleotide kinase phosphatase (PNKP) and aprataxin (APTX), which then interact with DNA polymerase β (POLB) and DNA ligase III α (LIG3).[99,100] POLB replaces the missing nucleotides in the damaged DNA strand. Once the gap is repaired, LIG3 seals the nick in the DNA backbone, finalizing the repair process.[101–103]

1.3.2 PARP-1 inhibitors

Due to its critical role in DNA repair and its overexpression in several tumours, such as breast, uterine, ovarian, lung, and pancreatic cancers, PARP-1 has emerged as a druggable target for anticancer therapy in the past decade.[104,105] A PARPi directly targets the catalytically active site of PARP molecules, competing with NAD+ and halting the formation of the ADP-ribose extensions. PARP inhibitors are also able to trap PARP-1 at the level of the SSB, interfering with the whole repair mechanism.[106–108]

They have been strictly linked to the concept of SL, especially when administered in BRCA–mutated cancers, which are HR deficient and, therefore, rely on PARP-1 and BER for survival.[109–111] This combination marked a milestone for cancer therapy, representing the first personalized and targeted therapy specifically designed for addressing ovarian cancer and affirming the validation of the concept of SL in the development of oncological drugs.

To date, four PARPi have been approved by the FDA to treat different BRCA1/2 mutated tumours: olaparib (Lynparza), rucaparib (Rubraca), niraparib (Zejula) and talazoparib (Talzenna). (Fig. 7) A fifth PARPi, veliparib (ABT-888), is currently undergoing several clinical trials for breast and lung cancers; however, it is not yet approved for use in clinical practice.[112,113] Additionally, two other PARPi were approved in China: fuzuloparib (AiRuiYi) and pamiparib (PARTRUVIX™). The first has received approval to treat ovarian cancer; phase II and III trials are currently exploring its

potential for treating other solid cancers, such as those affecting the pancreas, breast, prostate, and lungs.[114] Pamiparib (PARTRUVIX™) was approved for the treatment of germline BRCA-mutated, recurrent and advanced ovarian, fallopian tube, or primary peritoneal cancers, which were previously subjected to two or more lines of chemotherapy.[115]

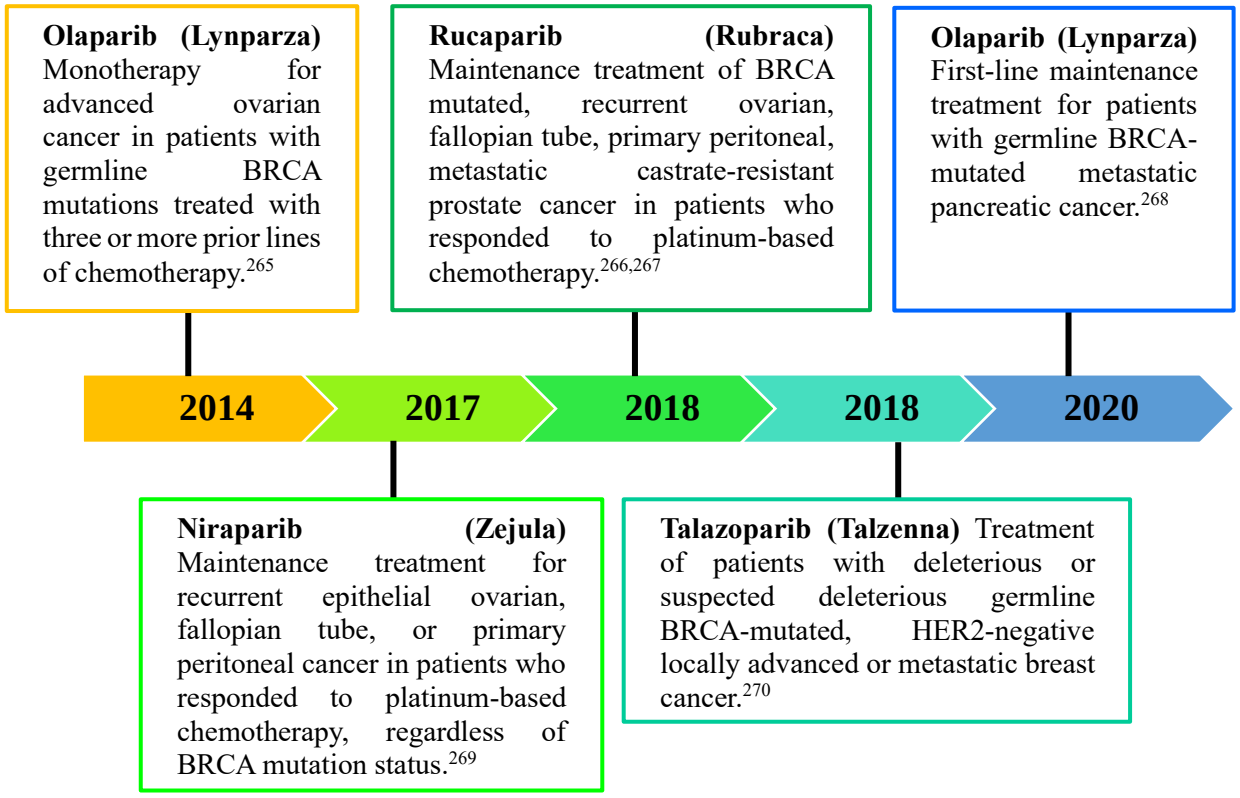

Figure 7. *Timeline FDA approval for PARPi.*

1.3.3 Talazoparib

In October 2018, the FDA approved the PARPi talazoparib (TLZ) to treat adult patients diagnosed with human epidermal growth factor receptor 2 (HER2)-negative, locally advanced, or metastatic breast cancer with suspected or confirmed deleterious germline BRCA mutations.[116] This decision was based on the results of the phase III EMBRACA trial.[117] The trial demonstrated that TLZ treatment, compared to single-agent chemotherapy not involving platinum (such as capecitabine, eribulin, gemcitabine, or vinorelbine), exhibited significant enhancements in progression-free

survival (median 8.6 vs. 5.6 months).[118] Cytotoxicity of PARPi is linked to their combined ability to inhibit the catalytic NAD+ domain and trap PARP-1 at the DNA damage site is the basis for PARPi cytotoxicity. TLZ was shown to be characterized by greater stereospecific PARP-DNA trapping ability, being 100-fold more potent than niraparib, which in turn shows higher effectiveness than rucaparib and olaparib.[119,120] Moreover, TLZ is active at lower concentrations compared to the other PARPi (PARP-1 IC_{50}= 0.57 nM vs Olaparib PARP-1 IC_{50}= 1 nM).[121]

TLZ is currently in early-phase clinical development, and studies are ongoing to analyse its effectiveness in different solid tumours, such as lung, ovarian, prostate, and pancreatic cancers.[122–124] To date, it is considered a promising inhibitor with potentially advantageous features in the PARPi drug class.

1.3.4 DNA double-strand breaks

A DNA DSB represents one of the most harmful types of DNA damage.[125] Programmed formation of DSBs happens during different cellular processes, such as meiosis I for ensuring normal chromosome segregation, formation of T-cell receptors, or class switching of immunoglobulins in B-lymphocytes.[126,127] However, there are several inadvertent causes of DSBs, which can be divided into:

- *Endogenous factors*. They include ROS generated during cellular metabolism or errors that can occur during normal cellular processes like DNA replication or recombination.[128,129]
- *Exogenous factors*. Examples are chemotherapeutic drugs, including DNA-alkylating agents such as cisplatin, methyl methanosulfonate and temozolomide, and ionizing radiation (X-rays or gamma rays).[130,131]

If DSBs are not properly repaired, the main consequence is the rise of genomic instability, which may contribute to several diseases such as cancer; furthermore, persistent unrepaired DSBs can trigger cell death pathways. Therefore, cells have evolved complex DNA repair mechanisms to address DSBs correctly; among these, HR is considered the most accurate.

1.3.5 Focus on homologous recombination

HR is a high-fidelity and error-free DNA double-strand break repair process (Fig. 8).[132] The DSBs recognition is achieved through different serine-threonine kinases that act as damage sensor-proteins, such as ataxia-telangiectasia mutated (ATM), Ataxia telangiectasia and Rad3-related protein (ATR), DNA-dependent protein kinase (DNA-PK).[133] To allow the DNA repair process, ATM phosphorylates different checkpoint proteins, such as P53, checkpoint kinase 1 (CHK1), and checkpoint kinase 2 (CHK2), which stop the progression of the cell cycle. Overall, ATM and the other damage sensor-proteins can phosphorylate about 900 factors; one of them is the H2A histone family member X (H2AX), referred to as γ-H2AX in its phosphorylated form, which generates focal points and co-localizes with other DNA damage repair-related proteins, such as those of the MRN complex.[134,135] This complex is composed of three proteins: the double-strand break repair meiotic recombination protein MRE11, the DNA repair protein RAD50, and the Nijmegen breakage syndrome 1 protein NBS1.[136]

NBS1 interacts with the other members of the MRN complex through its C-terminal domain and with γ-H2AX through its N-terminal domain, allowing the recruitment of the entire MRN complex into the nucleus at the DSB site.[137] DNA repair by HR can be conceptually divided into three steps: pre-synapsis, synapsis, and post-synapsis.

The pre-synapsis stage is aimed at performing the DNA-end resection needed for repair. The MRN complex, together with the DNA endonuclease RBBP8 (also called CtIP), operates a nucleotide cleavage necessary for creating the 3' tailed ssDNA overhang useful for DNA repair, after which exonuclease 1 (ExoI) or endonuclease DNA2 together with bloom syndrome helicase (BLM) promote extensive resection.[138,139,140]

At this stage, ATM promotes the coating of the generated ssDNA by the Replication Protein complex (RPA1, RPA2, RPA3); this step is essential to preserve the integrity of the ssDNA and to prevent the annealing with other homologous ssDNA.[141] Then, the ATR protein, along with its binding partner ATR-interacting protein (ATRIP), is recruited to the RPA-coated ssDNA to further promote the checkpoint signalling. It phosphorylates different substrates such as the partner and localizer of BRCA2 (PALB2), which, together with BRCA1-BARD1 (BRCA1 Associated RING Domain 1) proteins, recruits BRCA2 protein.[142,143] BRCA2 is critical for the recruitment of the Radiation Sensitive Protein 51 (RAD51) at the DNA damage site. In particular, BRCA2, together with its partner Exoribonuclease II, mitochondrial (DSS1), is able to displace RPA proteins, to promote RAD51 filament formation on the ssDNA, leading to RAD51 searching and invasion of

the homologous DNA sequence.[144] Different proteins support the elongation and stabilization of the RAD51 filaments: RAD51B, RAD51C, RAD51D, XRCC2 (X-Ray Repair Cross Complementing 2), XRCC3 (X-Ray Repair Cross Complementing 3), SWS1 (Short-wavelength sensitive opsin) and SWSAP1 (SWIM-Type Zinc Finger 7 Associated Protein 1), which form three functional complexes: the BCDX2 complex (RAD51B, RAD51C, RAD51D and XRCC2) the CX3 complex (RAD51C and XRCC3) and the Shu complex (SWS1 and SWSAP1).[145,144,146]

During the synapsis step, the BRCA1-BARD1-PALB2 complex assists the BRCA2-DSS1-RAD51 complex in the search for a double-stranded (ds) homologous template. The RAD51 nucleoprotein filament invades the homologous donor dsDNA, causing the formation of the so-called synaptic complex, consisting of three encased DNA strands. The 3′ end of the invading strand intertwined with its complementary donor DNA leads to the formation of a displacement loop (D-loop) intermediate.[147,148] RAD54 protein removes RAD51 from DNA, thus allowing polymerases δ (POLδ) to bind and use the annealed 3' overhang as a primer for DNA synthesis; furthermore, POLδ extends the D-loop and relaxes the DNA template.[149,150]

In the post-synapsis step, two different pathways are involved in resolving the D-loop: Synthesis-Dependent Strand Annealing (SDSA) and Double-Strand Break Repair (DSBR).

SDSA is the preferred pathway during mitosis.[151] It leads to the extension of the invaded strand and the creation of a newly synthesized DNA strand, which is subsequently disengaged from the DNA template and re-anneals with the original DNA strand, replacing the damaged or broken section. Importantly, SDSA does not involve a crossover, which is the exchange of DNA between the paired homologous DNA templates. Instead, it restores the original sequence while preserving the integrity of the flanking regions.[152,153]

DSBR is the most important pathway during meiosis.[154] It generates the so-called Holliday junctions, which form two homo-duplex/two hetero-duplex structures and result in the exchange of genetic material between the two DNA molecules.[155]

Since the complex interplay and coordination between RAD51 and BRCA2 is the core of HR pathway, it has garnered significant attention, also given its implications in several tumour types.

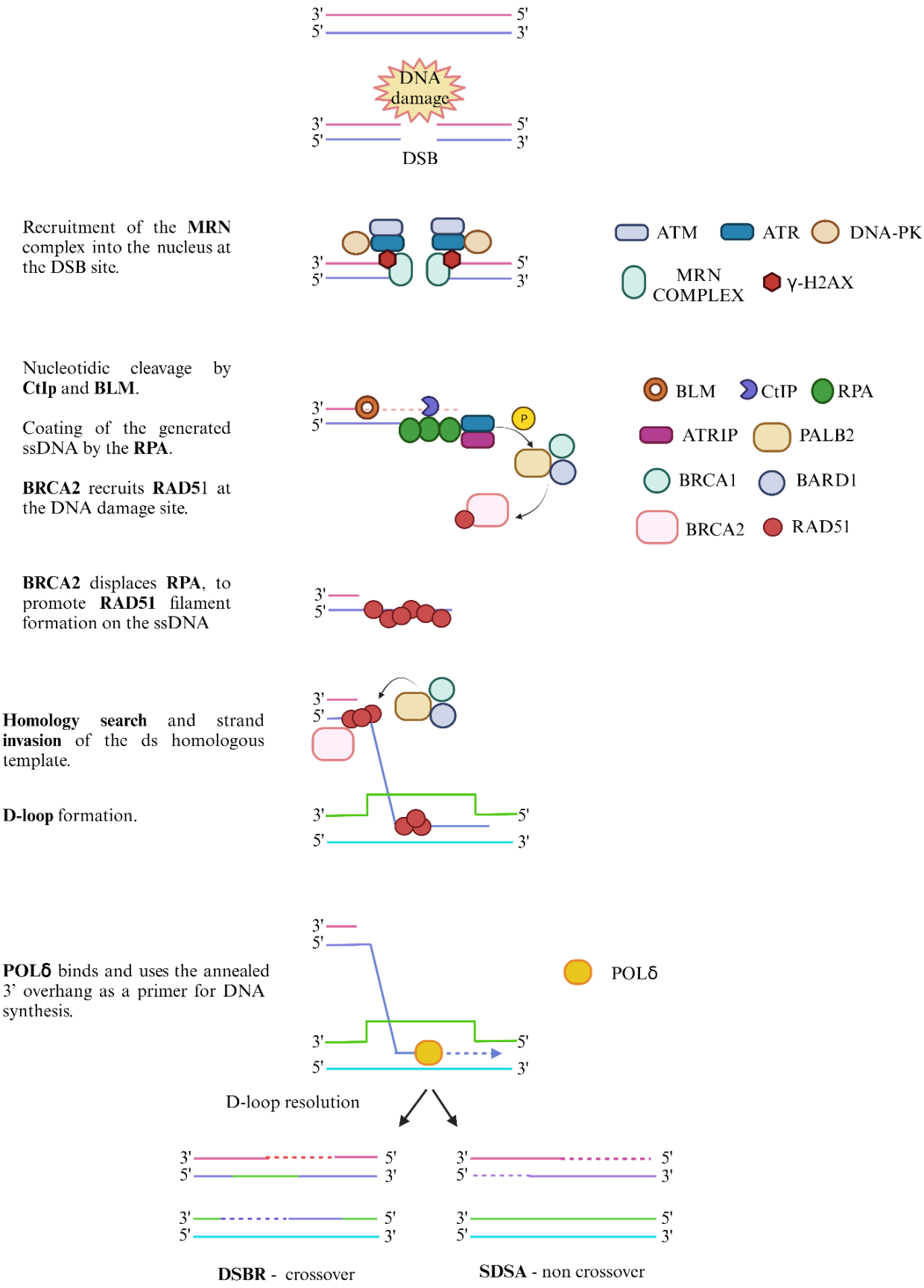

Figure 8. *Schematic representation of the HR pathway.*

1.3.6 RAD51 and BRCA2, the HR core proteins

RAD51 is an ATP-dependent recombinase of 339 amino acids, whose gene is localized on chromosome 15. It is mainly present in an equilibrium between monomers and homo-oligomers in the cytosol. Each RAD51 monomer consists of an N-terminal domain, which is joined to the C-terminal ATPase domain by a small helical linker.[156–158] The ATP-binding sites are critical for the protein's function in HR. ATP hydrolysis is involved in the dynamics of RAD51 filament assembly and disassembly.[159,160] Moreover, two flexible DNA binding loops (L1 and L2) are present within the ATPase domain (Fig.9).[161]

Since RAD51 lacks the nuclear localization sequence, it needs BRCA2 as a carrier for the transport into the nucleus at the site of DNA damage, where it forms nucleoprotein filament covering the 3' tailed ssDNA. Then, it promotes search and invasion of the homologous DNA sequence essential for the accurate repair of the DSB.[162,163]

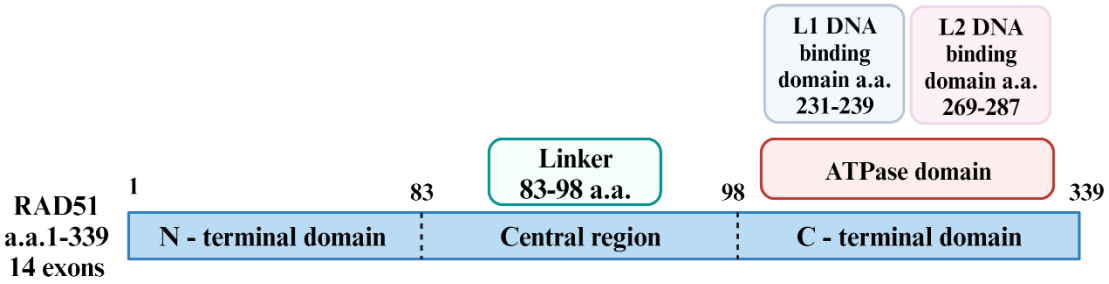

Figure 9. Schematic representation of RAD51 domains.

In several cancer forms (ovarian, lung, breast, pancreatic, and prostate tumours), different studies have correlated the overexpression of RAD51 protein with worse survival and prognosis, making this protein an attractive therapeutic target to investigate.[164–168]. In particular, Zhang et al. demonstrated that RAD51 promotes tumoral cell proliferation by enhancing aerobic glycolysis in pancreatic cancer.[169] R. Sarwar et al. showed a direct correlation between RAD51 increased expression and large tumour size, proximal lymph node, and distant metastases in several cases of thyroid carcinoma.[170] J. Hu et al. connected RAD51 overexpression with poor lung cancer patients' survival, demonstrating that depletion of RAD51 resulted in enhanced DNA double-strand breaks, defective colony formation, and increased cell death.[168] Overexpression of RAD51 is reported to be associated with enhanced resistance to DNA damage induced by chemical agents and/or ionizing radiation. Min-Shao Tsai et al. suggested that the suppression of RAD51 expression may be

considered as a potential therapeutic target to overcome the chemoresistance of gemcitabine in non–non-small-cell lung cancer (NSCLC).[171] Moreover, RAD51 protein level seems to be correlated also to increased resistance of Etoposide (VP16) in small cell lung cancer (SCLC), and reduced radiation- and chemo-sensitivity in osteosarcoma cells.[172,173]

BRCA2 is a tumour suppressor protein, whose gene is localized on chromosome 13. It is a large protein (3418 amino acids) characterized by an N-terminal domain that interacts with PALB2 and shows a DNA binding domain whose specific role is unknown;[174,175] a central region (exon 11) that is mainly involved in the direct interaction with RAD51 through eight well-conserved composed of 35-40 amino acids and called BRC repeats;[176] a C-terminal domain that can bind both ssDNA and dsDNA and also shows an additional RAD51 binding motif that stabilizes the RAD51 filament.[177,178] Moreover, the C-terminal domain contains three nuclear localization signals (NLS) that control BRCA2 localization (Fig.10).[179,180]

BRCA2 function in HR can promote both RAD51 defibrillation and defibrillation. In the cytoplasm, it induces RAD51 defibrillation to support its nuclear translocation; in the nucleus, the same function is implemented following the DNA repair.[181] On the contrary, RAD51 fibrillation is promoted at the DNA-damaged sites, thus favouring the formation of an active RAD51 nucleoprotein filament; furthermore, BRCA2 stabilizes the RAD51 fibrils and hides the protein nuclear export signal when RAD51 nuclear retention is necessary. [182–184]

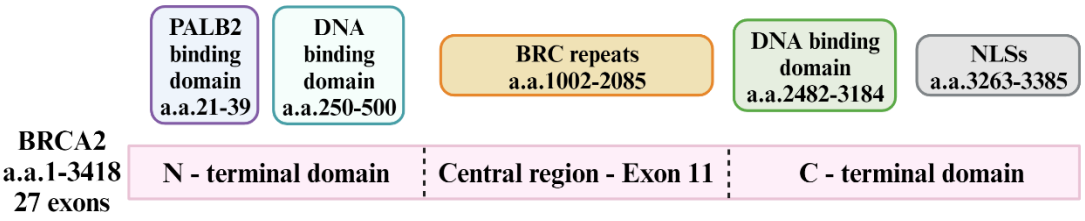

Figure 10. Schematic representation of BRCA2 domains.

Mutations of BRCA2 predispose to different types of cancer; in particular, they are directly associated with an increased possibility of developing early-onset breast cancer.[185] They have a role also in the onset and development of additional types of human malignancies, including prostate, colorectal, stomach, and pancreatic cancers.[186,187] To date, more than 1800 different mutations have been identified in the BRCA2 gene; the most common are shift or missense mutations, resulting in premature truncation or non-functional protein, and are prevalently sited in exon 11.[186,188,189] BRCA

mutations are considered markers indicating a deficiency in repairing double-strand breaks through the HR pathway and, therefore, predicting a favourable response to PARPi.[190,191]

Among the eight BRC repeats of the central region of BRCA2, BRC4 was shown to be the most efficient in binding RAD51 and, to date, the interaction between BRC4 and RAD51 is the only structurally elucidated.[192] Two BRC4 hydrophobic pockets are critical for its interaction with RAD51: the first one (1524-FxxA1527 sequence, zone-I) is located at its N-terminal and the second one (1545-LFDE-1548 sequence, zone-II) at the C-terminal.

The 1524-FxxA1527 mimics the oligomerization motifs of RAD51 monomer and is involved in the inhibition of RAD51 filament formation. [181,192] On the contrary, the 1545-LFDE-1548 sequence interacts with RAD51 with a binding that is not expected to perturb the RAD51 inter-protomer interface and was hypothesized to promote RAD51 filament formation, which, as stated above, is essential for its function in DNA repair. [193,194]

The BRC4 sequence is often used as a model to reproduce the BRCA2-RAD51 interaction, a key step in the HR pathway and a promising therapeutic target.

To date, different small molecules and peptides have been reported to disrupt the interaction between RAD51 and the BRC repeats, or between RAD51 multimers.[195–201] However, due to its promising relevance as an effective therapeutic approach, the exploration and development of new, more potent compounds are currently ongoing.

[This page is intentionally left blank]

2. AIM OF THE THESIS

My Ph.D. project is contextualized within the AIRC project "A chemical biology approach to synthetic lethality by means of DNA repair inhibitors," which originated from a collaboration between the Italian Institute of Technology of Genova (IIT) and the University of Bologna. It is based on the hypothesis that the disruption of the RAD51/BRCA2 protein interaction, which is crucial in the DNA double-strand breaks repair by HR, could trigger SL in combination with PARPi. In fact, according to the concept of SL, the simultaneous impairment of two different DNA repair mechanisms - DNA SSBs repair by PARPi and DNA DSBs repair by RAD51/BRCA2 inhibitors - is expected to cause cell death in cancer cells characterized by high genetic instability.

Importantly, patients with BRCA2-defective tumours exhibit increased sensibility to PARPi, such as olaparib, which has received FDA approval for treating BRCA-mutant tumours. Unfortunately, the applicability of these treatments is restricted to tumours that carry the desired mutation.

In this context, our research group recently proposed a new anticancer drug discovery concept, dubbed "fully small-molecule-induced synthetic lethality", that combines the administration of RAD51-BRCA2 disruptors with PARPi to BRCA2-wild type models of pancreatic cancer. The compounds' combination is supposed to mimic the increased sensitivity to PARPi observed in oncology patients with BRCA2 deficiencies, widening the population of patients eligible for treatment with PARPi.

The research field was restricted to pancreatic cancer and, in particular, to its most malignant subtype: pancreatic adenocarcinoma. It lacks markers of early detection and screening programs, and most efforts to improve the current therapy regimens fail in advanced clinical trials, leading to a low 5-year overall survival rate and making pancreatic adenocarcinoma an important oncological need.

The potential applicability of the "fully small-molecule-induced synthetic lethality" was previously validated by our group, providing the basis for identifying more powerful RAD51-BRCA2 inhibitors.[202–204]

The aim of my research project was to characterize the biological effects of novel RAD51-BRCA2 disruptors, active at low concentration and potentially able to trigger SL in combination with PARPi, in BRCA2 wild-type models of pancreatic adenocarcinoma. For this study, both 2D and 3D cell cultures were used. My work can be structured into two sections.

Section I was mainly devoted to elucidating the biological effects of RAD51/BRCA2 disruption in cultured cells; to this aim, we exposed cell cultures to a synthetic BRC4 peptide since, as

explained in the Introduction paragraph 1.3.6, the fourth BRC repeat of BRCA2 lacks the protein's nuclear localization sequence and is involved in the control of RAD51 fibril polymerization/de-polymerization.

Section II describes the effect of a novel RAD51/BRCA2 small molecule inhibitor, identified and synthesized by chemists colleagues from IIT and University of Bologna. Taking advantage of an in-house fluorinated fragment library, a ^{19}Fluorine Nuclear Magnetic Resonance (^{19}F NMR) screening on the oligomeric RAD51 protein was performed. The hits derived from the ^{19}F NMR screening were subjected to structure-activity relationship (SAR) studies generating two series of compounds. These studies allowed to identify a molecule (ARN24922, referred to as **46** in the published article and in the present thesis) which, in both 2D and 3D models of pancreatic cancer, showed the ability to reproduce the effects of RAD51/BRCA2 disruption and to trigger SL in combination with the PARPi talazoparib.

[This page is intentionally left blank]

3. SECTION I

The BRC4 peptide: a tool for studying the effects of RAD51/BRCA2 inhibition

3.1 Introduction

As explained in paragraph 1.3.6, RAD51/BRCA2 interaction is mediated by eight evolutionarily conserved motifs, called BRC repeats, each consisting of about 35 amino acids. They show a significantly different capacity to bind RAD51, with BRC4 exhibiting the highest affinity. Consequently, BRC4 appears to be the most suitable and specific tool for studying the molecular consequences of RAD51/BRCA2 disruption.

In preliminary evaluations, we observed that in its native form, BRC4 exhibited inefficient cytoplasmic penetration. To overcome this problem, we adopted a myristoylated form of this peptide, in which a reducible disulfide links a C-terminal BRC4 Cys to a myristoylated Cys-Lys(Myr)-Lys-Lys-Lys sequence, allowing both membrane permeation and intracellular release.

In my experiments, I analysed the BRC4 effects on HR pathway activity and on pancreatic cancer cell line viability. Finally, a proteomic analysis was applied to identify a proteomic fingerprint of HR impairment.

The obtained data can be useful in view of future investigation of novel RAD51-BRCA2 small molecule inhibitors.

3.2 Materials and methods

3.2.1 Cell cultures

Two PDAC lines, BxPC-3 and HPAC, were used for this study. Both cell lines express functional BRCA2.[205,206] They were grown in RPMI 1640 (Merck, Cat. #R0883) supplemented with 10% FBS, 100 U/mL penicillin/streptomycin, 2 mM glutamine. The two PDAC cell lines express a functional BRCA2 protein. The cell cultures were routinely tested for Mycoplasma contamination.

3.2.2 BRC4 Peptide

Native and myristoylated BRC4 (myrBRC4) peptides were purchased from Thermo-Fisher Scientific. The complete myrBRC4 sequence was as follows: KEPTLLGFHTASGKKVKIAKESLDKVKNLFDEKEQ[C][C][K(myristoyl]KKKNH2, (MW 4902.47 Da). A scrambled myrBRC4 peptide carrying a double mutation [F1524A, T1526A] was used in control, untreated samples.

3.2.3 Homologous Recombination Quick Assay (HR-QA)

HR was assessed by using a commercially available kit (Norgen, Cat. #35600). This assay is based on cell transfection with two plasmids able to recombine upon cell entry. The efficiency of HR was assessed by Real-Time PCR, using primer mixtures included in the assay kit. Different primer mixtures allow to differentiate between the original plasmid backbones and their recombination product. BxPC-3 cells (2×10^5 per well) were seeded in a 24-well plate and allowed to adhere overnight. Co-transfection with the two plasmids (1 µg each) was performed in Lipofectamine 2000 (Invitrogen, Cat. #11668019), according to the manufacturer's instructions. The transfection lasted 5 h, during which different doses of compounds, dissolved in culture medium supplemented with 0.6% DMSO, were administered to cells. After washing with PBS, cells were harvested, and DNA was isolated using QIAamp DNA Mini kit (Qiagen, Cat. #51304). Sample concentration was measured using an ONDA Nano Genius photometer. The efficiency of HR was assessed by Real-Time PCR, using 25 ng of template and primer mixtures included in the assay kit, following the protocol indicated by the manufacturer. Data analysis was based on the $2^{-\Delta\Delta Ct}$ method:

(Recombination Product/Backbone Plasmids) treated versus (Recombination Product/Backbone Plasmids) control.

3.2.4 Cell immunofluorescence assay

Immunofluorescence was used for studying RAD51 nuclear translocation. To visualize RAD51 in cell nuclei, BxPC-3 cells were seeded on glass coverslips placed in a 6-well culture plate (2×10^5 cells/well) and allowed to adhere overnight. Cultures were then preincubated with the desired compounds for 1 h and subsequently exposed to 50 μM cisplatin (CPL) (MedChemExpress, Cat. #HY-17394) or 200 nM doxorubicin (DOXO) (Selleckchem, Cat. # S1208) for an additional 1.5 h. Medium containing CPL or DOXO was removed, and cells were maintained in the presence of the desired compounds for 5 h. After this time, cultures were fixed in PBS containing 4% formalin for 15 min, permeabilized in 70% ethanol, air-dried, and washed twice with PBS. Samples were incubated in 5% bovine serum albumin (BSA) in PBS for 30 min and subsequently exposed to anti-RAD51 rabbit monoclonal antibody (1:1000 in 5% BSA/PBS, BioAcademia, Cat. #70-001) overnight at 4 °C. After washing, coverslips were incubated with a secondary anti-rabbit rhodamine-labelled (Novus Biologicals, Cat. #NB120-6792, 1:1000 in 5% BSA/PBS), for 30 min, washed, air-dried, and mounted with a solution 2 μg/mL DAPI in DABCO. Images were acquired using a Nikon fluorescent microscope equipped with filters for FITC, TRITC, and DAPI. The percentage of cells bearing RAD51 nuclear foci was estimated by two independent observers analysing approximately 200 cells for each treatment sample.

3.2.5 Cell viability assay

Cell viability was assessed with the CellTiter-Glo Luminescent Cell Viability Assay (Promega, Cat. #G7571). For this experiment, 2×10^4 cells were seeded using the complete medium in a 96-multiwell white plate and allowed to adhere overnight. The next day, the medium was replaced, and treatments were conducted entirely in the absence of serum. After a brief wash, cells were pre-incubated with 5 μM myrBRC4 for 1 h. CPL (50 and 100 μM) or DOXO (200 nM and 1 μM) was subsequently added to wells for 1.5 h. The medium was then removed to eliminate the chemotherapeutic agents, and cells were maintained in the presence of 5 μM myrBRC4 for an additional 48 h. After treatments, the multiwell plate was allowed to equilibrate at room temperature for 30 min, and the CellTiter-Glo reactive was directly added to each well. The plate was kept on a

shaker for 10 min to induce cell lysis, and its luminescence was measured following the manufacturer's instructions using a Fluoroskan Ascent FL reader (Labsystems).

3.2.6 Western Blot Analysis

BxPC-3 and HPAC cells were seeded in T25 flasks and allowed to adhere overnight. Cells were then treated with 5 μM myrBRC4 peptide; 24 h after the treatment, they were harvested and lysed in RIPA buffer containing protease (Roche, Cat. #04693124001) and phosphatase (Merck, Cat. #78420) inhibitors. The homogenates were left for 10 min on ice and then centrifuged for 20 min at 12000 rpm. 100 μg protein of the supernatants (measured according to Bradford) was loaded onto a 4–12% polyacrylamide gel for electrophoresis and run at 170 V. The separated proteins were blotted on a low fluorescent PVDF membrane (Amersham Hybord Cat. #GE10600060) using a standard apparatus for wet transfer with an electrical field of 70 mA for 16 h. The blotted membrane was blocked with 5% BSA in TBS-Tween and probed with the primary antibodies (Abcam). The antibodies were: rabbit anti-RPA3 (1:200 in BSA/TBS tween, Cat. #ab97436), rabbit anti-FANCI (1:1000 in BSA/TBS-Tween, Cat. #ab245219), rabbit anti-FANCD2 (1:5000 in BSA/TBS tween, Cat. #ab178705), and rabbit anti-Actin (Sigma-Aldrich, Cat. #A2066, 1:2000 in BSA/TBS-Tween). Binding was revealed by a Cy5-labelled secondary antibody (anti-rabbit-IgG, Jackson Immunoresearch, Cat. #111175144). The fluorescence of the blots was assayed with the Pharos FX Scanner (BioRad) at a resolution of 100 μm, using the Quantity One software (BioRad).

3.3 Results and Discussion

3.3.1 BRC4 peptide inhibits HR activity

The ability of the BRC4 peptide to inhibit the HR pathway was analysed by using BxPC-3 cells. The treatment was performed in the absence of serum to avoid interference with peptide activity due to degradation by proteases contained in the serum.[207]

As shown in Fig.11 A, the wild-type myrBRC4 peptide (red bars) showed a dose-dependent HR inhibition, reaching 85.1% at 30 μM, with an estimated $IC_{50} \approx 10$ μM. In its scrambled form (black bars), myrBRC4 was unable to impair HR at 5 μM, while, surprisingly, it led to HR inhibition at both 10 μM and 30 μM, although its effect was weaker than of BRC4 wild-type; these results suggest off-target effects probably caused by increasing dose of the peptide. Therefore, the 5 μM myrBRC4 dose was selected for the next experiments.

3.3.2 Evaluation of RAD51 nuclear foci as a marker for compromised HR

Further evidence of compromised HR was gathered by examining the RAD51 localization in BxPC-3 cell nuclei following DNA damage. To induce massive DNA damage, cells were treated with cisplatin (CPL) or doxorubicin (DOXO). In particular, DOXO represents the major anti-cancer treatment in clinical use. It hinders topoisomerase II, an enzyme involved in DNA regulation, which usually facilitates DNA unwinding during transcription. This interference prevents the proper rejoining of the DNA double-strand, ultimately halting the process of DNA replication.[208,209]

CPL is one of the most powerful chemotherapeutic drugs, especially administered in combination with other compounds. It is used to treat several cancers, including ovarian, breast, lung, and prostate tumours. It covalently binds to DNA bases, forming DNA adducts that inhibit transcription and DNA synthesis.[210,211] An immunofluorescence assay was performed to detect RAD51 nuclear foci. In detail, BxPC-3 cells were treated with 50 μM CPL or 200 nM DOXO for 1.5 hours, followed by 5 μM myrBRC4 treatment. As depicted in Fig. 11 B, the immunohistochemical assessment of RAD51 revealed remarkable nuclear foci in BxPC-3 cells treated with 50 μM CPL and 200 nM DOXO. However, this effect was significantly reduced when the drug was co-administered with 5 μM myrBRC4. Additionally, the percentage of RAD51-labeled nuclei in cultures exposed to 5 μM myrBRC4 alone mirrored that observed in cells treated with the combination of CPL or DOXO and

5 μM myrBRC4. Notably, the scrambled peptide in combination with CPL or DOXO did not significantly affect the RAD51 nuclear foci, supporting the expected mechanism of action of the 5 μM myrBRC4 peptide.

3.3.3 HR impairment increases the cytotoxic effects of anticancer drugs

As a following step, we studied whether the HR impairment and RAD51 nuclear foci reduction observed in myrBRC4 exposed cells result in increased toxicity of the two used chemotherapeutic agents. The effect of the combined administration of myrBRC4 with CPL or DOXO was then evaluated by using a cell viability assay (Fig. 11 C). BxPC-3 cells were treated with 5 μM wild-type myrBRC4 or scrambled myrBRC4 peptides for 48 hours. Cells were maintained in a medium without serum. The bar graph represented in Fig. 10 C shows a significant decrease in cell viability when BxPC-3 cells were treated with 5 μM myrBRC4 in combination with 50 and 100 μM CPL or 1 μM DOXO, compared to cells treated with CPL or DOXO alone.

These data suggest that myrBRC4 peptide is able to increase the cytotoxicity effects of the chemotherapy drugs, suggesting the impairment of DNA repair pathways concurrently with the induction of DNA damage as a promising anticancer strategy.

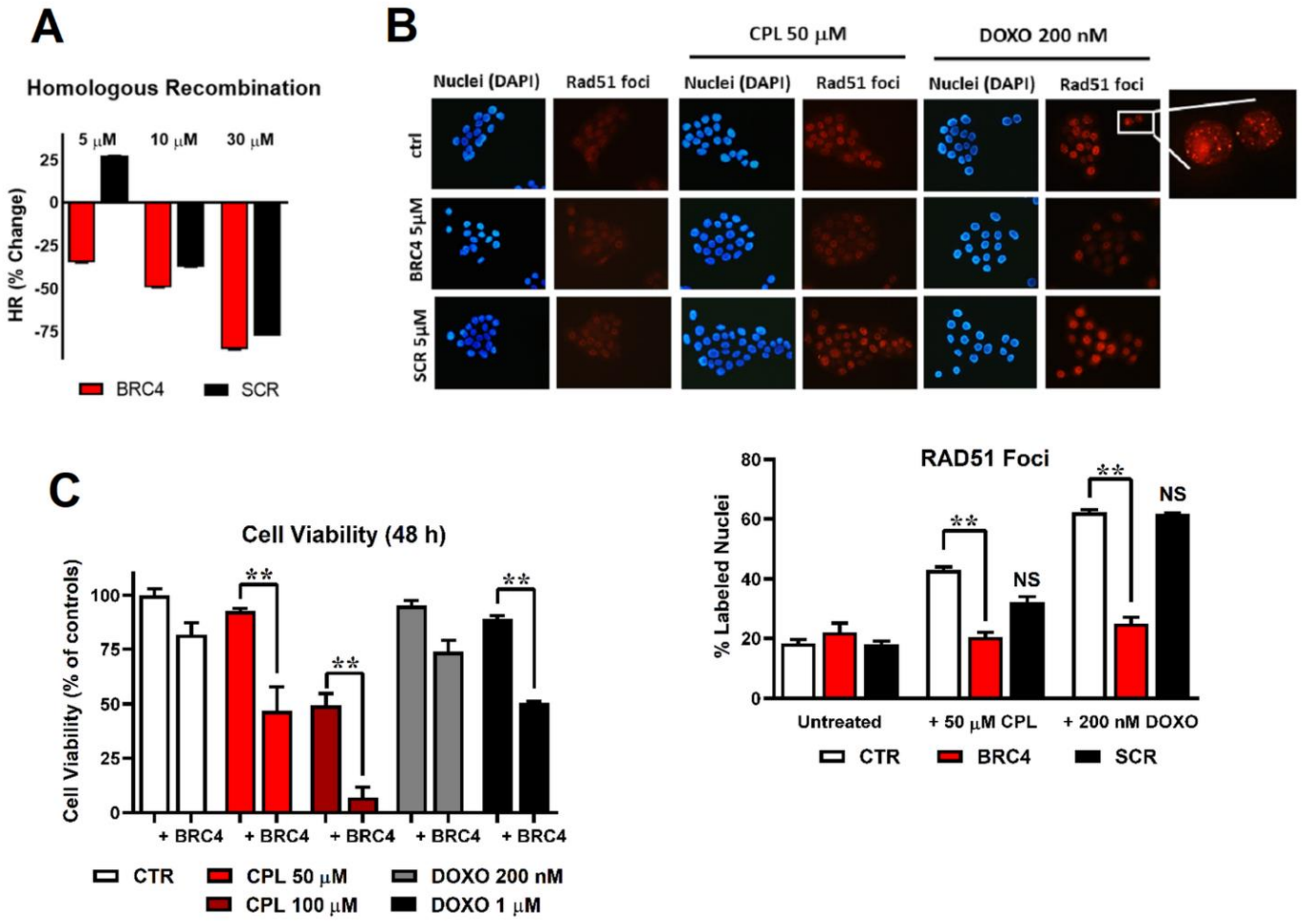

Figure 11. ***(A)*** *homologous recombination (HR) assay: evaluation of the percentage of HR inhibition at 5, 10, and 30 μM myrBRC4 peptide (red) or scrambled myrBRC4 peptide (black).*
(B) *Immunofluorescence detection of RAD51 foci in BxPC-3 cells nuclei. 50 μM CPL or 200 nM DOXO were administered alone or in combination with 5 μM myrBRC4 or scrambled myrBRC4 peptides to cells. Representative pictures showing DAPI-stained cell nuclei and the corresponding labelling of RAD51 nuclear localization. A higher magnification detail of the 200 nM DOXO-treated sample is included. The bar graph shows the percentage of RAD51-lableled nuclei obtained by analysing approximately 300 cells for each treatment. Data were statistically evaluated by applying the two-way ANOVA with multiple comparisons. A statistically significant difference was found between cells treated with myrBRC4 in combination with CPL or DOXO compared to cells treated with CPL or DOXO alone.*
(C) *Cell viability assessed in BxPC-3 cultures exposed to CPL (50 or 100 μM, 1.5 h) or doxorubicin (DOXO, 200 nM or 1 μM, 1.5 h) and treated for 48 h with 5 μM myrBRC4 or scrambled myrBRC4. Data were analysed by two-way ANOVA with multiple comparisons.** $p < 0.01$.*

3.3.4 Proteomic profile of BxPC-3 cells following myrBRC4 peptide treatment

BRC4 can be considered the most appropriate and precise tool for investigating the molecular outcomes resulting from RAD51/BRCA2 disruption. To deeply characterize the impact of the inhibition of RAD51/BRCA2 interaction also on cellular pathways different from HR, a mass spectrometry (MS) proteomic campaign was carried out in collaboration with Dr. Giorgio Oliviero from the University College of Dublin on BxPC-3 cells treated with 5 μM myrBRC4 for 24 hours. The proteomic data analysis was performed by Dr. Viola Previtali and Dr. Sam Myers (IIT) and is completely reported in the published article.

This study led to the identification of a total of 3595 proteins, which were filtered with specific criteria (p-value < 0.05 and $\log_2$ (fold change) > 1 or < − 1), resulting in the detection of 225 proteins displaying differential expression between myrBRC4-treated and untreated cells. Among these, 29 exhibited upregulation, while 196 showed downregulation. Following more stringent criteria (p-value < 0.01 or 0.001 as significant threshold, and $\log_2$ (fold change) > 2 or < − 2 as differential abundance threshold), 20 proteins were identified in the treated samples compared to untreated, as the top hits with significant up- or downregulation.

To enhance the identification of specific proteomic signatures following myrBRC4 peptide treatment, the proteins exhibiting upregulation and downregulation were cross-referenced with the RAD51 and BRCA2 interactomes obtained via the BioGRID tool (Biological General Repository for Interaction Datasets). Two proteins were found at the intersection of RAD51 and BRCA2 networks (FANCI: Fanconi anemia, complementation group I, and FANCD2: Fanconi anemia group D2 protein). Thus, attention was turned to FANCI and FANCD2 proteins, which appeared to be downregulated following myrBRC4 peptide treatment and are in common with BRCA2 and RAD51 interactomes. FANCI and FANCD2 belong to the FA family, which is constituted of 22 proteins.[212] FANCI and -D2 form the so-called ID complex that coordinates the ICL DNA damage repair and the response to replication stress, as well as the apoptosis signalling in case of a DNA damage repair failure.[213–215] Moreover, the ID complex plays a crucial role in stabilizing RAD51 filaments by directly engaging with RAD51, a pivotal step in the HR process.[216,217] It is also remarkable that the overexpression of both FANCI and FANCD2 proved to be markers of poor prognosis in a wide spectrum of cancers.[218–222] Among all the differentially expressed proteins, we also considered RPA3, which is in common only to the RAD51 interactome but showed downregulation with the highest observed statistical significance. Furthermore, this protein is functionally related to both

FANCI and FANCD2 (Fig. 12). RPA3 is one of the three subunits of the RPA complex, a nuclear factor binding to single-stranded DNA and involved in several DNA repair processes, including HR.[223] Elevated levels of all three RPA subunits denote increased resistance to radiotherapy and poorer prognoses among patients in different cancer types.[224]

To confirm the proteomic analysis, the level of FANCI, FANCD2, and RPA3 was assessed in myrBRC4 exposed cells by immunoblotting.

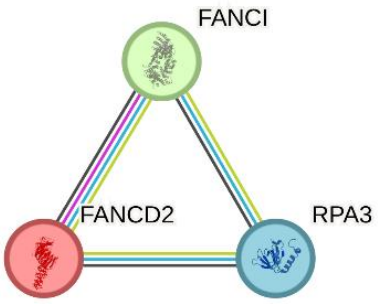

Figure 12. Functional interaction network among the proteins identified using the proteomic analysis*. The image was downloaded from http://string-db.org. The protein-protein interaction enrichment p-value is 0.000619; according to STRING database, this level of enrichment indicates that the proteins are at least partially biologically correlated, as a group.*

3.3.5 Validation of FANCI, FANCD2, and RPA3 protein downregulation in pancreatic cancer cells

To validate the downregulation of FANCI, FANCD2, and RPA3 proteins, a western blot analysis was performed on the same pancreatic cancer cell line (BxPC-3) used for the MS and proteomic analysis.

As for the proteomic analysis, cells were treated with 5 μM myrBRC4 peptide for 24 h in a serum-free medium.

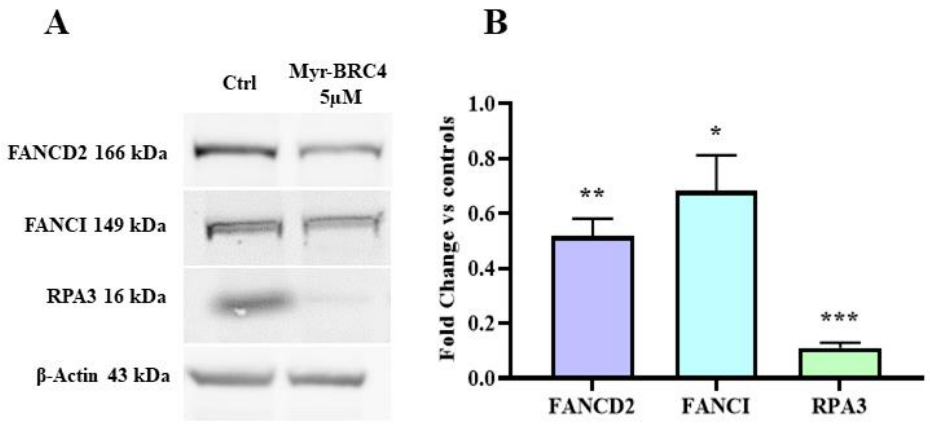

Figure 13. Immunoblotting evaluation of FANCD2, FANCI, and RPA3 proteins after a 24-hour treatment with 5 μM myrBRC4 peptide in BxPC-3 cell line. (A) *Immunoblotting images.* ***(B)*** *Protein level changes were assessed through bands densitometric reading. For each protein, the levels measured in myrBRC4 treated cells were compared to the corresponding values obtained in untreated cultures, and normalized on actin levels. *, **, *** correspond to $p < 0.05$, 0.01, and 0.001, respectively, as assessed by Tukey's Multiple Comparisons test.*

In BxPC-3 cells treated with the myrBRC4 peptide, a statistically significant decrease was observed for all three proteins compared to the untreated control cultures (Fig. 13). Specifically, a decrease of approximately 50%, 30%, and 90% was observed for FANCD2, FANCI, and RPA3, respectively, corroborating the proteomic analysis.

BxPC-3 cell line is a reliable model to study different aspects of pancreatic adenocarcinoma, since it is characterized by P53 mutation, as usually observed in the pancreatic tumours encountered in clinical practice.[225–229] However, a further validation of the proteomic analysis was carried out using a different pancreatic cancer cell line: HPAC. Compared to BxPC-3 cells, this cell line is characterized by the expression of wild-type TP53 and shows distinct proliferation timing.[206] Notably, TP53 and cell proliferation duration are critical factors influencing DNA damage repair and responses to anticancer treatments.

As illustrated in Figure 14, despite these distinctions, the results obtained in myrBRC4-exposed HPAC cells were at least in part aligned with the proteomic data obtained in BxPC-3 cells, showing a 20% and 30% decreased level for FANCI and RPA3, respectively. However, the FANCD2 protein resulted in an increase. This discrepancy can be explained by considering that FA proteins aren't consistently active but become activated during specific phases of the cell cycle. Consequently, the different cell proliferation timings might have influenced the response to a 24-hour RAD51/ BRCA2 inhibition induced by the myrBRC4 peptide.

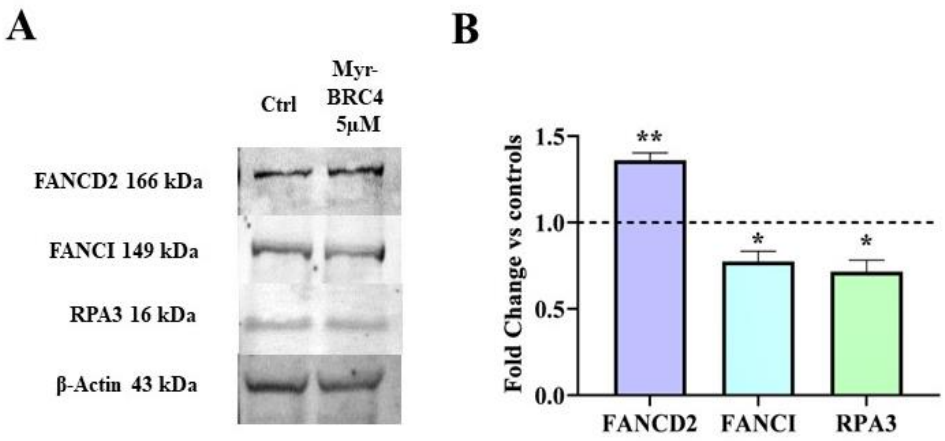

***Figure 14. Immunoblotting evaluation of FANCD2, FANCI and RPA3 proteins after a 24 h treatment with 5 µM myrBRC4 peptide in HPAC cell line**. **(A)** Immunoblotting images. **(B)** Protein level changes were assessed through bands densitometric reading. For each protein, the levels measured in myrBRC4 treated cells were compared to the corresponding values obtained in untreated cultures and normalized on actin levels. *, ** correspond to $p < 0.01$ and $p < 0.05$ respectively, as assessed by Tukey's Multiple Comparisons test.*

3.4 Conclusions - SECTION I

Among the eight BRC repeats localized in the central domain of BRCA2, the BRC4 repeat shows the highest affinity for RAD51.[192] Previous reports in the literature have shown that small synthetic peptides resembling the BRC4 repeat, as well as small organic molecules that mimic BRC4, can hinder RAD51-BRCA2 interaction.[203,230] To date, the BRC4 peptide has demonstrated a superior affinity compared to non-peptide compounds and is considered the most fitting tool to further explore the complexity of the HR pathway. In this context, it was selected to mimic the interaction between RAD51 and BRCA2 proteins to better characterize the outcomes of HR pathway inhibition, which could be significant in designing innovative anticancer treatments.

For the described experiments, the BRC4 peptide was derivatized with myristic acid since, as well known, myristoylation is a reversible modification that increases cell permeation and allows intracellular release.[231–233]

We demonstrated that the myrBRC4 peptide, in a low micromolar dose, interferes with the correct mechanism of HR DNA damage repair in BxPC-3 cells (Fig. 10 A). Confirmation of HR impairment by myrBRC4 was obtained by observing that the peptide treatment can prevent RAD51 nuclear foci after the DNA damage caused in BxPC-3 cultures by two widely used genotoxic chemotherapeutic agents (CPL and DOXO) (Fig. 10 B). The absence of RAD51 at the DNA injury

sites made BxPC-3 cancer cells unable to repair DNA damage, leading to an increased cell response to the two chemotherapeutic agents (Fig. 10 C). These data also suggested the myrBRC4 peptide as a promising and powerful tool for better characterising the outcomes of RAD51/BRCA2 inhibition.

For these reasons, a proteomic fingerprint of BxPC-3 pancreatic adenocarcinoma cells was obtained following treatment with myrBRC4. It showed that peptide treatment affected the level of several proteins involved in different molecular functions.

To be consistent with the Ph.D. project aim, the analysis was restricted to the proteins shared by the RAD51 and BRCA2 interactomes; the study resulted in the identification of FANCI and FANCD2 as downregulated proteins in common to both interactomes. A third protein (RPA3) was also considered for further studies due to its strong statistical significance and its interaction with FANCI and FANCD2 (Fig. 11). The downregulation evidenced by the proteomic analysis was validated in immunoblotting experiments performed in two different pancreatic cancer cell lines: BxPC-3 cells (Fig. 12) – the culture used for the MS and for the following proteomic analysis, and HPAC cells (Fig. 13) – a pancreatic cancer cell line, characterized by conserved TP53 function and a different proliferation rate compared to BxPC-3 cells. Among the three proteins, RPA3 displayed the most evident reduction, an outcome confirming the robust statistical evidence derived from the proteomic analysis. RPA3 is a nuclear protein binding to ssDNA, contributing not only to HR but also to various other DNA repair mechanisms. Interestingly, elevated RPA3 levels have been correlated with poorer prognoses in patients with different cancer types, particularly those displaying increased RAD51 nuclear foci post-irradiation. [234]

FANCI and FANCD2 are among the 22 FA-associated proteins involved also in the HR pathway, alongside the key proteins BRCA2 and RAD51. Notably, the FANCI-FANCD2 complex directly engages with RAD51 and is crucial for filament stabilization - a critical step in HR.[235] Overexpression of FANCI, FANCD2 is connected to poor prognosis.[218–222]

The results propose FANCI, FANCD2, and RPA3 as markers of HR inhibition and could serve as a reference point for exploring and characterizing different RAD51/BRCA2 small molecule disruptors' activity. Moreover, the induction of HR deficiency through the BRC4 peptide might be considered as a possible approach to broaden the use of PARP inhibitors, which to date have shown success only in breast and ovarian cancer patients carrying germline BRCA1 or BRCA2 mutations.

The described results also encourage the exploration of advanced formulations, such as nanoparticles and intelligent delivery methods, aiming at enhancing the drug-like properties of the BRC4 peptide itself for its potential use in oncology medicine.

[This page is intentionally left blank]

4. SECTION II

Biological validation of a RAD51/BRCA2 small molecule inhibitor as a promising candidate to synergize with PARPi in 2D and 3D models of pancreatic cancer

4.1 Introduction

RAD51/BRCA2 interaction has been studied in a variety of medicinal chemistry approaches. Ligand-based Nuclear Magnetic Resonance (NMR) has been successfully exploited for the hit identification in Fragment-Based Drug Discovery (FBDD).[236,237] FBDD allows a more accurate exploration of chemical space, the use of high throughput screening, and a better understanding of protein-ligand molecular interactions.[238] By using this approach and exploiting a chimeric RadA-RAD51 construct, Scott et al. successfully identified fragments able to disrupt the BRC4-RAD51 interaction.[239] Nevertheless, to the best of our knowledge, no NMR fragment-based screening on the full-length wild-type form of human RAD51 has been performed so far. Therefore, we decided to exploit the full-length RAD51 protein and performed a ^{19}F NMR fragment-based screening aimed at identifying novel hits able to disrupt the RAD51/BRCA2 interaction. To this aim, we took advantage of the IIT in-house fluorinated fragment library, built following the Local Fluorine-Environment (LEF) approach.[236] This initial screening led to the identification of two hit compounds subsequently developed in SAR studies that generated two distinct series of derivatives, among which the pyrazolopyrimidine derivative **46** (Fig.15) showed the most appealing biological profile, inhibiting RAD51/BRCA2 in both biophysical and biochemical assays.

The aim of the experiments described in Section II was to enhance the biological study of **46** in different pancreatic cancer cell lines. For this reason, I also spent a six-month period at the Dublin City University, under the supervision of Dr. Naomi Walsh, where I had the opportunity to analyse the effects of **46** in combination with the PARPi talazoparib also in 3D pancreatic cancer models.

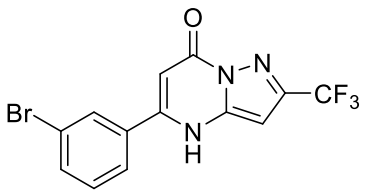

Figure 15. 46 chemical structure.

4.2 Materials and methods

4.2.1 Cell cultures

Three different pancreatic ductal adenocarcinoma cell lines were used: BxPC-3 cells were grown in RPMI 1640 (Merck, Cat. #R0883) supplemented with 10 % FBS, 100 U/mL penicillin/streptomycin, 2 mM glutamine; AsPC-1 and HPAC cells were grown in RPMI 1640 supplemented with 5 % FBS, 100 U/mL penicillin/streptomycin, 2 mM glutamine. HEK-293 cell line was grown in DMEM High Glucose (Merck, Cat. #D6546) supplemented with 10 % FBS, 100 U/mL penicillin/streptomycin, and 2 mM glutamine. A normal human pancreatic epithelial cell culture was obtained by Cell Biologics (Cat. #H6037). It was grown in its specific medium (Cell biologics, Cat. #H6621) and added with epithelial cell growth supplements (Cell biologics, Cat. #H6621-Kit). All the cultures were routinely tested for Mycoplasma contamination.

4.2.2 Organoid cultures

The PT291 organoid was derived from xenografts of invasive pancreatic adenocarcinoma/cholangiocarcinoma of a female patient.[240,241] The PDM41 organoid (pancreatic ductal adenocarcinoma) is commercially available from ATCC (Cat. #HCM-CSHL-0094-C25). The Complete Human Feeding Media (CHFM) components were as follows: DMEM/F12 GlutaMAX™ Supplement (Thermofisher, Cat. #10565018), Antibiotic Antimycotic 100 X (Merck, Cat. #A5955), L-WRN (Wnt3a-R-spondin3 Noggin) conditioned media (50 % v/v), 500 nM A83-01 (Merck, Cat. #SML0788), 50 ng/mL EGF (ThermoFisher, Cat. #PHG0311), 100 ng/mL hFGF10 (Biolegend, Cat. #559308), 0.01 µM Gastrine (Tocris, Cat. #3006), 1.25 mM N-acetylcysteine (R&D, Cat. #5619), 10 mM Nicotinammide (Merck, Cat. # N0636), B-27 Supplement 1X (Life Technologies, Cat. #17504-044) 10.5 µM ROCKi (Merck, Cat. #Y-27632). The organoid establishment was performed as follows: cells were resuspended in Cultrex BME (R&D System Biotechne, Cat. #3432-005-01); 20 µL of organoid in BME solution was pipetted onto a 24-multiwell poly-HEMA coated plate. The plate was placed at 37 ˚C for 15 min to allow the BME to polymerize, and then CHFM with 10.5 µM ROCKi was added to each well. Two days after establishing the organoid sample, cells were fed using CHFM without ROCKi, then subsequently fed every two days.

4.2.3 Homologous Recombination Quick Assay (HR-QA)

Homologous recombination (HR) was assessed using a commercially available kit (Norgen, Cat. #35600). This assay is based on cell transfection with two plasmids able to recombine upon cell entry. The efficiency of HR was assessed by Real-Time PCR, using primer mixtures included in the assay kit. Different primer mixtures allow differentiation between the original plasmid backbones and their recombination product. Briefly, BxPC3 cells (2×10^5 per well) were seeded in a 24-well plate and allowed to adhere overnight. Co-transfection with the two plasmids (1 µg each) was performed in Lipofectamine 2000 (Invitrogen, Cat. #11668019), according to the manufacturer's instructions. During the 5 h of transfection, cells were exposed to different doses of compounds, dissolved in DMSO. After washing with PBS, cells were harvested, and DNA was isolated using QIAamp DNA Mini kit (Qiagen, Cat. #51304). Sample concentration was measured using an ONDA Nano Genius photometer. The efficiency of HR was assessed by Real-Time PCR, using 25 ng of template and primer mixtures included in the assay kit, following the protocol indicated by the manufacturer. Data analysis was based on the $2^{-\Delta\Delta Ct}$ method: (Recombination Product/ Backbone Plasmids) treated versus (Recombination Product/Backbone Plasmids) control.

4.2.4 mClover Lamin A Homologous Recombination assay (mCl-HR)

50 µM **46** was added to HEK293 cells (6×10^4/well) grown on coverslips in a 24-well plate 1 h before transfection. Cells were transfected with 500 ng sgRNA plasmid targeting Lamin A (pUC CBA-SpCas9.EF1a-BFP. sgLMNA, Addgene Plasmid, Cat. #98971) and 500 ng donor plasmid (pCAGGS Donor mClover-LMNA, Addgene Plasmid, Cat. #98970) using Lipofectamine2000 (Invitrogen, Cat. #11668019). The next day, cell culture media was replaced by fresh media containing 50 µM **46**. 3 days after transfection, cells were fixed in PBS containing 4 % formalin for 15 min and washed twice with PBS before mounting. Images acquired using a Nikon fluorescent microscope equipped with filters for FITC, TRITC and DAPI were analysed by using the Cell Counter Plug-in of the ImageJ software.

4.2.5 Cells immunofluorescence assay

Immunofluorescence was used for studying RAD51 nuclear translocation. To visualize RAD51 in cell nuclei, BxPC-3 cells were seeded on glass coverslips placed in a 6-well culture plate (2×10^5

cells/well) and allowed to adhere overnight. Cultures were then pre-incubated with 30 μM **46** for 1 h and subsequently exposed to 50 μM cisplatin for an additional 1.5 h. Medium was removed, and cells were maintained in the presence of 30 μM **46** for 5 h. After this time, cultures were fixed in PBS containing 4 % formalin for 13 min, permeabilized in 70 % ethanol, air-dried, and washed twice with PBS. Samples were incubated in 5 % bovine serum albumin (BSA) in PBS for 30 min and subsequently exposed to anti-RAD51 rabbit monoclonal antibody (1:1000 in 5 % BSA/PBS, BioAcademia, Cat. #70-001) overnight at 4 ◦C. After washing, coverslips were incubated with a secondary antirabbit rhodamine-labelled (Amersham Hybord, Cat. #10600060 1:1000 in 5 % BSA/ PBS), for 30 min, washed, air-dried, and mounted with a solution 2 μg/ mL DAPI in DABCO. Images were acquired using a Nikon fluorescent microscope equipped with filters for FITC, TRITC, and DAPI. The percentage of cells bearing RAD51 nuclear foci was estimated by two independent observers analysing approximately 200 cells for each treatment sample.

4.2.6 Cell viability assay

Cell viability was assessed with the PrestoBlue cell viability kit (Thermofisher, Cat. #A13261). 1–10 × 10^3 cells, depending on cell type and incubation time, in 200 μL of culture medium were seeded in a 96-multiwell plate and allowed to adhere overnight. The day after, cells were treated with different doses of compounds, alone or in combination. Cell viability was assessed with the PrestoBlue cell viability kit (Thermofisher, Cat. #A13261). 1–10 × 10^3 cells, depending on cell type and incubation time, were seeded in 200 μL of culture medium in a 96-multiwell plate and allowed to adhere overnight. The day after, cells were treated with different doses of compounds, alone or in combination. After 6 days of treatment, 20 μL of the PrestoBlue cell Viability Reagent was added to each well, and incubated for 4 h at 37 ◦C. The fluorescence intensity was measured with the i-control™ Microplate Reader Software by Tecan.

4.2.7 Cell death inhibitors assay

BxPC-3 and HPAC cells were seeded in a 96-multiwell plate and allowed to adhere overnight. The day after, cells were treated with 2 μM talazoparib and 30 μM **46**, alone and in combination. 72 h later, 20 μM Z-VAD-FMK or 20 μM Nec-1 (Merck, Cat. #627610; #480065) was added and then re-added to cultures every 24 h until the sixth day of treatment. The cell viability was assessed by using the PrestoBlue cell viability kit (Thermofisher, Cat. #A13261), as described previously.

4.2.8 Organoid viability assay

Organoid viability was assessed using the CellTiter-Glo® 3D Cell Viability Assay (Promega, Cat. #G9681). 5×10^3 cells in 10 µL of Cultrex Basement Membrane were seeded into each well of a 96-multiwell polyHEMA-coated black-sided, clear bottom plate. The plate was incubated at 37 °C for 20 min to allow the BME to solidify; then, 100 µL of CHFM, supplemented with ROCKi, was added to each well. After 3 days, organoids were treated with 2X concentration of talazoparib and **46** in 100 µL of CHFM and maintained for 6 days, alone or in combination. At the end of the treatment, 25 µL of the viability reagent was added to each well. After 5 min shaking and 25 min room temperature incubation, the luminescence intensity was measured with the i-control™ Microplate Reader Software by Tecan.

4.2.9 Immunofluorescence organoid assay

PT291 was seeded on glass coverslips placed in an 8-chamber plate (1×10^4 cells/well) and allowed to adhere and grow for 3 days. PT291 was treated with 50 µM **46** for 24 h. The medium was removed, and organoids were washed with PBS containing 0.1 % Tween and 2 % BSA (wash buffer) for 5 min. Then, they were fixed in 4 % Formalin in PBS for 20 min, permeabilized in 0.5 % Triton-X for 45 min, and washed twice with the wash buffer. Samples were blocked for 1.5 h with 10 % FBS in PBS and subsequently exposed to the anti- γ-H2AX mouse monoclonal antibody (BioLegend, Cat. #613402) 1:250 in wash buffer) overnight at 4 °C. After washing, coverslips were incubated with an anti-mouse FITC-conjugated secondary antibody (Novus Biologicals, Cat. #NB720-F, 1:200 in wash buffer) for 1 h at room temperature, washed, and counterstained with DAPI for 5 min. Images were acquired using a Nikon fluorescent microscope equipped with filters for FITC, TRITC, and DAPI. Images were analysed by using the Cell Counter Plug-in of the ImageJ software.

4.3 Results and Discussion

4.3.1 Evaluation of HR impairment following 46 treatment through different assays

The HR-QA assay was performed as a first experiment aimed at evaluating HR inhibition by **46**. It is a rapid tool used for compounds screening that, in our experience, can give a reliable indication of a cell's HR efficiency in a relatively high-throughput manner.[203,204] The compound was administered at a wide range of doses (1–400 μM) to BxPC-3 cells. As shown in Figure 16, **46** produced a statistically significant dose−response effect in reducing cell HR up to 30 μM; a plateau effect was observed for doses higher doses, indicating that the compound has reached its maximum HR inhibition rate. The calculated IC_{50} value was 7.83 ± 3.19 μM.

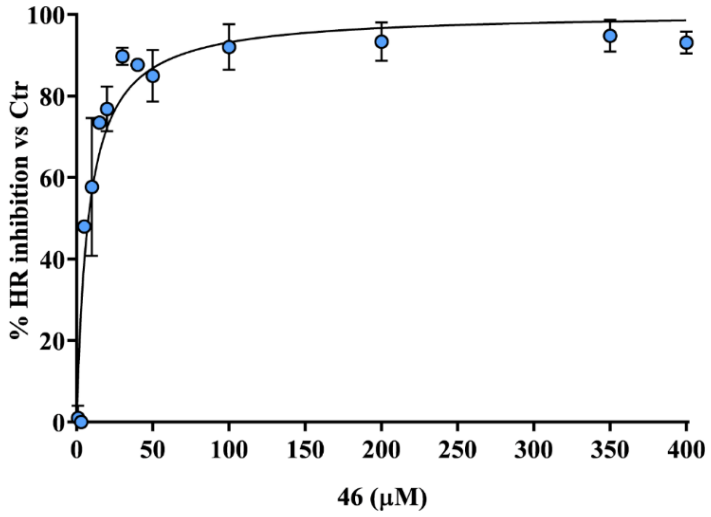

Figure 16. HR inhibition caused by increasing doses of 46 administered to BxPC-3 cells during 5 h of plasmid transfection. *HR was evaluated by real-time PCR, as described in the Experimental Methods section. A plateau effect was observed for doses higher than 30 μM, with no statistically significant difference in the HR inhibitory power caused by* ***46****, measured in the dose range 30–400 μM (assessed by ANOVA). To extrapolate the IC50 value, data were analysed by applying the least squares regression fit; the theoretical regression curve (R^2 = 0.91) is shown in the graph.*

A further HR inhibition study was performed by applying the m-Clover Lamin A assay (mCl-HR).[242,243] This assay relies on the HR-dependent incorporation of a mClover-carrying sequence into a DSB generated by Cas-9 within the LMNA gene. Following the cleavage performed by Cas-9, the DNA DSB is repaired through HR utilizing the mClover donor plasmid containing the corresponding sequence, resulting in the reconstitution of a fluorescent mClover-Lamin A fusion

protein (Fig. 17). This assay requires cells that are highly proliferative and transfection-permissive, thus it was conducted using embryonic kidney cells (HEK-293) instead of BxPC-3 cells, which have limited transfection efficacy and a slower growth rate.[244,245]

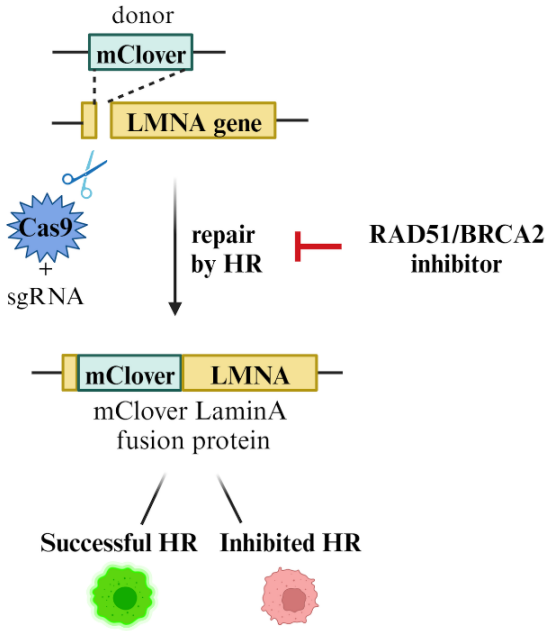

Figure 17. Schematic depiction of the mClover-LaminA assay for DNA repair by HR. *HEK-293 cells were transfected with the assay plasmids (Lamin A-targeting sgRNA and mClover Lamin A donor constructs) and analysed for mClover Lamin A-positive cells, following treatment with the desired RA51/BRCA2 inhibitor.*

First, the transfection efficacy of HEK-293 cells was evaluated using a GFP-bearing plasmid, revealing an efficiency of approximately 45% (Fig. 18), and thus confirming HEK-293 as a transfection-permissive cell line.

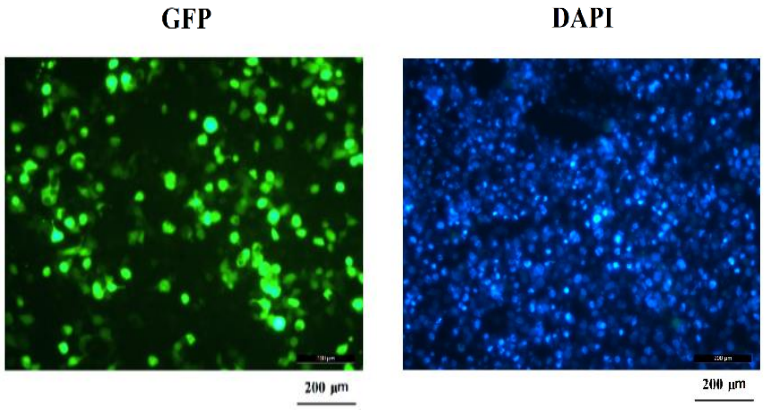

Figure 18. Representative microscopic fields showing fluorescence of HEK-293 cells transfected with the GFP plasmid as a transfection control. *The GFP-transfected cells fluorescence (on the left) intensity was found to be ≈ 45%, compared to the DAPI staining of cells nuclei (on the right). The fluorescent analysis was performed by using the Cell Counter Plug-in of the ImageJ software.*

Even though the HR-QA identified 30 µM as the **46** lowest effective dose for inhibiting HR activity, mClover-transfected HEK-293 cultures were exposed to 50 µM. This slightly higher dose was chosen considering the longer incubation period required for the mCl-HR assay (3 days compared to the 5 hours for HR-QA). As illustrated in Figure 19, the untreated m-Clover-transfected cultures (Ctr) exhibited ≈ 20% cells with Lamin A fluorescence. However, treatment with compound **46** notably decreased the number of Lamin A fluorescent cells to approximately 3.7%. This significant reduction in HR inhibition (about 80%) mirrored the outcomes observed in BxPC-3 cells using the HR-QA assay, highlighting the potential of compound **46** as a BRCA2-RAD51 inhibitor.

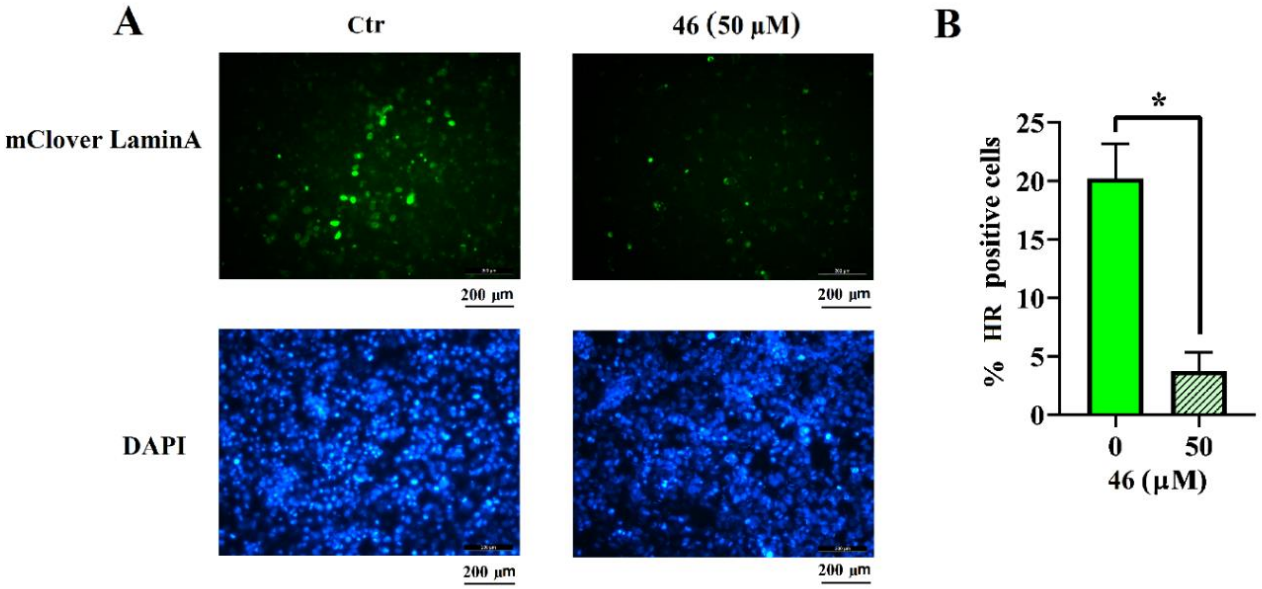

Figure 19. mCl-HR assay on HEK-293 cells. *A) Representative microscopic fields showing fluorescence of HEK-293 transfected with the assay plasmids (Lamin A-targeting sgRNA-spCas9 and mClover Lamin A donor).* ***46*** *(50 µM) administration led to a remarkable decrease in HR positive cells, compared to the Ctr. The blue fluorescence shows DAPI-stained DNA. Scale bar, 200 µm. B) The graph shows the percentage of HR-proficient cells in untreated and* ***46*** *(50 µM) exposed samples, highlighting a statistically significant decrease (* p = 0.0199) due to the treatment. Approximately 200 cells per sample were analysed in two independent experiments, and the fluorescence intensity was measured by using the ImageJ software. Statistical significance was assessed by Student's t-test.*

To validate the results obtained in the HR inhibition assays, an immunofluorescence detection of RAD51 nuclear foci was carried out following treatment with DNA-damaging agents. In fact, a decrease in RAD51 nuclear foci is a recognized indicator of compromised HR. To achieve this, extensive DNA damage was induced in BxPC-3 cells by 50 µM CPL for 1.5 hours. Subsequently, cells were treated with 30 µM of compound **46** for 5 hours. As shown in Fig. 20, the administration

of compound **46** alone did not appear to induce DNA damage, as RAD51 foci were not observed in BxPC-3 cultures. On the contrary, as expected, RAD51 foci were visible in approximately 35% of cells in the CPL-treated cultures. However, upon the addition of compound **46**, RAD51 foci were significantly reduced. These observations are in agreement with the results obtained in the HR experiments, providing substantial support for the expected mechanism of action of the compound.

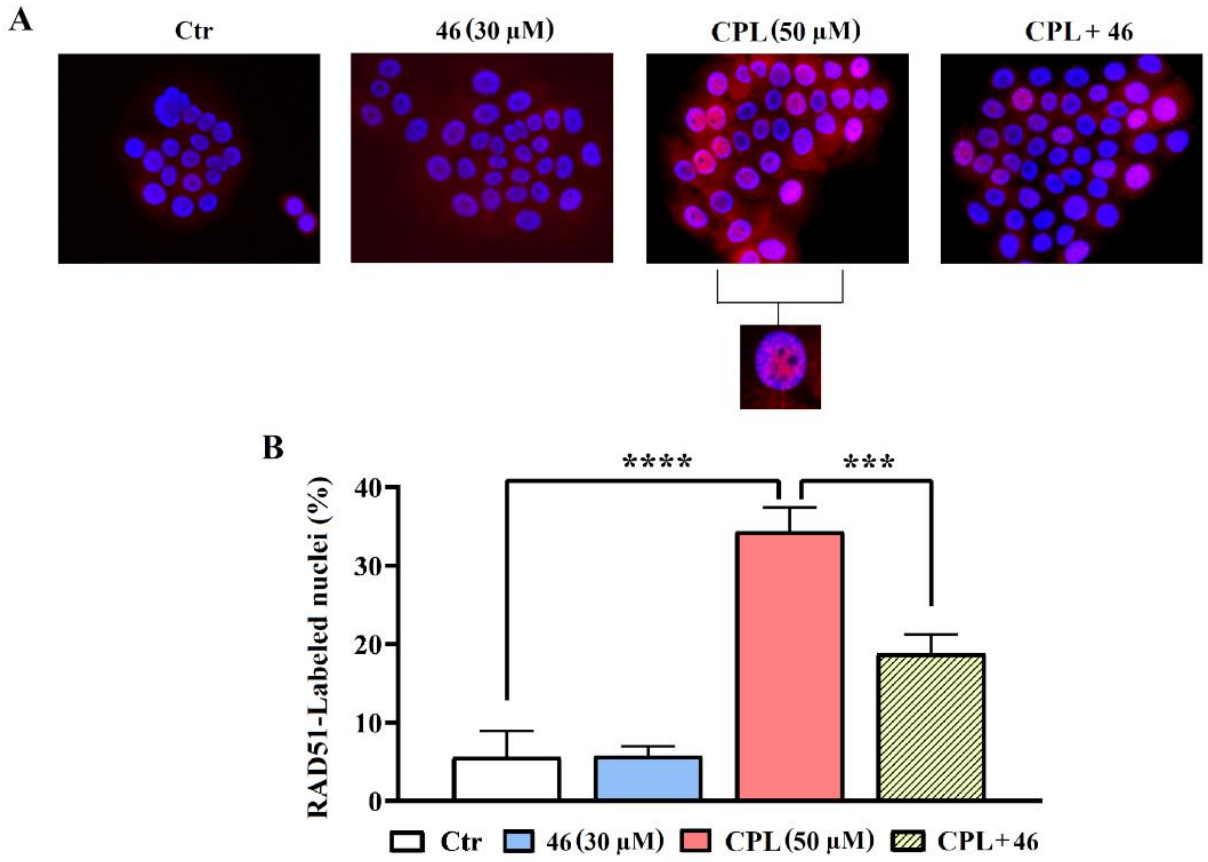

Figure 20. Immunofluorescence detection of RAD51 nuclear foci. *A) Representative pictures showing DAPI-stained BxPC-3 cell nuclei merged with the corresponding RAD51-labelling. A higher magnification detail of RAD51 nuclear foci was included for the CPL-exposed culture. B) The bar graph shows the percentage of labelled assessed in the cell cultures. In CPL-exposed cultures, RAD51 labelling was detected in 35% nuclei (**** $p < 0.0001$, compared to Ctr); in cells exposed to both* ***46*** *and CPL only 18% cell nuclei showed RAD51 labelling, a statistically significant reduction compared to CPL-exposed cells (*** $p = 0.0004$). RAD51-labeled nuclei were assessed by two independent observers who analysed the treated cultures, counting approximately 200 cells for each treatment sample. Data were statistically evaluated by applying the one-way ANOVA test.*

4.3.2 Analysis of 46/talazoparib combination in three different BRCA2- proficient pancreatic cancer cell lines

According to the concept of SL, the impairment of RAD51/BRCA2 interaction mediated by **46** is expected to increase the antineoplastic activity of PARPi. When RAD51 functions in HR DNA damage repair are compromised, cells become more reliant on alternative repair pathways like PARP-mediated repair.[246,247]

The effects on cell viability of the RAD51/BRCA2 inhibition combined with PARP inhibition by TLZ were evaluated in three PDAC cell lines: HPAC, BxPC-3, and AsPC-1. HPAC and BxPC-3 are cell lines derived from a primary tumour, while the AsPC-1 line was isolated from the ascitic fluid of a PDAC metastasis.[206,248–250] The heatmap graph reported in Fig. 21 illustrates the different expression of relevant genes related to the HR pathway in these cell lines.

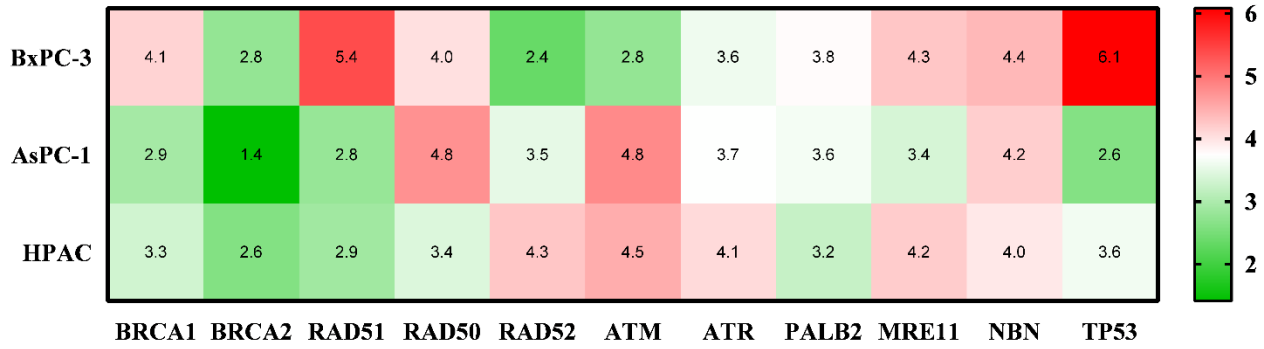

Figure 21. Different HR gene expression among BxPC-3, AsPC-1, HPAC cells. *The Heatmap graph was obtained using Depmap, the Cancer Dependency Map portal (https://depmap.org/portal/); as reported in Depmap, relative gene expression values are inferred from RNA-seq data using the RSEM tool and are reported after log2 transformation, using a pseudo-count of 1; log2(TPM+1). It shows the gene expression profile of the main HR genes (indicated at the bottom of the graph) in the three PDAC cell lines used (indicated at the left of the graph). The reported colours are referred to the scale on the right: the more intense the red, the more expressed the gene; otherwise, the more intense the green, the less expressed the gene.*

Specifically, BxPC-3 cells exhibit elevated levels of RAD51, a condition associated with cell survival, drug resistance, and unfavourable patient prognosis.[165,251] These cells also display the highest P53 expression, even though, together with AsPC-1 cells, carry various loss-of-function or missense mutations resulting in either the absence or impaired function of the protein. Conversely, HPAC is the only cell line expressing wild-type P53.[252,253] In this aspect, HPAC cells represent an exception within the landscape of common PDACs in clinical practice, where these cancer types

typically exhibit mutated P53.[254,255] Nonetheless, we considered valuable to incorporate this model into our experiments for the investigative purposes of our study.

The ability of **46** to improve the antineoplastic effect of TLZ, was investigated in the three selected PDAC cultures. TLZ, an FDA-approved PARPi since 2018, is used for treating adult patients diagnosed with HER2-negative, locally advanced, or metastatic breast cancer with suspected or confirmed deleterious germline BRCA mutations.[116] Ongoing research on pancreatic cancer has also been exploring TLZ's efficacy.[256–258] Compared to other PARPi, TLZ shares a similar mechanism of action and demonstrates higher antineoplastic activity in vitro. Additionally, TLZ was found to be approximately 100 times more potent in trapping PARP1.[108,120]

In preliminary experiments, all the three cell cultures were exposed to different doses of TLZ (0–5 μM) for six days to determine the IC_{50} values (Fig. 22). Remarkably, the calculated IC_{50} values were similar across the cell lines: 1.8 μM for BxPC-3, 2.27 μM for HPAC, and 2.66 μM for AsPC-1. Consequently, a standardized dose of 2 μM TLZ was chosen to investigate its combined effect with **46** across all three cultures.

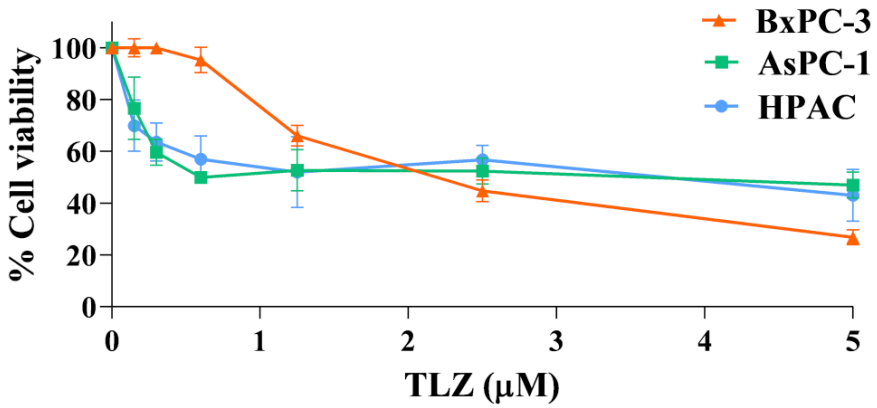

Figure 22. Dose-response curves of TLZ in HPAC, AsPC-1 and BxPC-3 cells. *Six days of TLZ treatment (0-5 μM); IC_{50} was calculated by applying polynomial regression to the collected data.*

46 was administered at 30 and 50 μM, either alone or in combination with TLZ, for six days. This long exposure time was selected because cell death is expected to be a consequence of progressive DNA damage accumulation due to the simultaneous impairment of DNA SSBs and DSBs repair induced by PARPi and **46**, respectively. In BxPC-3 cells, the administration of **46** alone led to a 25–30% reduction in cell viability at both doses (Fig. 23). Interestingly, this effect was amplified by the addition of TLZ, displaying a 60% reduction (with $p < 0.05$). This outcome is in

agreement with the HR-QA data (Fig. 16), demonstrating consistent effects for both **46** doses and aligning with the mCl-HR experiment illustrated in Fig. 19.

A similar statistically significant impact of the **46**/TLZ combination was observed in HPAC cells. In contrast, the effect appeared less marked in AsPC-1, yet remaining statistically significant at the 50 µM concentration. A plausible explanation for this observation can be inferred from the heatmap depicted in Fig. 21. Specifically, AsPC-1 cells exhibit notably lower BRCA2 expression compared to BxPC-3 and HPAC cells, while the expression level of RAD52 is more than 2-fold higher than BRCA2. Therefore, it can be hypothesized that in AsPC-1 cells, alternative HR mechanisms, particularly the RAD52-mediated HR, which is independent of BRCA2, might prevail, thus explaining the compromised efficacy of RAD51/BRCA2 inhibition.[259,260]

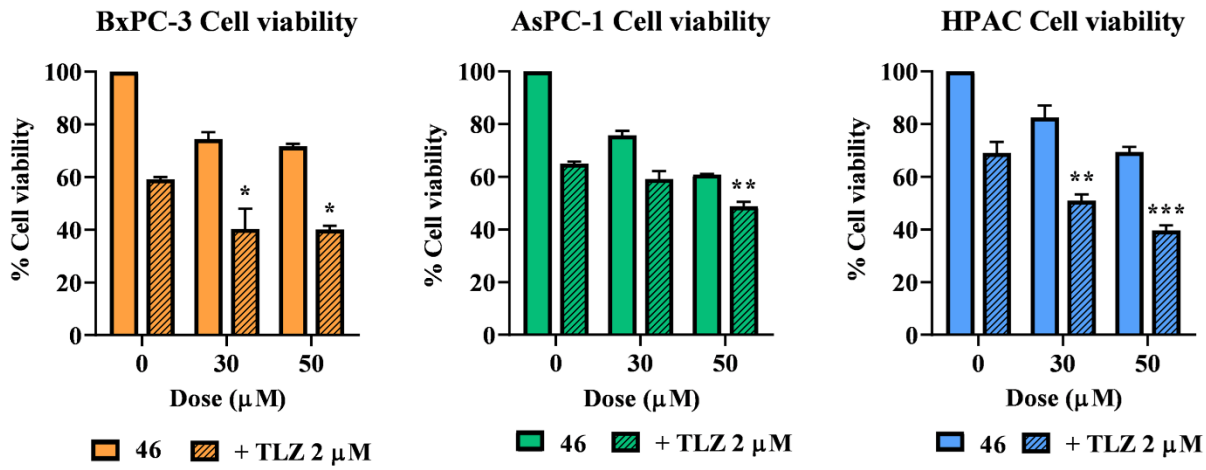

Figure 23. Evaluation of BxPC-3, AsPC-1, HPAC cell viability following 46/TLZ combination. *Antiproliferative effect caused by **46**, administered at 30 and 50 µM singularly or in combination with 2 µM TLZ, measured in BxPC-3, AsPC-1 and HPAC cells after six days of treatment. Data were statistically analysed using the two-way ANOVA followed by Tukey's multiple comparisons test, to evaluate the differences between the effects caused by the compounds' combination vs those caused by the single TLZ treatment. * $p < 0.05$; ** $p < 0.005$; *** $p = 0.0001$.*

Subsequently, we explored whether the results shown in Fig. 23 could be explained by the involvement of cell death, which is a desired outcome in antineoplastic treatments. Given the reduced efficacy observed in AsPC-1 cultures, this experiment was performed in HPAC and BxPC-3 cells. These cells were treated with the **46**/TLZ combination for six days, in the presence of either 20 µM Z-VAD-FMK (a widely-used pan-caspase inhibitor) or 20 µM Necrostatin-1 (Nec-1, a necroptosis inhibitor).[261,262] **46** was administered at 30 µM, which is the lowest dose causing

statistically significant effects in the cell viability experiments (Fig. 23). Upon treating cultures with the **46**/TLZ combination, the addition of Z-VAD-FMK resulted in a statistically significant increase in cell viability (Fig. 24 A). On the contrary, the administration of Nec-1 did not affect the antiproliferative effect of the **46**/TLZ combination (Fig. 24 B). These results confirmed the involvement of apoptosis, reproducing the desired mechanism of SL triggered by the combination of RAD51/BRCA2 and PARP inhibitors.

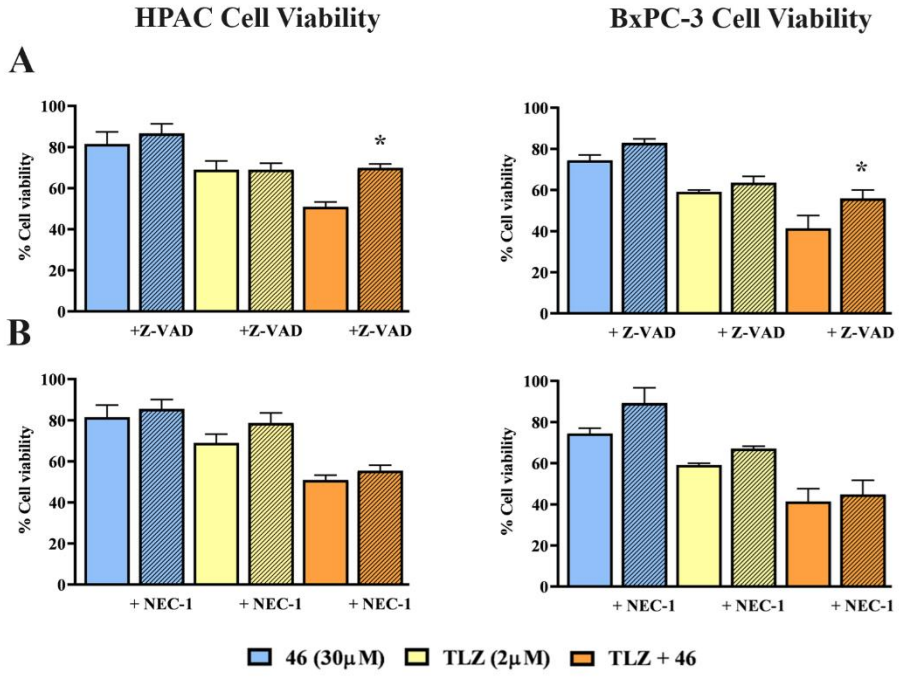

Figure 24. Evidence of cell death pathways following the 46/TLZ treatment in HPAC (left) and BxPC-3 (right) cells. (A) *Involvement of apoptosis. Cells were treated for six days with 30 μM* ***46****, given singularly or in combination with 2 μM TLZ. 20 μM Z-VAD-FMK was added mid-treatment and then every 24 h. Data were statistically analysed using two-way ANOVA followed by Tukey's multiple comparisons test (*p < 0.05, compared to the culture treated with* ***46****/TLZ).*
(B) *Involvement of necroptosis. Cells were treated for six days with 30 μM* ***46****, singularly or in combination with 2 μM TLZ. 20 μM Nec-1 was added mid-treatment and then every 24 h. Data were statistically analysed using two-way ANOVA followed by Tukey's multiple comparisons test. No evidence of necroptosis was observed.*

To investigate the selectivity of the **46**/TLZ combination for cancer cells, we assessed the toxicity of this combination on normal epithelial cells isolated from the human pancreas (H-6037). H-6037 cells were treated with either 30 μM **46** alone or in combination with 2 μM TLZ for six days. As shown in Fig. 25, administration of TLZ had no impact on the viability of H-6037 cells, while the effect of **46** alone resulted in a mild inhibition, ≤ 20%. These effects were lower than those

observed in the cancer models (Fig. 23). Additionally, the administration of **46** was unable to increase the antiproliferative effects of TLZ, since no statistically significant difference was observed between the cells exposed to **46** alone and those receiving the combination treatment. Though preliminary, these findings align with the hypothesis that concurrent inhibition of PARP and RAD51/BRCA2 function should preferentially affect cancer cells.

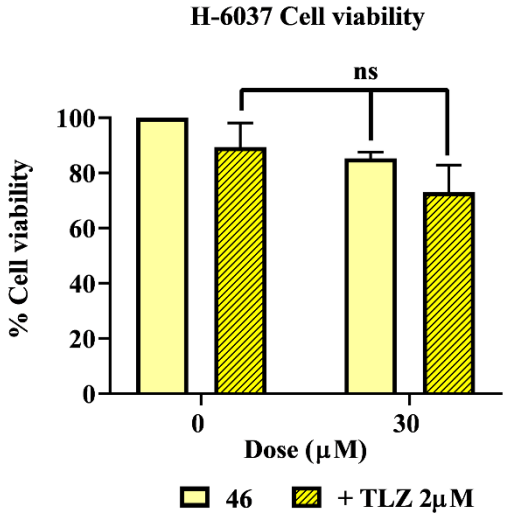

Figure 25. Evaluation of H-6037 cell viability following treatment with 46/TLZ combination for after six days. *H-6037 were treated with 30 μM* ***46*** *and 2 μM TLZ, given alone or in combination. Data were statistically analysed by two-way ANOVA followed by Tukey's multiple comparisons test. 30 μM* ***46*** *caused a ≈ 20% inhibition of H-6037 cell viability ($p < 0.05$). No statistically significant difference was observed when the effect of the* ***46****/TLZ combination was compared with those caused by the two compounds administered as single treatments; ns= not significant.*

4.3.3 Analysis of 46/talazoparib combination in 3D models of pancreatic adenocarcinoma

In two-dimensional (2D) cell culture, cells are grown on flat surfaces, thus forced into a planar shape, and exposed to a uniform administration of nutrients, growth factors, and drugs. Moreover, in 2D cultures, cells lack complex cell-cell and cell-environment interactions found in living tissues. Conversely, in three-dimensional (3D) cultures, cells are embedded in a gel or scaffold that mimics the natural extracellular matrix (ECM) and provides a three-dimensional structure, allowing for *in vivo*-like cell-cell and cell-environment interactions. Moreover, 3D cultures are characterized by heterogenous cell polarities and phenotypes, which are more representative of native tissue

architecture, allowing researchers to study cell behaviour in conditions that better mimic *in vivo* situations (Fig. 26). [263,264]

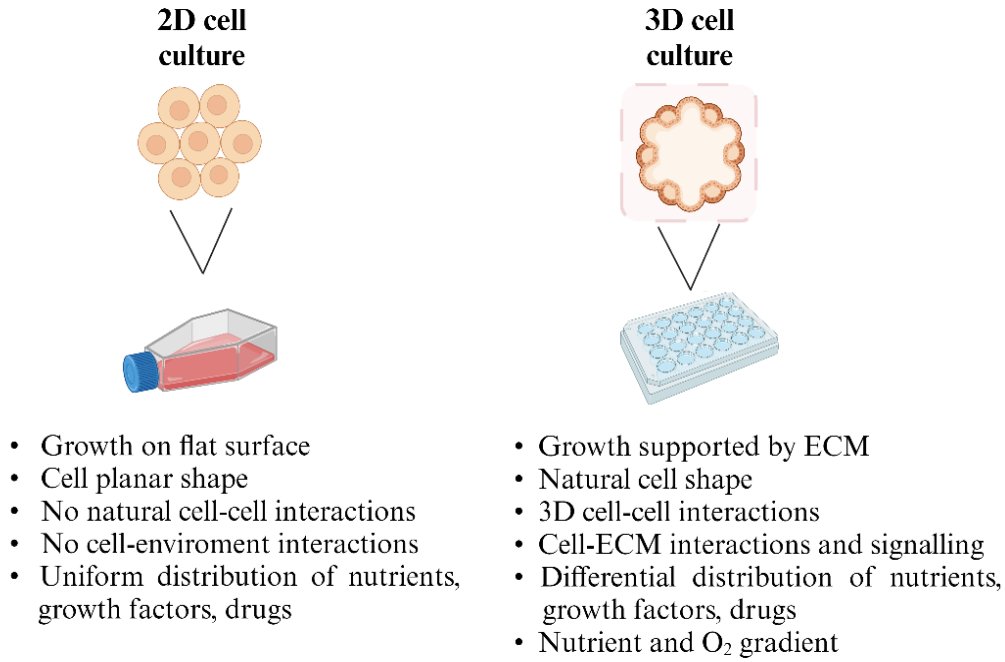

Figure 26. Differences between 2D and 3D culture models. *A schematic representation of the traditional 2D monolayer cell culture and 3D cell culture systems and their main differences.*

Consequently, the effect of the compounds' association (50 µM **46** with 2 µM TLZ) was assessed on two distinct PDAC organoids, PT291 and PDM41. The PT291 organoid was derived from xenografts of an invasive pancreatic adenocarcinoma/cholangiocarcinoma from a female patient (Fig. 27); the PDM41 organoid is characterized by an adenocarcinoma ductal type histology and is commercially available (Fig. 28) (details reported in section 4.2.2).

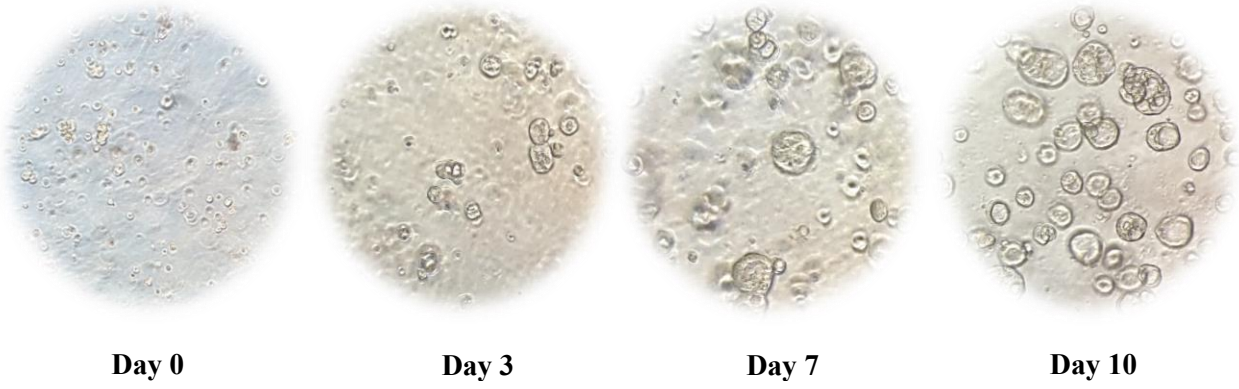

Figure 27. PT291 organoid growth and development*. Representative images showing PT291 on day 0, day 3, day 7 and day 10.*

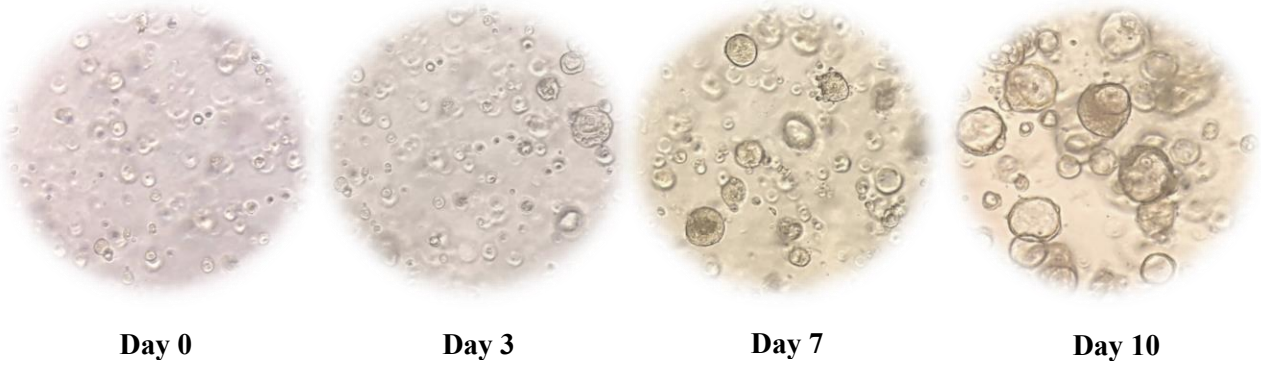

***Figure 28. PDM41 organoid growth and development**. Representative images showing PDM41 on day 0, day 3, day 7 and day 10.*

The impairment of organoid viability caused by the **46**/TLZ combination following a six-day treatment is represented in Fig. 29. The combination treatment significantly increased the effects of TLZ in both organoid models, in agreement with the results obtained in the 2D cellular assays. Particularly, in PT291 the co-administration with **46** resulted in a 50% decrease in cell viability compared to the treatment with TLZ alone.

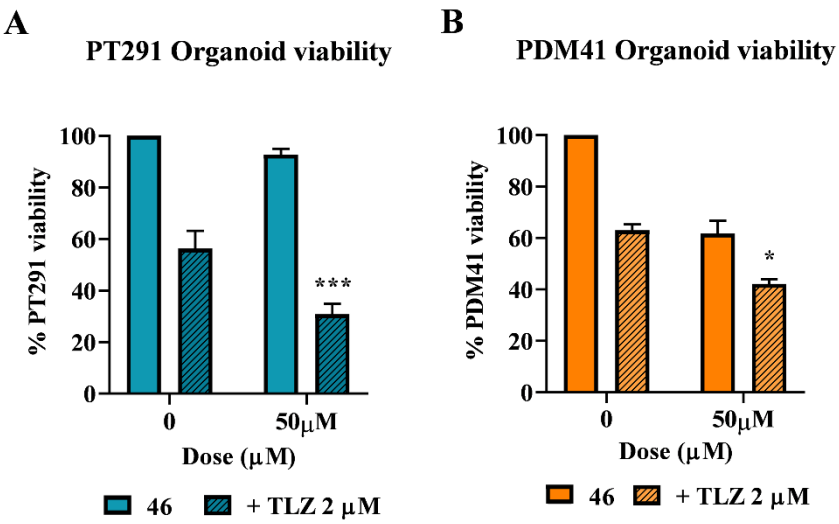

Figure 29. Antiproliferative effect caused by 46 administered singularly or in combination with 2 μM TLZ and evaluated in two different 3D models of PDAC: the PT291 (A) and the PDM41 (B).** **(A)** The six-day co-administration of the two compounds led to a marked decrease in organoids' viability, strongly potentiating the anti-proliferative effect of TLZ. The two-way ANOVA test, followed by Tukey's multiple comparisons test, indicated a statistically significant difference produced by the coadministration compared to the single TLZ treatment (p = 0.0003). **(B)** In PDM41 PDAC organoid culture the compounds' association showed a less remarkable, but statistically significant effect (* p = 0.0116, compared the single TLZ treatment).*

In a final experiment, we verified whether the combined treatment **46**/TLZ can produce increased DNA damage, as expected in cells with both HR repair and PARP function impairment. This

experiment was performed in the PT291 organoid. Following the **46**/TLZ treatment, the DNA damage level was evaluated using an immunofluorescent assay for detecting γ-H2AX foci, a recognized DNA damage marker (Fig. 30). Interestingly, when given as single treatments, both **46** and TLZ did not cause significant γ-H2AX labelling, compared to the untreated PT291. However, their combination resulted in a threefold increased level of γ-H2AX foci, in line with the viability experiment results (Fig. 29).

These data are in agreement with the postulated mechanism of action of the compounds, which are expected to significantly compromise DNA integrity when administered in combination. Moreover, these findings further confirmed the data of the previous experiments.

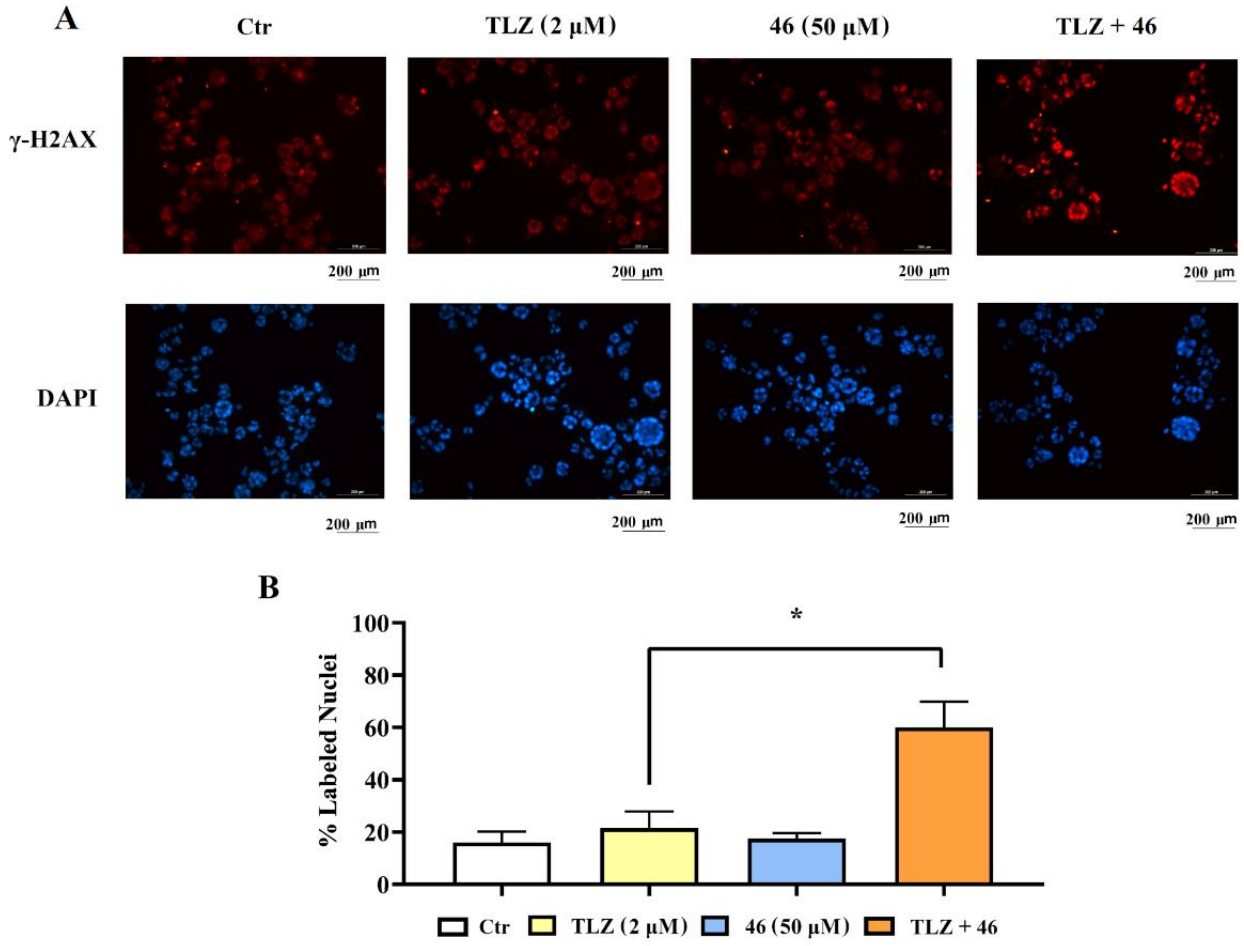

Figure 30. Evaluation of DNA damage in the PT291 organoid culture treated for 24 h with 2 µM TLZ and 50 µM 46, given singularly or in combination. (A) *Representative pictures showing DAPI-stained cell nuclei and the corresponding immune-labelling of γ-H2AX, a marker of DNA damage. In PT291, the coadministration of* ***46*** *and TLZ led to increased γ-H2AX labelling.* ***(B)*** *The bar graph shows the percentage of γ-H2AX labelled nuclei, assessed with the aid of ImageJ software. The statistical analysis was carried out by applying one-way ANOVA followed by Tukey's multiple comparisons test; a statistically significant difference was found between the organoid culture treated with TLZ alone and that exposed to the compounds' combination. * p = 0.0127.*

4.4 Conclusions – SECTION II

Compound **46**, which is derived from a ^{19}F NMR fragment screening on the oligomeric RAD51 form, proved to inhibit HR in a low micromolar range. Two different HR inhibition assays (HR-QA and mCl-HR) proved its supposed mechanism of action. Importantly, in combination with TLZ, **46** induced cell apoptosis, which is a desired anticancer goal and represents a confirmation of the desired SL induction. Notably, the combination was studied on three PDAC cell lines with the aim of providing a more comprehensive understanding of the potential efficacy and limitations of the RAD51/BRCA2 inhibitor. In fact, the used cell lines are characterized by different expression patterns of the main HR genes and are derived from PDAC with different clinical features. The study of **46**/TLZ combination was also implemented in 3D culture systems, which represent a more physiologically and clinically relevant platform for drug discovery research. Taken together, all the obtained results confirmed **46** as a promising RAD51/BRCA2 small molecule inhibitor able to increase the antineoplastic effect of PARPi TLZ.

This work adds credence to the SL paradigm for tackling unmet oncological needs such as pancreatic cancer. Moreover, **46** can be considered as a useful tool for further investigation of the SL mechanism based on RAD51, as well as a starting point for further drug discovery campaigns.

[This page is intentionally left blank]

5. CONCLUSIONS

SL exploits the inherent vulnerabilities of cancer cells by targeting specific genetic or molecular weaknesses, representing a promising avenue for medicinal chemistry in the field of anticancer therapies. In the context of DNA damage repair, the SL concept can be applied by targeting two separate DNA repair pathways; when a pathway is defective, cells can still survive by relying on the alternative pathway. However, if the two pathways are simultaneously compromised, cells become vulnerable.

In this context, the described research project was aimed at inhibiting the HR DNA repair pathway by targeting the interaction between RAD51 and BRCA2 proteins, which makes cancer cells more sensitive to PARPi. To inhibit the RAD51/BRCA2 interaction, the experiments reported in Section I used a peptide derived from a BRCA2 sequence (BRC4), which is directly involved in the interaction with RAD51; this study enabled to outline the potential outcomes of HR inhibition. Moreover, for the first time, it allowed to obtain a proteomic fingerprint consequent to HR inhibition after cell exposure to BRC4. The acquired data can be useful in view of further investigations aimed at obtaining a biological characterization of novel RAD51/BRCA2 small molecule inhibitors. Section II reports studies aimed at characterizing the biological activity of a potential RAD51/BRCA2 disruptor identified during a drug discovery campaign performed at IIT and University of Bologna: compound **46**. The performed experiments highlighted the potential of **46** to trigger SL in combination with talazoparib. Talazoparib is a potent PARPi approved by FDA in 2018 for treating adult patients diagnosed with HER2-negative, locally advanced, or metastatic breast cancer with suspected or confirmed deleterious germline BRCA mutations.

Overall, the present study added important notions useful for the application of a chemical biology approach involving the use of small molecules, to trigger synthetic lethality by means of DNA repair inhibitors. This approach has the potential to enhance the efficacy of anticancer treatments targeting DNA damage repair, making them applicable to a broader spectrum of patients.

[This page is intentionally left blank]

6. BIBLIOGRAPHY

1. Walter E, Scott M. The life and work of Rudolf Virchow 1821–1902: "Cell theory, thrombosis and the sausage duel." *J Intensive Care Soc*. 2017;18(3):234-235. doi:10.1177/1751143716663967

2. Cancer, World Health Organization. Accessed December 29, 2023. https://www.who.int/health-topics/cancer#tab=tab_1

3. Bisoyi P. A brief tour guide to cancer disease. In: *Understanding Cancer*. Elsevier; 2022:1-20. doi:10.1016/B978-0-323-99883-3.00006-8

4. Johnson DE, Burtness B, Leemans CR, Lui VWY, Bauman JE, Grandis JR. Head and neck squamous cell carcinoma. *Nat Rev Dis Primers*. 2020;6(1):92. doi:10.1038/s41572-020-00224-3

5. Sung H, Ferlay J, Siegel RL, et al. Global Cancer Statistics 2020: GLOBOCAN Estimates of Incidence and Mortality Worldwide for 36 Cancers in 185 Countries. *CA Cancer J Clin*. 2021;71(3):209-249. doi:10.3322/caac.21660

6. Chaitanya Thandra K, Barsouk A, Saginala K, Sukumar Aluru J, Barsouk A. Epidemiology of lung cancer. *Współczesna Onkologia*. 2021;25(1):45-52. doi:10.5114/wo.2021.103829

7. Mattiuzzi C, Lippi G. Current Cancer Epidemiology. *J Epidemiol Glob Health*. 2019;9(4):217. doi:10.2991/jegh.k.191008.001

8. Siegel RL, Miller KD, Fuchs HE, Jemal A. Cancer statistics, 2022. *CA Cancer J Clin*. 2022;72(1):7-33. doi:10.3322/caac.21708

9. Ilic I, Ilic M. International patterns in incidence and mortality trends of pancreatic cancer in the last three decades: A joinpoint regression analysis. *World J Gastroenterol*. 2022;28(32):4698-4715. doi:10.3748/wjg.v28.i32.4698

10. Petrin K, Bowen DJ, Alfano CM, Bennett R. Adjusting to pancreatic cancer: Perspectives from first-degree relatives. *Palliat Support Care*. 2009;7(3):281-288. doi:10.1017/S1478951509990204

11. Rawla P, Sunkara T, Gaduputi V. Epidemiology of Pancreatic Cancer: Global Trends, Etiology and Risk Factors. *World J Oncol*. 2019;10(1):10-27. doi:10.14740/wjon1166

12. Rawla P, Sunkara T, Gaduputi V. Epidemiology of Pancreatic Cancer: Global Trends, Etiology and Risk Factors. *World J Oncol*. 2019;10(1):10-27. doi:10.14740/wjon1166

13. McGuigan A, Kelly P, Turkington RC, Jones C, Coleman HG, McCain RS. Pancreatic cancer: A review of clinical diagnosis, epidemiology, treatment and outcomes. *World J Gastroenterol*. 2018;24(43):4846-4861. doi:10.3748/wjg.v24.i43.4846

14. Accessed December 27, 2023, https://visualsonline.cancer.gov/about.cfm

15. Louvet C, Philip PA. Accomplishments in 2007 in the treatment of metastatic pancreatic cancer. *Gastrointest Cancer Res*. 2008;2(3 Suppl):S37-41.

16. Sarantis P, Koustas E, Papadimitropoulou A, Papavassiliou AG, Karamouzis M V. Pancreatic ductal adenocarcinoma: Treatment hurdles, tumor microenvironment and immunotherapy. *World J Gastrointest Oncol*. 2020;12(2):173-181. doi:10.4251/wjgo.v12.i2.173

17. Sears HF, Kim Y, Strawitz J. Squamous cell carcinoma of the pancreas. *J Surg Oncol*. 1980;14(3):261-265. doi:10.1002/jso.2930140312

18. Simone CG, Zuluaga Toro T, Chan E, Feely MM, Trevino JG, George TJ. Characteristics and outcomes of adenosquamous carcinoma of the pancreas. *Gastrointest Cancer Res*. 2013;6(3):75-79.

19. Orcutt ST, Coppola D, Hodul PJ. Colloid Carcinoma of the Pancreas: Case Report and Review of the Literature. *Case Rep Pancreat Cancer*. 2016;2(1):40-45. doi:10.1089/crpc.2016.0006

20. Siegel RL, Miller KD, Jemal A. Cancer statistics, 2020. *CA Cancer J Clin*. 2020;70(1):7-30. doi:10.3322/caac.21590

21. Yadav D, Lowenfels AB. The Epidemiology of Pancreatitis and Pancreatic Cancer. *Gastroenterology*. 2013;144(6):1252-1261. doi:10.1053/j.gastro.2013.01.068

22. Becker AE. Pancreatic ductal adenocarcinoma: Risk factors, screening, and early detection. *World J Gastroenterol*. 2014;20(32):11182. doi:10.3748/wjg.v20.i32.11182

23. Werner J, Combs SE, Springfeld C, Hartwig W, Hackert T, Büchler MW. Advanced-stage pancreatic cancer: therapy options. *Nat Rev Clin Oncol*. 2013;10(6):323-333. doi:10.1038/nrclinonc.2013.66

24. Gillen S, Schuster T, Meyer zum Büschenfelde C, Friess H, Kleeff J. Preoperative/Neoadjuvant Therapy in Pancreatic Cancer: A Systematic Review and Meta-analysis of Response and Resection Percentages. *PLoS Med*. 2010;7(4):e1000267. doi:10.1371/journal.pmed.1000267

25. Versteijne E, van Dam JL, Suker M, et al. Neoadjuvant Chemoradiotherapy Versus Upfront Surgery for Resectable and Borderline Resectable Pancreatic Cancer: Long-Term Results of the Dutch Randomized PREOPANC Trial. *Journal of Clinical Oncology*. 2022;40(11):1220-1230. doi:10.1200/JCO.21.02233

26. Meneses-Medina MI, Gervaso L, Cella CA, et al. Chemotherapy in pancreatic ductal adenocarcinoma: When cytoreduction is the aim. A systematic review and meta-analysis. *Cancer Treat Rev*. 2022;104:102338. doi:10.1016/j.ctrv.2022.102338

27. Conroy T, Desseigne F, Ychou M, et al. FOLFIRINOX versus Gemcitabine for Metastatic Pancreatic Cancer. *New England Journal of Medicine*. 2011;364(19):1817-1825. doi:10.1056/NEJMoa1011923

28. Zhang B, Zhou F, Hong J, et al. The role of FOLFIRINOX in metastatic pancreatic cancer: a meta-analysis. *World J Surg Oncol*. 2021;19(1):182. doi:10.1186/s12957-021-02291-6

29. SEER Cancer Stat Facts: Pancreatic Cancer; 2019.

30. Conroy T, Desseigne F, Ychou M, et al. FOLFIRINOX versus Gemcitabine for Metastatic Pancreatic Cancer. *New England Journal of Medicine*. 2011;364(19):1817-1825. doi:10.1056/NEJMoa1011923

31. Mohammed S, Van Buren G, Fisher WE. Pancreatic cancer: advances in treatment. *World J Gastroenterol*. 2014;20(28):9354-9360. doi:10.3748/wjg.v20.i28.9354

32. Burris HA, Moore MJ, Andersen J, et al. Improvements in survival and clinical benefit with gemcitabine as first-line therapy for patients with advanced pancreas cancer: a randomized trial. *Journal of Clinical Oncology*. 1997;15(6):2403-2413. doi:10.1200/JCO.1997.15.6.2403

33. Moore MJ, Goldstein D, Hamm J, et al. Erlotinib Plus Gemcitabine Compared With Gemcitabine Alone in Patients With Advanced Pancreatic Cancer: A Phase III Trial of the National Cancer Institute of Canada Clinical Trials Group. *Journal of Clinical Oncology*. 2007;25(15):1960-1966. doi:10.1200/JCO.2006.07.9525

34. Conroy T, Desseigne F, Ychou M, et al. FOLFIRINOX versus Gemcitabine for Metastatic Pancreatic Cancer. *New England Journal of Medicine*. 2011;364(19):1817-1825. doi:10.1056/NEJMoa1011923

35. Von Hoff DD, Ervin T, Arena FP, et al. Increased Survival in Pancreatic Cancer with nab-Paclitaxel plus Gemcitabine. *New England Journal of Medicine*. 2013;369(18):1691-1703. doi:10.1056/NEJMoa1304369

36. Ouyang G, Wu Y, Liu Z, et al. Efficacy and safety of gemcitabine-capecitabine combination therapy for pancreatic cancer. *Medicine*. 2021;100(48):e27870. doi:10.1097/MD.0000000000027870

37. Neoptolemos JP, Palmer DH, Ghaneh P, et al. Comparison of adjuvant gemcitabine and capecitabine with gemcitabine monotherapy in patients with resected pancreatic cancer (ESPAC-4): a multicentre, open-label, randomised, phase 3 trial. *The Lancet*. 2017;389(10073):1011-1024. doi:10.1016/S0140-6736(16)32409-6

38. Vernucci E, Abrego J, Gunda V, et al. Metabolic Alterations in Pancreatic Cancer Progression. *Cancers (Basel)*. 2019;12(1):2. doi:10.3390/cancers12010002

39. Grasso C, Jansen G, Giovannetti E. Drug resistance in pancreatic cancer: Impact of altered energy metabolism. *Crit Rev Oncol Hematol*. 2017;114:139-152. doi:10.1016/j.critrevonc.2017.03.026

40. Nakano Y, Tanno S, Koizumi K, et al. Gemcitabine chemoresistance and molecular markers associated with gemcitabine transport and metabolism in human pancreatic cancer cells. *Br J Cancer*. 2007;96(3):457-463. doi:10.1038/sj.bjc.6603559

41. Oria VO, Bronsert P, Thomsen AR, et al. Proteome Profiling of Primary Pancreatic Ductal Adenocarcinomas Undergoing Additive Chemoradiation Link ALDH1A1 to Early Local Recurrence and Chemoradiation Resistance. *Transl Oncol*. 2018;11(6):1307-1322. doi:10.1016/j.tranon.2018.08.001

42. Gottesman MM, Fojo T, Bates SE. Multidrug resistance in cancer: role of ATP–dependent transporters. *Nat Rev Cancer*. 2002;2(1):48-58. doi:10.1038/nrc706

43. Bridges C.B. The origin of variation. *Amer Nat* . 1922;56:51-63.

44. Dobzhansky T. Genetics of natural populations. XIII. Recombination and variability in populations of Drosphila pseudoobscura. *Genetics*. 1946;31:269-290.

45. Hennessy KM, Lee A, Chen E, Botstein D. A group of interacting yeast DNA replication genes. *Genes Dev*. 1991;5(6):958-969. doi:10.1101/gad.5.6.958

46. Huang A, Garraway LA, Ashworth A, Weber B. Synthetic lethality as an engine for cancer drug target discovery. *Nat Rev Drug Discov*. 2020;19(1):23-38. doi:10.1038/s41573-019-0046-z

47. Li S, Topatana W, Juengpanich S, et al. Development of synthetic lethality in cancer: molecular and cellular classification. *Signal Transduct Target Ther*. 2020;5(1):241. doi:10.1038/s41392-020-00358-6

48. Dey P, Baddour J, Muller F, et al. Genomic deletion of malic enzyme 2 confers collateral lethality in pancreatic cancer. *Nature*. 2017;542(7639):119-123. doi:10.1038/nature21052

49. Muller FL, Aquilanti EA, DePinho RA. Collateral Lethality: A New Therapeutic Strategy in Oncology. *Trends Cancer*. 2015;1(3):161-173. doi:10.1016/j.trecan.2015.10.002

50. Reid RJD, Du X, Sunjevaric I, et al. A Synthetic Dosage Lethal Genetic Interaction Between *CKS1B* and *PLK1* Is Conserved in Yeast and Human Cancer Cells. *Genetics*. 2016;204(2):807-819. doi:10.1534/genetics.116.190231

51. Zhang B, Tang C, Yao Y, et al. The tumor therapy landscape of synthetic lethality. *Nat Commun*. 2021;12(1):1275. doi:10.1038/s41467-021-21544-2

52. Chari S, Dworkin I. The Conditional Nature of Genetic Interactions: The Consequences of Wild-Type Backgrounds on Mutational Interactions in a Genome-Wide Modifier Screen. *PLoS Genet*. 2013;9(8):e1003661. doi:10.1371/journal.pgen.1003661

53. Li S, Topatana W, Juengpanich S, et al. Development of synthetic lethality in cancer: molecular and cellular classification. *Signal Transduct Target Ther*. 2020;5(1):241. doi:10.1038/s41392-020-00358-6

54. Bailey ML, O'Neil NJ, van Pel DM, Solomon DA, Waldman T, Hieter P. Glioblastoma Cells Containing Mutations in the Cohesin Component *STAG2* Are Sensitive to PARP Inhibition. *Mol Cancer Ther*. 2014;13(3):724-732. doi:10.1158/1535-7163.MCT-13-0749

55. Sharma S, Kelly TK, Jones PA. Epigenetics in cancer. *Carcinogenesis*. 2010;31(1):27-36. doi:10.1093/carcin/bgp220

56. Bian Y, Kitagawa R, Bansal PK, Fujii Y, Stepanov A, Kitagawa K. Synthetic genetic array screen identifies PP2A as a therapeutic target in Mad2-overexpressing tumors. *Proceedings of the National Academy of Sciences*. 2014;111(4):1628-1633. doi:10.1073/pnas.1315588111

57. Seshacharyulu P, Pandey P, Datta K, Batra SK. Phosphatase: PP2A structural importance, regulation and its aberrant expression in cancer. *Cancer Lett*. 2013;335(1):9-18. doi:10.1016/j.canlet.2013.02.036

58. Fang G, Yu H, Kirschner MW. The checkpoint protein MAD2 and the mitotic regulator CDC20 form a ternary complex with the anaphase-promoting complex to control anaphase initiation. *Genes Dev*. 1998;12(12):1871-1883. doi:10.1101/gad.12.12.1871

59. Reid RJD, Du X, Sunjevaric I, et al. A Synthetic Dosage Lethal Genetic Interaction Between *CKS1B* and *PLK1* Is Conserved in Yeast and Human Cancer Cells. *Genetics*. 2016;204(2):807-819. doi:10.1534/genetics.116.190231

60. Zhan F, Colla S, Wu X, et al. CKS1B, overexpressed in aggressive disease, regulates multiple myeloma growth and survival through SKP2- and p27Kip1-dependent and -independent mechanisms. *Blood*. 2007;109(11):4995-5001. doi:10.1182/blood-2006-07-038703

61. Choi BH, Pagano M, Dai W. Plk1 Protein Phosphorylates Phosphatase and Tensin Homolog (PTEN) and Regulates Its Mitotic Activity during the Cell Cycle. *Journal of Biological Chemistry*. 2014;289(20):14066-14074. doi:10.1074/jbc.M114.558155

62. Thng DKH, Toh TB, Chow EKH. Capitalizing on Synthetic Lethality of MYC to Treat Cancer in the Digital Age. *Trends Pharmacol Sci*. 2021;42(3):166-182. doi:10.1016/j.tips.2020.11.014

63. Roman M, Hwang E, Sweet-Cordero EA. Synthetic Vulnerabilities in the KRAS Pathway. *Cancers (Basel)*. 2022;14(12):2837. doi:10.3390/cancers14122837

64. Pang Y, Cheng M, Chen M, et al. Synthetic lethality in personalized cancer therapy. *Genome Instab Dis*. 2022;4(2):121-135. doi:10.1007/s42764-022-00080-3

65. Emerling BM, Hurov JB, Poulogiannis G, et al. Depletion of a Putatively Druggable Class of Phosphatidylinositol Kinases Inhibits Growth of p53-Null Tumors. *Cell*. 2013;155(4):844-857. doi:10.1016/j.cell.2013.09.057

66. Williamson CT, Miller R, Pemberton HN, et al. ATR inhibitors as a synthetic lethal therapy for tumours deficient in ARID1A. *Nat Commun*. 2016;7(1):13837. doi:10.1038/ncomms13837

67. Bryant HE, Schultz N, Thomas HD, et al. Specific killing of BRCA2-deficient tumours with inhibitors of poly(ADP-ribose) polymerase. *Nature*. 2005;434(7035):913-917. doi:10.1038/nature03443

68. Farmer H, McCabe N, Lord CJ, et al. Targeting the DNA repair defect in BRCA mutant cells as a therapeutic strategy. *Nature*. 2005;434(7035):917-921. doi:10.1038/nature03445

69. Jerez Y, Márquez-Rodas I, Aparicio I, Alva M, Martín M, López-Tarruella S. Poly (ADP-ribose) Polymerase Inhibition in Patients with Breast Cancer and BRCA 1 and 2 Mutations. *Drugs*. 2020;80(2):131-146. doi:10.1007/s40265-019-01235-5

70. Li LY, Guan Y Di, Chen XS, Yang JM, Cheng Y. DNA Repair Pathways in Cancer Therapy and Resistance. *Front Pharmacol*. 2021;11. doi:10.3389/fphar.2020.629266

71. Swenberg JA, Lu K, Moeller BC, et al. Endogenous versus Exogenous DNA Adducts: Their Role in Carcinogenesis, Epidemiology, and Risk Assessment. *Toxicological Sciences*. 2011;120(Supplement 1):S130-S145. doi:10.1093/toxsci/kfq371

72. Jackson SP, Bartek J. The DNA-damage response in human biology and disease. *Nature*. 2009;461(7267):1071-1078. doi:10.1038/nature08467

73. Scharer OD. Nucleotide Excision Repair in Eukaryotes. *Cold Spring Harb Perspect Biol*. 2013;5(10):a012609-a012609. doi:10.1101/cshperspect.a012609

74. Lehmann AR, McGibbon D, Stefanini M. Xeroderma pigmentosum. *Orphanet J Rare Dis*. 2011;6(1):70. doi:10.1186/1750-1172-6-70

75. Marteijn JA, Lans H, Vermeulen W, Hoeijmakers JHJ. Understanding nucleotide excision repair and its roles in cancer and ageing. *Nat Rev Mol Cell Biol*. 2014;15(7):465-481. doi:10.1038/nrm3822

76. Wallace SS, Murphy DL, Sweasy JB. Base excision repair and cancer. *Cancer Lett*. 2012;327(1-2):73-89. doi:10.1016/j.canlet.2011.12.038

77. Robertson AB, Klungland A, Rognes T, Leiros I. DNA Repair in Mammalian Cells. *Cellular and Molecular Life Sciences*. 2009;66(6):981-993. doi:10.1007/s00018-009-8736-z

78. Caldecott KW. Single-strand break repair and genetic disease. *Nat Rev Genet*. 2008;9(8):619-631. doi:10.1038/nrg2380

79. Caldecott KW. Causes and consequences of DNA single-strand breaks. *Trends Biochem Sci*. Published online November 2023. doi:10.1016/j.tibs.2023.11.001

80. Krokan HE, Bjoras M. Base Excision Repair. *Cold Spring Harb Perspect Biol*. 2013;5(4):a012583-a012583. doi:10.1101/cshperspect.a012583

81. Sinicrope FA, Sargent DJ. Molecular Pathways: Microsatellite Instability in Colorectal Cancer: Prognostic, Predictive, and Therapeutic Implications. *Clinical Cancer Research*. 2012;18(6):1506-1512. doi:10.1158/1078-0432.CCR-11-1469

82. Li K, Luo H, Huang L, Luo H, Zhu X. Microsatellite instability: a review of what the oncologist should know. *Cancer Cell Int*. 2020;20(1):16. doi:10.1186/s12935-019-1091-8

83. Clauson C, Scharer OD, Niedernhofer L. Advances in Understanding the Complex Mechanisms of DNA Interstrand Cross-Link Repair. *Cold Spring Harb Perspect Biol*. 2013;5(10):a012732-a012732. doi:10.1101/cshperspect.a012732

84. Michl J, Zimmer J, Tarsounas M. Interplay between Fanconi anemia and homologous recombination pathways in genome integrity. *EMBO J*. 2016;35(9):909-923. doi:10.15252/embj.201693860

85. Kee Y, D'Andrea AD. Molecular pathogenesis and clinical management of Fanconi anemia. *Journal of Clinical Investigation*. 2012;122(11):3799-3806. doi:10.1172/JCI58321

86. Cannan WJ, Pederson DS. Mechanisms and Consequences of Double-Strand DNA Break Formation in Chromatin. *J Cell Physiol*. 2016;231(1):3-14. doi:10.1002/jcp.25048

87. Prado F, Aguilera A. Impairment of replication fork progression mediates RNA polII transcription-associated recombination. *EMBO J*. 2005;24(6):1267-1276. doi:10.1038/sj.emboj.7600602

88. Lieber MR. The Mechanism of Double-Strand DNA Break Repair by the Nonhomologous DNA End-Joining Pathway. *Annu Rev Biochem*. 2010;79(1):181-211. doi:10.1146/annurev.biochem.052308.093131

89. Katsuki Y, Jeggo PA, Uchihara Y, Takata M, Shibata A. DNA double-strand break end resection: a critical relay point for determining the pathway of repair and signaling. *Genome Instab Dis*. 2020;1(4):155-171. doi:10.1007/s42764-020-00017-8

90. Hossain Md, Lin Y, Yan S. Single-Strand Break End Resection in Genome Integrity: Mechanism and Regulation by APE2. *Int J Mol Sci*. 2018;19(8):2389. doi:10.3390/ijms19082389

91. Kuzminov A. Single-strand interruptions in replicating chromosomes cause double-strand breaks. *Proceedings of the National Academy of Sciences*. 2001;98(15):8241-8246. doi:10.1073/pnas.131009198

92. Pourquier P, Pommier Y. Topoisomerase I-mediated DNA damage. In: ; 2001:189-216. doi:10.1016/S0065-230X(01)80016-6

93. Pommier Y, Sun Y, Huang S yin N, Nitiss JL. Roles of eukaryotic topoisomerases in transcription, replication and genomic stability. *Nat Rev Mol Cell Biol*. 2016;17(11):703-721. doi:10.1038/nrm.2016.111

94. Yan S, Sorrell M, Berman Z. Functional interplay between ATM/ATR-mediated DNA damage response and DNA repair pathways in oxidative stress. *Cellular and Molecular Life Sciences*. 2014;71(20):3951-3967. doi:10.1007/s00018-014-1666-4

95. Caldecott KW. Single-strand break repair and genetic disease. *Nat Rev Genet*. 2008;9(8):619-631. doi:10.1038/nrg2380

96. Jubin T, Kadam A, Jariwala M, et al. The PARP family: insights into functional aspects of poly (ADP-ribose) polymerase-1 in cell growth and survival. *Cell Prolif*. 2016;49(4):421-437. doi:10.1111/cpr.12268

97. Ray Chaudhuri A, Nussenzweig A. The multifaceted roles of PARP1 in DNA repair and chromatin remodelling. *Nat Rev Mol Cell Biol*. 2017;18(10):610-621. doi:10.1038/nrm.2017.53

98. Kim MY, Zhang T, Kraus WL. Poly(ADP-ribosyl)ation by PARP-1: `PAR-laying' NAD $^{+}$ into a nuclear signal. *Genes Dev*. 2005;19(17):1951-1967. doi:10.1101/gad.1331805

99. Caldecott KW. XRCC1 protein; Form and function. *DNA Repair (Amst)*. 2019;81:102664. doi:10.1016/j.dnarep.2019.102664

100. Harris JL, Jakob B, Taucher-Scholz G, Dianov GL, Becherel OJ, Lavin MF. Aprataxin, poly-ADP ribose polymerase 1 (PARP-1) and apurinic endonuclease 1 (APE1) function together to protect the genome against oxidative damage. *Hum Mol Genet*. 2009;18(21):4102-4117. doi:10.1093/hmg/ddp359

101. Caldecott KW. Causes and consequences of DNA single-strand breaks. *Trends Biochem Sci*. Published online November 2023. doi:10.1016/j.tibs.2023.11.001

102. Leppard JB, Dong Z, Mackey ZB, Tomkinson AE. Physical and Functional Interaction between DNA Ligase IIIα and Poly(ADP-Ribose) Polymerase 1 in DNA Single-Strand Break Repair. *Mol Cell Biol*. 2003;23(16):5919-5927. doi:10.1128/MCB.23.16.5919-5927.2003

103. Koczor CA, Saville KM, Andrews JF, et al. Temporal dynamics of base excision/single-strand break repair protein complex assembly/disassembly are modulated by the PARP/NAD+/SIRT6 axis. *Cell Rep*. 2021;37(5):109917. doi:10.1016/j.celrep.2021.109917

104. Xu F, Sun Y, Yang S, et al. Cytoplasmic PARP-1 promotes pancreatic cancer tumorigenesis and resistance. *Int J Cancer*. 2019;145(2):474-483. doi:10.1002/ijc.32108

105. Ossovskaya V, Koo IC, Kaldjian EP, Alvares C, Sherman BM. Upregulation of Poly (ADP-Ribose) Polymerase-1 (PARP1) in Triple-Negative Breast Cancer and Other Primary Human Tumor Types. *Genes Cancer*. 2010;1(8):812-821. doi:10.1177/1947601910383418

106. Lau CH, Seow KM, Chen KH. The Molecular Mechanisms of Actions, Effects, and Clinical Implications of PARP Inhibitors in Epithelial Ovarian Cancers: A Systematic Review. *Int J Mol Sci*. 2022;23(15):8125. doi:10.3390/ijms23158125

107. Cortesi L TA. Molecular Mechanisms of PARP Inhibitors in BRCA-related Ovarian Cancer. *J Cancer Sci Ther*. 2013;05(11). doi:10.4172/1948-5956.1000234

108. Murai J, Huang S yin N, Das BB, et al. Trapping of PARP1 and PARP2 by Clinical PARP Inhibitors. *Cancer Res*. 2012;72(21):5588-5599. doi:10.1158/0008-5472.CAN-12-2753

109. Ragupathi A, Singh M, Perez AM, Zhang D. Targeting the BRCA1/2 deficient cancer with PARP inhibitors: Clinical outcomes and mechanistic insights. *Front Cell Dev Biol*. 2023;11. doi:10.3389/fcell.2023.1133472

110. Farmer H, McCabe N, Lord CJ, et al. Targeting the DNA repair defect in BRCA mutant cells as a therapeutic strategy. *Nature*. 2005;434(7035):917-921. doi:10.1038/nature03445

111. Bryant HE, Schultz N, Thomas HD, et al. Specific killing of BRCA2-deficient tumours with inhibitors of poly(ADP-ribose) polymerase. *Nature*. 2005;434(7035):913-917. doi:10.1038/nature03443

112. Daei Sorkhabi A, Fazlollahi A, Sarkesh A, et al. Efficacy and safety of veliparib plus chemotherapy for the treatment of lung cancer: A systematic review of clinical trials. *PLoS One*. 2023;18(9):e0291044. doi:10.1371/journal.pone.0291044

113. Xu J, Keenan TE, Overmoyer B, et al. Phase II trial of veliparib and temozolomide in metastatic breast cancer patients with and without BRCA1/2 mutations. *Breast Cancer Res Treat*. 2021;189(3):641-651. doi:10.1007/s10549-021-06292-7

114. Lee A. Fuzuloparib: First Approval. *Drugs*. 2021;81(10):1221-1226. doi:10.1007/s40265-021-01541-x

115. Markham A. Pamiparib: First Approval. *Drugs*. 2021;81(11):1343-1348. doi:10.1007/s40265-021-01552-8

116. Hoy SM. Talazoparib: First Global Approval. *Drugs*. 2018;78(18):1939-1946. doi:10.1007/s40265-018-1026-z

117. Clinical Trials.gov. A study evaluating talazoparib (BMN 673), a PARP inhibitor, in advanced and/or metastatic breast cancer patients with BRCA mutation (EMBRACA Study) (EMBRACA). 2022. Accessed December 28, 2023. https://clinicaltrials.gov/ct2/show/NCT01945775

118. Litton JK, Rugo HS, Ettl J, et al. Talazoparib in Patients with Advanced Breast Cancer and a Germline *BRCA* Mutation. *New England Journal of Medicine*. 2018;379(8):753-763. doi:10.1056/NEJMoa1802905

119. Murai J, Huang SYN, Renaud A, et al. Stereospecific PARP Trapping by BMN 673 and Comparison with Olaparib and Rucaparib. *Mol Cancer Ther*. 2014;13(2):433-443. doi:10.1158/1535-7163.MCT-13-0803

120. Shen Y, Rehman FL, Feng Y, et al. BMN 673, a Novel and Highly Potent PARP1/2 Inhibitor for the Treatment of Human Cancers with DNA Repair Deficiency. *Clinical Cancer Research*. 2013;19(18):5003-5015. doi:10.1158/1078-0432.CCR-13-1391

121. Boussios S, Abson C, Moschetta M, et al. Poly (ADP-Ribose) Polymerase Inhibitors: Talazoparib in Ovarian Cancer and Beyond. *Drugs R D*. 2020;20(2):55-73. doi:10.1007/s40268-020-00301-8

122. Owonikoko TK, Redman MW, Byers LA, et al. Phase 2 Study of Talazoparib in Patients With Homologous Recombination Repair–Deficient Squamous Cell Lung Cancer: Lung-MAP Substudy S1400G. *Clin Lung Cancer*. 2021;22(3):187-194.e1. doi:10.1016/j.cllc.2021.01.001

123. Kachmazov A, Bolotina L, Kornietskaya A, Kuznetsova O, Ivanov M, Fedenko A. Complete response to talazoparib in patient with pancreatic adenocarcinoma harboring somatic PALB2 mutation: A case report and literature review. *Front Oncol*. 2022;12. doi:10.3389/fonc.2022.953908

124. Mittra A, Coyne GHOS, Zlott J, et al. Pharmacodynamic effects of the PARP inhibitor talazoparib (MDV3800, BMN 673) in patients with BRCA-mutated advanced solid tumors. *Cancer Chemother Pharmacol*. Published online November 27, 2023. doi:10.1007/s00280-023-04600-0

125. Khanna KK, Jackson SP. DNA double-strand breaks: signaling, repair and the cancer connection. *Nat Genet*. 2001;27(3):247-254. doi:10.1038/85798

126. Soulas-Sprauel P, Rivera-Munoz P, Malivert L, et al. V(D)J and immunoglobulin class switch recombinations: a paradigm to study the regulation of DNA end-joining. *Oncogene*. 2007;26(56):7780-7791. doi:10.1038/sj.onc.1210875

127. de Massy B. Initiation of Meiotic Recombination: How and Where? Conservation and Specificities Among Eukaryotes. *Annu Rev Genet*. 2013;47(1):563-599. doi:10.1146/annurev-genet-110711-155423

128. Syeda AH, Hawkins M, McGlynn P. Recombination and Replication. *Cold Spring Harb Perspect Biol*. 2014;6(11):a016550-a016550. doi:10.1101/cshperspect.a016550

129. Woodbine L, Brunton H, Goodarzi AA, Shibata A, Jeggo PA. Endogenously induced DNA double strand breaks arise in heterochromatic DNA regions and require ataxia telangiectasia mutated and Artemis for their repair. *Nucleic Acids Res*. 2011;39(16):6986-6997. doi:10.1093/nar/gkr331

130. Mehta A, Haber JE. Sources of DNA Double-Strand Breaks and Models of Recombinational DNA Repair. *Cold Spring Harb Perspect Biol*. 2014;6(9):a016428-a016428. doi:10.1101/cshperspect.a016428

131. Tchounwou PB, Dasari S, Noubissi FK, Ray P, Kumar S. Advances in Our Understanding of the Molecular Mechanisms of Action of Cisplatin in Cancer Therapy. *J Exp Pharmacol*. 2021;Volume 13:303-328. doi:10.2147/JEP.S267383

132. Li X, Heyer WD. Homologous recombination in DNA repair and DNA damage tolerance. *Cell Res*. 2008;18(1):99-113. doi:10.1038/cr.2008.1

133. Jackson SP, Bartek J. The DNA-damage response in human biology and disease. *Nature*. 2009;461(7267):1071-1078. doi:10.1038/nature08467

134. Saito YFHKJ. Role of NBS1 in DNA damage response and its relationship with cancer development. *Transl Cancer Res*. 2013;2(3):178-189.

135. Matsuoka S, Ballif BA, Smogorzewska A, et al. ATM and ATR Substrate Analysis Reveals Extensive Protein Networks Responsive to DNA Damage. *Science (1979)*. 2007;316(5828):1160-1166. doi:10.1126/science.1140321

136. Sun Y, McCorvie TJ, Yates LA, Zhang X. Structural basis of homologous recombination. *Cellular and Molecular Life Sciences*. 2020;77(1):3-18. doi:10.1007/s00018-019-03365-1

137. Lamarche BJ, Orazio NI, Weitzman MD. The MRN complex in double-strand break repair and telomere maintenance. *FEBS Lett*. 2010;584(17):3682-3695. doi:10.1016/j.febslet.2010.07.029

138. Kinner A, Wu W, Staudt C, Iliakis G. -H2AX in recognition and signaling of DNA double-strand breaks in the context of chromatin. *Nucleic Acids Res*. 2008;36(17):5678-5694. doi:10.1093/nar/gkn550

139. Chen L, Nievera CJ, Lee AYL, Wu X. Cell Cycle-dependent Complex Formation of BRCA1·CtIP·MRN Is Important for DNA Double-strand Break Repair. *Journal of Biological Chemistry*. 2008;283(12):7713-7720. doi:10.1074/jbc.M710245200

140. Sturzenegger A, Burdova K, Kanagaraj R, et al. DNA2 Cooperates with the WRN and BLM RecQ Helicases to Mediate Long-range DNA End Resection in Human Cells. *Journal of Biological Chemistry*. 2014;289(39):27314-27326. doi:10.1074/jbc.M114.578823

141. Kijas AW, Lim YC, Bolderson E, et al. ATM-dependent phosphorylation of MRE11 controls extent of resection during homology directed repair by signalling through Exonuclease 1. *Nucleic Acids Res*. 2015;43(17):8352-8367. doi:10.1093/nar/gkv754

142. Sun Y, McCorvie TJ, Yates LA, Zhang X. Structural basis of homologous recombination. *Cellular and Molecular Life Sciences*. 2020;77(1):3-18. doi:10.1007/s00018-019-03365-1

143. Buisson R, Niraj J, Rodrigue A, et al. Coupling of Homologous Recombination and the Checkpoint by ATR. *Mol Cell*. 2017;65(2):336-346. doi:10.1016/j.molcel.2016.12.007

144. Kwon Y, Rösner H, Zhao W, et al. DNA binding and RAD51 engagement by the BRCA2 C-terminus orchestrate DNA repair and replication fork preservation. *Nat Commun*. 2023;14(1):432. doi:10.1038/s41467-023-36211-x

145. Sullivan MR, Bernstein KA. RAD-ical New Insights into RAD51 Regulation. *Genes (Basel)*. 2018;9(12):629. doi:10.3390/genes9120629

146. Holloman WK. Unraveling the mechanism of BRCA2 in homologous recombination. *Nat Struct Mol Biol*. 2011;18(7):748-754. doi:10.1038/nsmb.2096

147. Wright WD, Shah SS, Heyer WD. Homologous recombination and the repair of DNA double-strand breaks. *Journal of Biological Chemistry*. 2018;293(27):10524-10535. doi:10.1074/jbc.TM118.000372

148. Tavares EM, Wright WD, Heyer WD, Le Cam E, Dupaigne P. In vitro role of Rad54 in Rad51-ssDNA filament-dependent homology search and synaptic complexes formation. *Nat Commun*. 2019;10(1):4058. doi:10.1038/s41467-019-12082-z

149. McVey M, Khodaverdian VY, Meyer D, Cerqueira PG, Heyer WD. Eukaryotic DNA Polymerases in Homologous Recombination. *Annu Rev Genet*. 2016;50(1):393-421. doi:10.1146/annurev-genet-120215-035243

150. Li X, Zhang XP, Solinger JA, et al. Rad51 and Rad54 ATPase activities are both required to modulate Rad51-dsDNA filament dynamics. *Nucleic Acids Res*. 2007;35(12):4124-4140. doi:10.1093/nar/gkm412

151. Krejci L, Altmannova V, Spirek M, Zhao X. Homologous recombination and its regulation. *Nucleic Acids Res*. 2012;40(13):5795-5818. doi:10.1093/nar/gks270

152. Rodgers K, McVey M. Error-Prone Repair of DNA Double-Strand Breaks. *J Cell Physiol*. 2016;231(1):15-24. doi:10.1002/jcp.25053

153. Miura T, Yamana Y, Usui T, Ogawa HI, Yamamoto MT, Kusano K. Homologous Recombination via Synthesis-Dependent Strand Annealing in Yeast Requires the Irc20 and Srs2 DNA Helicases. *Genetics*. 2012;191(1):65-78. doi:10.1534/genetics.112.139105

154. Petronczki M, Siomos MF, Nasmyth K. Un Ménage à Quatre. *Cell*. 2003;112(4):423-440. doi:10.1016/S0092-8674(03)00083-7

155. Sansam CL, Pezza RJ. Connecting by breaking and repairing: mechanisms of DNA strand exchange in meiotic recombination. *FEBS J*. 2015;282(13):2444-2457. doi:10.1111/febs.13317

156. Sun Y, McCorvie TJ, Yates LA, Zhang X. Structural basis of homologous recombination. *Cellular and Molecular Life Sciences*. 2020;77(1):3-18. doi:10.1007/s00018-019-03365-1

157. Brouwer I, Moschetti T, Candelli A, et al. Two distinct conformational states define the interaction of human RAD51- ATP with single-stranded DNA. *EMBO J*. 2018;37(7). doi:10.15252/embj.201798162

158. Conway AB, Lynch TW, Zhang Y, et al. Crystal structure of a Rad51 filament. *Nat Struct Mol Biol*. 2004;11(8):791-796. doi:10.1038/nsmb795

159. Robertson RB, Moses DN, Kwon Y, et al. Structural transitions within human Rad51 nucleoprotein filaments. *Proceedings of the National Academy of Sciences*. 2009;106(31):12688-12693. doi:10.1073/pnas.0811465106

160. Kim H, Morimatsu K, Nordén B, Ardhammar M, Takahashi M. ADP stabilizes the human Rad51-single stranded DNA complex and promotes its DNA annealing activity. *Genes to Cells*. 2002;7(11):1125-1134. doi:10.1046/j.1365-2443.2002.00588.x

161. Matsuo Y, Sakane I, Takizawa Y, Takahashi M, Kurumizaka H. Roles of the human Rad51 L1 and L2 loops in DNA binding. *FEBS J*. 2006;273(14):3148-3159. doi:10.1111/j.1742-4658.2006.05323.x

162. Sung P, Krejci L, Van Komen S, Sehorn MG. Rad51 Recombinase and Recombination Mediators. *Journal of Biological Chemistry*. 2003;278(44):42729-42732. doi:10.1074/jbc.R300027200

163. Haber JE. DNA Repair: The Search for Homology. *BioEssays*. 2018;40(5):1700229. doi:10.1002/bies.201700229

164. Alshareeda AT, Negm OH, Aleskandarany MA, et al. Clinical and biological significance of RAD51 expression in breast cancer: a key DNA damage response protein. *Breast Cancer Res Treat*. 2016;159(1):41-53. doi:10.1007/s10549-016-3915-8

165. Nagathihalli NS, Nagaraju G. RAD51 as a potential biomarker and therapeutic target for pancreatic cancer. *Biochimica et Biophysica Acta (BBA) - Reviews on Cancer*. 2011;1816(2):209-218. doi:10.1016/j.bbcan.2011.07.004

166. Maacke H, Jost K, Opitz S, et al. DNA repair and recombination factor Rad51 is over-expressed in human pancreatic adenocarcinoma. *Oncogene*. 2000;19(23):2791-2795. doi:10.1038/sj.onc.1203578

167. Tripathi A, Balakrishna P, Agarwal N. PARP inhibitors in castration-resistant prostate cancer. *Cancer Treat Res Commun*. 2020;24:100199. doi:10.1016/j.ctarc.2020.100199

168. Hu J, Zhang Z, Zhao L, Li L, Zuo W, Han L. High expression of RAD51 promotes DNA damage repair and survival in KRAS-mutant lung cancer cells. *BMB Rep*. 2019;52(2):151-156. doi:10.5483/BMBRep.2019.52.2.213

169. Zhang X, Ma N, Yao W, Li S, Ren Z. RAD51 is a potential marker for prognosis and regulates cell proliferation in pancreatic cancer. *Cancer Cell Int*. 2019;19(1):356. doi:10.1186/s12935-019-1077-6

170. Sarwar R, Sheikh AK, Mahjabeen I, Bashir K, Saeed S, Kayani MA. Upregulation of RAD51 expression is associated with progression of thyroid carcinoma. *Exp Mol Pathol*. 2017;102(3):446-454. doi:10.1016/j.yexmp.2017.05.001

171. Tsai MS, Kuo YH, Chiu YF, Su YC, Lin YW. Down-Regulation of Rad51 Expression Overcomes Drug Resistance to Gemcitabine in Human Non–Small-Cell Lung Cancer Cells. *Journal of Pharmacology and Experimental Therapeutics*. 2010;335(3):830-840. doi:10.1124/jpet.110.173146

172. Du LQ, Wang Y, Wang H, Cao J, Liu Q, Fan FY. Knockdown of Rad51 expression induces radiation- and chemo-sensitivity in osteosarcoma cells. *Medical Oncology*. 2011;28(4):1481-1487. doi:10.1007/s12032-010-9605-1

173. Hansen LT, Lundin C, Spang-Thomsen M, Petersen LN, Helleday T. The role of RAD51 in etoposide (VP16) resistance in small cell lung cancer. *Int J Cancer*. 2003;105(4):472-479. doi:10.1002/ijc.11106

174. Buisson R, Dion-Côté AM, Coulombe Y, et al. Cooperation of breast cancer proteins PALB2 and piccolo BRCA2 in stimulating homologous recombination. *Nat Struct Mol Biol*. 2010;17(10):1247-1254. doi:10.1038/nsmb.1915

175. von Nicolai C, Ehlén Å, Martin C, Zhang X, Carreira A. A second DNA binding site in human BRCA2 promotes homologous recombination. *Nat Commun*. 2016;7(1):12813. doi:10.1038/ncomms12813

176. Carreira A, Kowalczykowski SC. Two classes of BRC repeats in BRCA2 promote RAD51 nucleoprotein filament function by distinct mechanisms. *Proceedings of the National Academy of Sciences*. 2011;108(26):10448-10453. doi:10.1073/pnas.1106971108

177. Yang H, Jeffrey PD, Miller J, et al. BRCA2 Function in DNA Binding and Recombination from a BRCA2-DSS1-ssDNA Structure. *Science (1979)*. 2002;297(5588):1837-1848. doi:10.1126/science.297.5588.1837

178. Esashi F, Galkin VE, Yu X, Egelman EH, West SC. Stabilization of RAD51 nucleoprotein filaments by the C-terminal region of BRCA2. *Nat Struct Mol Biol*. 2007;14(6):468-474. doi:10.1038/nsmb1245

179. Yano K ichi, Morotomi K, Saito H, Kato M, Matsuo F, Miki Y. Nuclear Localization Signals of the BRCA2 Protein. *Biochem Biophys Res Commun*. 2000;270(1):171-175. doi:10.1006/bbrc.2000.2392

180. Andreassen PR, Seo J, Wiek C, Hanenberg H. Understanding BRCA2 Function as a Tumor Suppressor Based on Domain-Specific Activities in DNA Damage Responses. *Genes (Basel)*. 2021;12(7):1034. doi:10.3390/genes12071034

181. Schipani F, Manerba M, Marotta R, et al. The Mechanistic Understanding of RAD51 Defibrillation: A Critical Step in BRCA2-Mediated DNA Repair by Homologous Recombination. *Int J Mol Sci*. 2022;23(15):8338. doi:10.3390/ijms23158338

182. Shahid T, Soroka J, Kong EH, et al. Structure and mechanism of action of the BRCA2 breast cancer tumor suppressor. *Nat Struct Mol Biol*. 2014;21(11):962-968. doi:10.1038/nsmb.2899

183. Daley JM, Niu H, Miller AS, Sung P. Biochemical mechanism of DSB end resection and its regulation. *DNA Repair (Amst)*. 2015;32:66-74. doi:10.1016/j.dnarep.2015.04.015

184. Jeyasekharan AD, Liu Y, Hattori H, et al. A cancer-associated BRCA2 mutation reveals masked nuclear export signals controlling localization. *Nat Struct Mol Biol*. 2013;20(10):1191-1198. doi:10.1038/nsmb.2666

185. Godet I, M. Gilkes D. BRCA1 and BRCA2 mutations and treatment strategies for breast cancer. *Integr Cancer Sci Ther*. 2017;4(1). doi:10.15761/ICST.1000228

186. Mersch J, Jackson MA, Park M, et al. Cancers associated with *BRCA1* and *BRCA2* mutations other than breast and ovarian. *Cancer*. 2015;121(2):269-275. doi:10.1002/cncr.29041

187. Cavanagh H, Rogers KMA. The role of BRCA1 and BRCA2 mutations in prostate, pancreatic and stomach cancers. *Hered Cancer Clin Pract*. 2015;13(1):16. doi:10.1186/s13053-015-0038-x

188. Xie C, Luo J, He Y, Jiang L, Zhong L, Shi Y. BRCA2 gene mutation in cancer. *Medicine*. 2022;101(45):e31705. doi:10.1097/MD.0000000000031705

189. Mehrgou A, Akouchekian M. The importance of BRCA1 and BRCA2 genes mutations in breast cancer development. *Med J Islam Repub Iran*. 2016;30:369.

190. Gorodetska I, Kozeretska I, Dubrovska A. *BRCA* Genes: The Role in Genome Stability, Cancer Stemness and Therapy Resistance. *J Cancer*. 2019;10(9):2109-2127. doi:10.7150/jca.30410

191. Ladan MM, van Gent DC, Jager A. Homologous Recombination Deficiency Testing for BRCA-Like Tumors: The Road to Clinical Validation. *Cancers (Basel)*. 2021;13(5):1004. doi:10.3390/cancers13051004

192. Pellegrini L, Yu DS, Lo T, et al. Insights into DNA recombination from the structure of a RAD51–BRCA2 complex. *Nature*. 2002;420(6913):287-293. doi:10.1038/nature01230

193. Short JM, Liu Y, Chen S, et al. High-resolution structure of the presynaptic RAD51 filament on single-stranded DNA by electron cryo-microscopy. *Nucleic Acids Res*. Published online September 5, 2016:gkw783. doi:10.1093/nar/gkw783

194. Rajendra E, Venkitaraman AR. Two modules in the BRC repeats of BRCA2 mediate structural and functional interactions with the RAD51 recombinase. *Nucleic Acids Res*. 2010;38(1):82-96. doi:10.1093/nar/gkp873

195. Ward A, Dong L, Harris JM, et al. Quinazolinone derivatives as inhibitors of homologous recombinase RAD51. *Bioorg Med Chem Lett*. 2017;27(14):3096-3100. doi:10.1016/j.bmcl.2017.05.039

196. Roberti M, Schipani F, Bagnolini G, et al. Rad51/BRCA2 disruptors inhibit homologous recombination and synergize with olaparib in pancreatic cancer cells. *Eur J Med Chem*. 2019;165:80-92. doi:10.1016/j.ejmech.2019.01.008

197. Nomme J, Renodon-Cornière A, Asanomi Y, et al. Design of Potent Inhibitors of Human RAD51 Recombinase Based on BRC Motifs of BRCA2 Protein: Modeling and Experimental Validation of a Chimera Peptide. *J Med Chem*. 2010;53(15):5782-5791. doi:10.1021/jm1002974

198. Falchi F, Giacomini E, Masini T, et al. Synthetic Lethality Triggered by Combining Olaparib with BRCA2–Rad51 Disruptors. *ACS Chem Biol*. 2017;12(10):2491-2497. doi:10.1021/acschembio.7b00707

199. Bagnolini G, Balboni B, Schipani F, et al. Identification of RAD51–BRCA2 Inhibitors Using *N* -Acylhydrazone-Based Dynamic Combinatorial Chemistry. *ACS Med Chem Lett*. 2022;13(8):1262-1269. doi:10.1021/acsmedchemlett.2c00063

200. Scott DE, Francis-Newton NJ, Marsh ME, et al. A small-molecule inhibitor of the BRCA2-RAD51 interaction modulates RAD51 assembly and potentiates DNA damage-induced cell death. *Cell Chem Biol*. 2021;28(6):835-847.e5. doi:10.1016/j.chembiol.2021.02.006

201. Shkundina IS, Gall AA, Dick A, Cocklin S, Mazin A V. New RAD51 Inhibitors to Target Homologous Recombination in Human Cells. *Genes (Basel)*. 2021;12(6):920. doi:10.3390/genes12060920

202. Bagnolini G, Balboni B, Schipani F, et al. Identification of RAD51–BRCA2 Inhibitors Using *N* -Acylhydrazone-Based Dynamic Combinatorial Chemistry. *ACS Med Chem Lett*. 2022;13(8):1262-1269. doi:10.1021/acsmedchemlett.2c00063

203. Roberti M, Schipani F, Bagnolini G, et al. Rad51/BRCA2 disruptors inhibit homologous recombination and synergize with olaparib in pancreatic cancer cells. *Eur J Med Chem*. 2019;165:80-92. doi:10.1016/j.ejmech.2019.01.008

204. Bagnolini G, Milano D, Manerba M, et al. Synthetic Lethality in Pancreatic Cancer: Discovery of a New RAD51-BRCA2 Small Molecule Disruptor That Inhibits Homologous Recombination and Synergizes with Olaparib. *J Med Chem*. 2020;63(5):2588-2619. doi:10.1021/acs.jmedchem.9b01526

205. Abbott DW, Holt JT, Freeman ML. Double-Strand Break Repair Deficiency and Radiation Sensitivity in BRCA2 Mutant Cancer Cells. *JNCI Journal of the National Cancer Institute*. 1998;90(13):978-985. doi:10.1093/jnci/90.13.978

206. Deer EL, González-Hernández J, Coursen JD, et al. Phenotype and Genotype of Pancreatic Cancer Cell Lines. *Pancreas*. 2010;39(4):425-435. doi:10.1097/MPA.0b013e3181c15963

207. Böttger R, Hoffmann R, Knappe D. Differential stability of therapeutic peptides with different proteolytic cleavage sites in blood, plasma and serum. *PLoS One*. 2017;12(6):e0178943. doi:10.1371/journal.pone.0178943

208. Taymaz-Nikerel H, Karabekmez ME, Eraslan S, Kırdar B. Doxorubicin induces an extensive transcriptional and metabolic rewiring in yeast cells. *Sci Rep*. 2018;8(1):13672. doi:10.1038/s41598-018-31939-9

209. Kciuk M, Gielecińska A, Mujwar S, et al. Doxorubicin—An Agent with Multiple Mechanisms of Anticancer Activity. *Cells*. 2023;12(4):659. doi:10.3390/cells12040659

210. Dasari S, Bernard Tchounwou P. Cisplatin in cancer therapy: Molecular mechanisms of action. *Eur J Pharmacol*. 2014;740:364-378. doi:10.1016/j.ejphar.2014.07.025

211. Brown A, Kumar S, Tchounwou PB. Cisplatin-Based Chemotherapy of Human Cancers. *J Cancer Sci Ther*. 2019;11(4).

212. Milletti G, Strocchio L, Pagliara D, et al. Canonical and Noncanonical Roles of Fanconi Anemia Proteins: Implications in Cancer Predisposition. *Cancers (Basel)*. 2020;12(9):2684. doi:10.3390/cancers12092684

213. Deans AJ, West SC. DNA interstrand crosslink repair and cancer. *Nat Rev Cancer*. 2011;11(7):467-480. doi:10.1038/nrc3088

214. Thompson EL, Yeo JE, Lee EA, et al. FANCI and FANCD2 have common as well as independent functions during the cellular replication stress response. *Nucleic Acids Res*. 2017;45(20):11837-11857. doi:10.1093/nar/gkx847

215. Shah RB, Kernan JL, van Hoogstraten A, et al. FANCI functions as a repair/apoptosis switch in response to DNA crosslinks. *Dev Cell*. 2021;56(15):2207-2222.e7. doi:10.1016/j.devcel.2021.06.010

216. Sato K, Shimomuki M, Katsuki Y, et al. FANCI-FANCD2 stabilizes the RAD51-DNA complex by binding RAD51 and protects the 5′-DNA end. *Nucleic Acids Res*. 2016;44(22):10758-10771. doi:10.1093/nar/gkw876

217. Schlacher K, Wu H, Jasin M. A Distinct Replication Fork Protection Pathway Connects Fanconi Anemia Tumor Suppressors to RAD51-BRCA1/2. *Cancer Cell*. 2012;22(1):106-116. doi:10.1016/j.ccr.2012.05.015

218. Li W, Yu M, Zhang J, et al. High expression levels of FANCI correlate with worse prognosis and promote tumor growth of lung adenocarcinoma partly via suppression of M1 macrophages. *Gene*. 2023;851:147053. doi:10.1016/j.gene.2022.147053

219. Liu X, Liu X, Han X. FANCI may serve as a prognostic biomarker for cervical cancer. *Medicine*. 2021;100(51):e27690. doi:10.1097/MD.0000000000027690

220. Yang Z, Song Y, Li Y, et al. Integrative analyses of prognosis, tumor immunity, and ceRNA network of the ferroptosis-associated gene FANCD2 in hepatocellular carcinoma. *Front Genet*. 2022;13. doi:10.3389/fgene.2022.955225

221. Fagerholm R, Sprott K, Heikkinen T, et al. Overabundant FANCD2, alone and combined with NQO1, is a sensitive marker of adverse prognosis in breast cancer. *Annals of Oncology*. 2013;24(11):2780-2785. doi:10.1093/annonc/mdt290

222. Hou Y, Li J, Yu A, et al. FANCI is Associated with Poor Prognosis and Immune Infiltration in Liver Hepatocellular Carcinoma. *Int J Med Sci*. 2023;20(7):918-932. doi:10.7150/ijms.83760

223. Cavero S, Limbo O, Russell P. Critical Functions of Rpa3/Ssb3 in S-Phase DNA Damage Responses in Fission Yeast. *PLoS Genet*. 2010;6(9):e1001138. doi:10.1371/journal.pgen.1001138

224. Dai Z, Wang S, Zhang W, Yang Y. Elevated Expression of RPA3 Is Involved in Gastric Cancer Tumorigenesis and Associated with Poor Patient Survival. *Dig Dis Sci*. 2017;62(9):2369-2375. doi:10.1007/s10620-017-4696-6

225. Thu KL, Radulovich N, Becker-Santos DD, et al. SOX15 is a candidate tumor suppressor in pancreatic cancer with a potential role in Wnt/β-catenin signaling. *Oncogene*. 2014;33(3):279-288. doi:10.1038/onc.2012.595

226. Rathos MJ, Joshi K, Khanwalkar H, Manohar SM, Joshi KS. Molecular evidence for increased antitumor activity of gemcitabine in combination with a cyclin-dependent kinase inhibitor, P276-00 in pancreatic cancers. *J Transl Med*. 2012;10(1):161. doi:10.1186/1479-5876-10-161

227. Huanwen W, Zhiyong L, Xiaohua S, Xinyu R, Kai W, Tonghua L. Intrinsic chemoresistance to gemcitabine is associated with constitutive and laminin-induced phosphorylation of FAK in pancreatic cancer cell lines. *Mol Cancer*. 2009;8(1):125. doi:10.1186/1476-4598-8-125

228. Fryer RA, Barlett B, Galustian C, Dalgleish AG. Mechanisms underlying gemcitabine resistance in pancreatic cancer and sensitisation by the iMiD^{TM} lenalidomide. *Anticancer Res*. 2011;31(11):3747-3756.

229. Tan MH, Nowak NJ, Loor R, et al. Characterization of a New Primary Human Pancreatic Tumor Line. *Cancer Invest*. 1986;4(1):15-23. doi:10.3109/07357908609039823

230. Zhu J, Zhou L, Wu G, et al. A novel small molecule RAD51 inactivator overcomes imatinib-resistance in chronic myeloid leukaemia. *EMBO Mol Med*. 2013;5(3):353-365. doi:10.1002/emmm.201201760

231. Nelson AR, Borland L, Allbritton NL, Sims CE. Myristoyl-Based Transport of Peptides into Living Cells. *Biochemistry*. 2007;46(51):14771-14781. doi:10.1021/bi701295k

232. Youn P, Chen Y, Furgeson DY. A Myristoylated Cell-Penetrating Peptide Bearing a Transferrin Receptor-Targeting Sequence for Neuro-Targeted siRNA Delivery. *Mol Pharm*. 2014;11(2):486-495. doi:10.1021/mp400446v

233. Li C, Liu H, Yang Y, et al. N-myristoylation of Antimicrobial Peptide CM4 Enhances Its Anticancer Activity by Interacting With Cell Membrane and Targeting Mitochondria in Breast Cancer Cells. *Front Pharmacol*. 2018;9. doi:10.3389/fphar.2018.01297

234. Qu C, Zhao Y, Feng G, et al. RPA3 is a potential marker of prognosis and radioresistance for nasopharyngeal carcinoma. *J Cell Mol Med*. 2017;21(11):2872-2883. doi:10.1111/jcmm.13200

235. Sato K, Shimomuki M, Katsuki Y, et al. FANCI-FANCD2 stabilizes the RAD51-DNA complex by binding RAD51 and protects the 5′-DNA end. *Nucleic Acids Res*. 2016;44(22):10758-10771. doi:10.1093/nar/gkw876

236. Vulpetti A, Hommel U, Landrum G, Lewis R, Dalvit C. Design and NMR-Based Screening of LEF, a Library of Chemical Fragments with Different Local Environment of Fluorine. *J Am Chem Soc*. 2009;131(36):12949-12959. doi:10.1021/ja905207t

237. Mureddu LG, Vuister GW. Fragment-Based Drug Discovery by NMR. Where Are the Successes and Where can It Be Improved? *Front Mol Biosci*. 2022;9. doi:10.3389/fmolb.2022.834453

238. Erlanson DA, Fesik SW, Hubbard RE, Jahnke W, Jhoti H. Twenty years on: the impact of fragments on drug discovery. *Nat Rev Drug Discov*. 2016;15(9):605-619. doi:10.1038/nrd.2016.109

239. Scott DE, Francis-Newton NJ, Marsh ME, et al. A small-molecule inhibitor of the BRCA2-RAD51 interaction modulates RAD51 assembly and potentiates DNA damage-induced cell death. *Cell Chem Biol*. 2021;28(6):835-847.e5. doi:10.1016/j.chembiol.2021.02.006

240. Nelson SR, Zhang C, Roche S, et al. Modelling of pancreatic cancer biology: transcriptomic signature for 3D PDX-derived organoids and primary cell line organoid development. *Sci Rep*. 2020;10(1):2778. doi:10.1038/s41598-020-59368-7

241. Roche S, O'Neill F, Murphy J, et al. Establishment and Characterisation by Expression Microarray of Patient-Derived Xenograft Panel of Human Pancreatic Adenocarcinoma Patients. *Int J Mol Sci*. 2020;21(3):962. doi:10.3390/ijms21030962

242. Buisson R, Niraj J, Rodrigue A, et al. Coupling of Homologous Recombination and the Checkpoint by ATR. *Mol Cell*. 2017;65(2):336-346. doi:10.1016/j.molcel.2016.12.007

243. Arnoult N, Correia A, Ma J, et al. Regulation of DNA repair pathway choice in S and G2 phases by the NHEJ inhibitor CYREN. *Nature*. 2017;549(7673):548-552. doi:10.1038/nature24023

244. Cowley GS, Weir BA, Vazquez F, et al. Parallel genome-scale loss of function screens in 216 cancer cell lines for the identification of context-specific genetic dependencies. *Sci Data*. 2014;1(1):140035. doi:10.1038/sdata.2014.35

245. Tan MH, Nowak NJ, Loor R, et al. Characterization of a New Primary Human Pancreatic Tumor Line. *Cancer Invest*. 1986;4(1):15-23. doi:10.3109/07357908609039823

246. Dedes KJ, Wilkerson PM, Wetterskog D, Weigelt B, Ashworth A, Reis-Filho JS. Synthetic lethality of PARP inhibition in cancers lacking *BRCA1* and *BRCA2* mutations. *Cell Cycle*. 2011;10(8):1192-1199. doi:10.4161/cc.10.8.15273

247. Lord CJ, Ashworth A. PARP inhibitors: Synthetic lethality in the clinic. *Science (1979)*. 2017;355(6330):1152-1158. doi:10.1126/science.aam7344

248. Tan MH, Nowak NJ, Loor R, et al. Characterization of a New Primary Human Pancreatic Tumor Line. *Cancer Invest*. 1986;4(1):15-23. doi:10.3109/07357908609039823

249. Gower WR, Risch RM, Godellas C V., Fabri PJ. HPAC, a new human glucocorticoid-sensitive pancreatic ductal adenocarcinoma cell line. *In Vitro Cell Dev Biol Anim*. 1994;30(3):151-161. doi:10.1007/BF02631438

250. Chen WH, Horoszewicz JS, Leong SS, et al. Human pancreatic adenocarcinoma: In vitro and in vivo morphology of a new tumor line established from ascites. *In Vitro*. 1982;18(1):24-34. doi:10.1007/BF02796382

251. Zhang X, Ma N, Yao W, Li S, Ren Z. RAD51 is a potential marker for prognosis and regulates cell proliferation in pancreatic cancer. *Cancer Cell Int*. 2019;19(1):356. doi:10.1186/s12935-019-1077-6

252. Wu W, Liu X, Wei L, et al. Tp53 Mutation Inhibits Ubiquitination and Degradation of WISP1 via Down-Regulation of Siah1 in Pancreatic Carcinogenesis. *Front Pharmacol*. 2018;9. doi:10.3389/fphar.2018.00857

253. Baugh EH, Ke H, Levine AJ, Bonneau RA, Chan CS. Why are there hotspot mutations in the TP53 gene in human cancers? *Cell Death Differ*. 2018;25(1):154-160. doi:10.1038/cdd.2017.180

254. Sun X, Yang D, Chen Y. Single-Cell Analysis Differentiates the Effects of p53 Mutation and p53 Loss on Cell Compositions of Oncogenic Kras-Driven Pancreatic Cancer. *Cells*. 2023;12(22):2614. doi:10.3390/cells12222614

255. Gao J, Chen X, Li X, et al. Differentiating TP53 Mutation Status in Pancreatic Ductal Adenocarcinoma Using Multiparametric MRI-Derived Radiomics. *Front Oncol*. 2021;11. doi:10.3389/fonc.2021.632130

256. Leal TA, Sharifi MN, Chan N, et al. A phase I study of talazoparib (BMN673) combined with carboplatin and paclitaxel in patients with advanced solid tumors (NCI9782). *Cancer Med*. 2022;11(21):3969-3981. doi:10.1002/cam4.4724

257. Gruber JJ, Afghahi A, Timms K, et al. A phase II study of talazoparib monotherapy in patients with wild-type BRCA1 and BRCA2 with a mutation in other homologous recombination genes. *Nat Cancer*. 2022;3(10):1181-1191. doi:10.1038/s43018-022-00439-1

258. Kachmazov A, Bolotina L, Kornietskaya A, Kuznetsova O, Ivanov M, Fedenko A. Complete response to talazoparib in patient with pancreatic adenocarcinoma harboring somatic PALB2 mutation: A case report and literature review. *Front Oncol*. 2022;12. doi:10.3389/fonc.2022.953908

259. Hanamshet K, Mazin A V. The function of RAD52 N-terminal domain is essential for viability of BRCA-deficient cells. *Nucleic Acids Res*. 2020;48(22):12778-12791. doi:10.1093/nar/gkaa1145

260. Carley AC, Jalan M, Subramanyam S, Roy R, Borgstahl GEO, Powell SN. Replication Protein A Phosphorylation Facilitates RAD52-Dependent Homologous Recombination in BRCA-Deficient Cells. *Mol Cell Biol*. 2022;42(2). doi:10.1128/mcb.00524-21

261. Cao L, Mu W. Necrostatin-1 and necroptosis inhibition: Pathophysiology and therapeutic implications. *Pharmacol Res*. 2021;163:105297. doi:10.1016/j.phrs.2020.105297

262. Van Noorden CJF. The history of Z-VAD-FMK, a tool for understanding the significance of caspase inhibition. *Acta Histochem*. 2001;103(3):241-251. doi:10.1078/0065-1281-00601

263. Barbosa MAG, Xavier CPR, Pereira RF, Petrikaitė V, Vasconcelos MH. 3D Cell Culture Models as Recapitulators of the Tumor Microenvironment for the Screening of Anti-Cancer Drugs. *Cancers (Basel)*. 2021;14(1):190. doi:10.3390/cancers14010190

264. Pampaloni F, Reynaud EG, Stelzer EHK. The third dimension bridges the gap between cell culture and live tissue. *Nat Rev Mol Cell Biol*. 2007;8(10):839-845. doi:10.1038/nrm2236

265. AstraZeneca: Highlights of prescribing information: LYNPARZA (olaparib) tablets, for oral use. Accessed December 27, 2023. https://www.accessdata.fda.gov/drugsatfda_docs/label/2018/208558s006lbl.pdf

266. Anscher MS, Chang E, Gao X, et al. FDA Approval Summary: Rucaparib for the Treatment of Patients with Deleterious *BRCA* -Mutated Metastatic Castrate-Resistant Prostate Cancer. *Oncologist*. 2021;26(2):139-146. doi:10.1002/onco.13585

267. FDA approves rucaparib for maintenance treatment of recurrent ovarian, fallopian tube, or primary peritoneal cancer. Accessed December 27, 2023. https://www.fda.gov/drugs/resources-information-approved-drugs/fda-approves-rucaparib-maintenance-treatment-recurrent-ovarian-fallopian-tube-or-primary-peritoneal

268. FDA approves olaparib for gBRCAm metastatic pancreatic adenocarcinoma. Accessed December 27, 2023. https://www.fda.gov/drugs/resources-information-approved-drugs/fda-approves-olaparib-gbrcam-metastatic-pancreatic-adenocarcinoma#:~:text=On%20December%2027%2C%202019%2C%20the,an%20FDA%2Dapproved%20test%2C%20whose

269. Zejula, Niraparib, Food and Drug Administration approval. Accessed December 27, 2023.

https://www.accessdata.fda.gov/drugsatfda_docs/label/2020/208447s015s017lbledt.pdf

270. FDA approves talazoparib for gBRCAm HER2-negative locally advanced or metastatic breast cancer. Accessed December 27, 2023. https://www.fda.gov/drugs/drug-approvals-and-databases/fda-approves-talazoparib-gbrcam-her2-negative-locally-advanced-or-metastatic-breast-cancer#:~:text=On%20October%2016%2C%202018%2C%20the,advanced%20or%20metastatic%20breast%20cancer.